What is the best map projection?

by

Reef Goudswaard

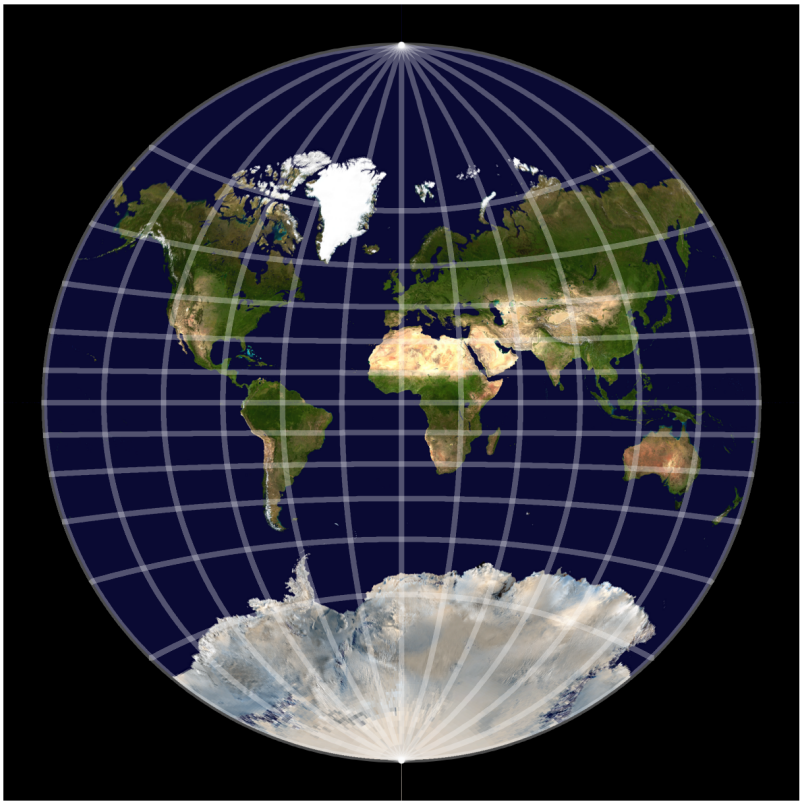

A Bachelors Thesis presented for the degree of Applied Mathematics
Delft Institute of Applied Mathematics
Delft University of Technology
Delft, The Netherlands
Dr. P.M. Visser and Dr. O. Jaïbi
March 2024

Contents

1 Introduction

For many thousands of years, humans have been involved in the creation of maps, ranging from charting simple lands, rivers and cities, all the way to projecting the entire Earth or even galaxies onto a map. Given that correct navigation of any area was, and is, of paramount importance to the development of humankind, one may not be surprised that maps of local territory have independently been invented by many different ancient cultures. Although much is still uncertain about the history of map creation and usage, also known as cartography, some estimates for the earliest maps date back to 25000 BC [15]. Some candidates for the earliest known maps include:

- A map carved into a mammoth tusk, depicting mountains, valleys, rivers and routes in Pavlov, Czech Republic. It has been dated back to around 25000 BC [15].
- A cylcon from the Aboriginal Australians which appears to depict the Darling river in Australia. It is thought to be from around 20000 BC. [2]
- A drawing of dots representing stars in the night sky on the walls of the caves at Lascaux, France. It is believed to be about 16500 years old. [10]

As time went on, larger and larger areas of Earth were being mapped, but, as up to and including the middle ages, any civilisation was only aware of at most half of Earth's coastlines (and even less of the interiors of the continents), creating a map of the world was impossible. With the start of the renaissance, however, a stark increase in exploration led to the first, somewhat accurate world maps appearing in the 1500's. By the mid 1700's, most of the Earth's coastlines were mapped, and over the coming 200 years so would the continental interiors. However, as the study of projecting the whole Earth onto a flat map began, some issues emerged; in their efforts of creating a perfect map, cartographers of the time started to suspect it might be impossible to project the surface of a sphere (or ellipsoid) onto a flat surface, without distortions of some sort. Their hunch was later proven correct by Johann Carl Friedrich Gauss some 300 years later in his famous "Theorema Egregium" [4]. This was problematic, as it implied no true two-dimensional map of the Earth can exist; one can, at best, create a map that has as few distortions as possible. As such, over the course of the last 500 years, many different world map projections have arisen; some more mathematically justified than others, and all with different purposes in mind. This, however, begs the question: of these map projections, what is the best projection? Over the course of the years, publishers of atlases have regularly swapped out their 'standard' world map projection for a new and supposedly 'better' projection, justified by a set of imprecise reasons that leave the user in the dark as to whether or not the map is actually of good quality. Naturally, different maps serve different purposes: some may need to display no change in area size, others may need to have roughly correct continent shapes and others may want to display direction correctly; no projection is the 'best' projection. Still though, it is useful to have a measure based on exact criteria that allows us to rank the projections in a list, after which the highest ranking projection fulfilling the given requirements can be chosen. By mathematically measuring the distortions, this reports aims to create a measure that ranks map projections according to the least distortion, thereby putting forward a list based on an exact criterion. To do this, we will first discuss what map projections are from a mathematical point of view in Chapter 2. This chapter contains all the necessary information for understanding map projections, allowing us to work our way to the mathematical definitions for the different sort of distortions at the end of the chapter. Consequently, Chapter 3 serves as a list of many different map projections. It includes the equations, inverse equations, quantified distortions as well as figures displaying the map projections and their distortions. Furthermore, a brief summary of the map projection including its properties and strengths and weaknesses is given. Chapter 4 then discusses the criterion on which the ranking is based and provides an ordered list of the map projections, all justified by the mathematics discussed in Chapter 2.

The code used for generating the map projections can be found in the following GitHub repository: `https://github.com/ReefG/mapprojections`.

Quantity	Symbol	meaning
Latitude	ϕ	The latitude represents the angular coordinate that determines the North-South position on the Earth and ranges from $-\pi/2$ to $\pi/2$. See: longitude
Longitude	λ	The longitude represents the angular coordinate that specifies the East-West position with respect to the prime meridian on the Earth and ranges from $-\pi$ to π. Together with the latitude it allows for measuring locations on the Earth.
x-coordinate	x	x represents the horizontal axis of the Cartesian coordinate system, henceforth called the plane, onto which the maps are projected.
y-coordinate	y	y represents the vertical axis of the plane onto which the maps are projected. Together with the x-coordinate, one can specify positions on the map projections.
Radius	R	$R \in \mathbb{R}_{>0}$ is the radius of the sphere that represents the Earth.
Map projections	T	T is a transformation from the latitude ϕ and longitude λ to the (x, y)-plane.
Scale factor along meridian	h	h is the scale factor along the meridians.
Scale factor along parallels	k	k represents the scale factor along the parallels.
Maximum scale factor	a	a is the maximum scale factor in a given point (ϕ, λ). It also represents the semi major axis of the Tissot's Indicatrix.
Minimum scale factor	b	b is the minimum scale factor in a given point (ϕ, λ). It also represents the semi minor axis of the Tissot's Indicatrix.
Singular value 1	σ_1	σ_1 corresponds to either a or b and hence is the maximum or minimum scale factor in a point, but is derived using singular value decomposition (see Section 2.9.3) rather than using geometry.
Singular value 2	σ_2	σ_2 is used together with σ_1 and corresponds to either a or b and hence is the maximum or minimum scale factor in a point. If σ_1 corresponds to a, then σ_2 corresponds to b and vice versa. It is derived using singular value decomposition (see Section 2.9.3) rather than using geometry.
Azimuthal radiating scale factor	h'	In azimuthal projections, h' represents the scale factor in the direction of a straight line radiating from the center of the projection.
Azimuthal perpendicular scale factor	k'	In azimuthal projections, k' represents the scale factor in the direction perpendicular to the straight lines radiating from the center of the projection.
Area distortion factor	s	s is the area distortion factor of the map projection at a given point (ϕ, λ). It is the factor by which the area is inflated or deflated at a given point.
Angular distortion	ω	ω represents the angular distortion in a point (ϕ, λ). It ranges from 0 to π.
Angular distortion number	μ_ω	μ_ω is the distortion number calculated for a map projection that allows one to rank map projections based on their angular distortion (see Section 4.1).
Area distortion number	μ_s	μ_s is the area distortion number calculated for a map projection that allows one to rank map projections based on their area distortion (see Section 4.1).
Overall distortion number	μ	μ is the distortion number calculated for a map projections that allows one to rank map projections on a combination of their angular and area distortion (see Section 4.1).

Table 1: Glossary of used symbols. This table lists the meaning of the different symbols used in the text.

2 Map projections and distortion analysis

In this Chapter, we define what a map projection is. Furthermore, we introduce some terminology, as well as some simplifications to be able to work around the difficulties of the problem at hand. Hereupon we treat the distortion analysis of map projections. Starting with cylindrical projections, we gradually work our way up to the mathematics that describes the angular distortion as well as the distortion in area size of map projections in general. In doing so, we examine the Tissot's indicatrix [12] and discuss its value in distortion analysis.

2.1 Geographic coordinate system

Before we can discuss map projections, we must first study the coordinate system that is often used for measuring locations on the surface of the Earth: the geographic coordinate system. This system uses an ordered list of two numbers, henceforth called a tuple, that consists of the latitude, denoted by ϕ, and longitude, denoted by λ, for determining positions on Earth. Figure 1 provides a visual aid in the explanation of these coordinates. In the geographic coordinate system, the latitude determines the North-South position on the globe. It is defined as the angle that ranges from -90° at the South Pole, to 90° at the North Pole, and has the equator at 0°. Circles of a certain latitude run from East to West, parallel to the equator and are hence called parallels. Similarly, the longitude specifies the East-West position on the Earth; it is given as an angle, and ranges from -180° to +180°. The semicircles of a certain longitude that run from pole to pole are called meridians. The meridian at 0° is defined as the prime meridian (also called the central meridian) and is usually chosen to be the Greenwich meridian, which is the meridian passing through the Royal Observatory in London known as Greenwich. Together, the latitude and longitude form the tuple (ϕ, λ) that allows one to assess any location on the surface of the Earth.

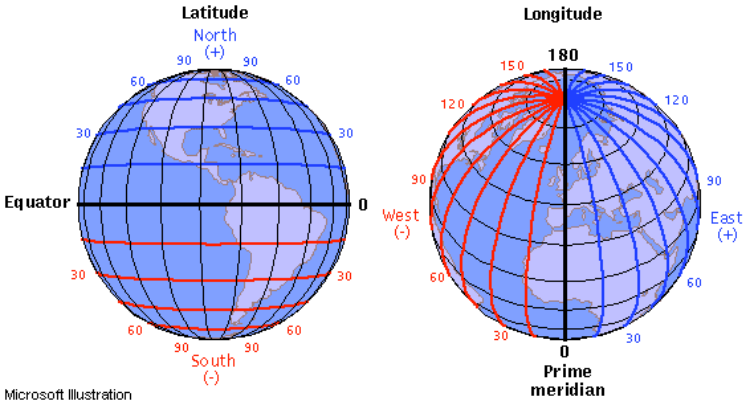

Figure 1: Illustration of the latitude and longitude coordinates that delineate the surface of the Earth. They range from -90° to 90° and from -180° and 180°, respectively. The negative values are represented by the colour red and the positive values by the colour blue. In radians, the ranges are from $-\pi/2$ to $+\pi/2$ and from $-\pi$ to $+\pi$, respectively. The prime meridian passes through Greenwich, London. Image from [3].

In mathematics, however, we prefer to use radians rather than degrees. Henceforth, we will assume the latitude ϕ to range from $-\pi/2$ to $+\pi/2$. Likewise, the longitude λ will range from $-\pi$ to $+\pi$.

2.2 What is a map projection?

A map projection T is a (non-linear) coordinate transformation from (a part of) the sphere with coordinates latitude ϕ and longitude λ to the plane. Hence

$$T : [-\pi/2, \pi/2] \times [-\pi, \pi) \to Z \subseteq \mathbb{R}^2, \tag{2.2.0.1}$$

and is defined as:

$$T(\phi, \lambda) = (x, y),$$

where x and y are functions of λ and ϕ:

$$x = x(\phi, \lambda),$$
$$y = y(\phi, \lambda).$$

If and only if both $x(\phi, \lambda)$ and $y(\phi, \lambda)$ are differentiable (and hence continuous) on their domain, then so is the map projection $T(\phi, \lambda)$. There are different ways of implementing a map projection, which are discussed in Chapter 3. However, the challenge of projecting the Earth onto a flat map (but perhaps also what makes it very interesting) is that no map projection that projects the surface of a sphere onto the plane can be created that does not involve some kind of distortion. Intuitively, this is shown in Figure 2 using an orange with the world map drawn on the orange's peel. Peeling the orange and trying to fold it so that it lies flat results in an odd and perhaps somewhat useless world map. As mentioned before, this

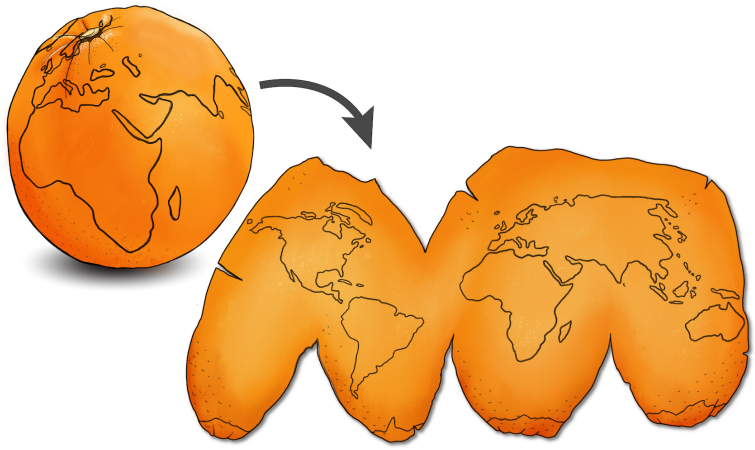

Figure 2: Visualisation of the inability to project a sphere onto a flat map without some kind of distortion or tearing up, using an orange. One notices that the folded out orange peel takes an odd shape [16].

has also been mathematically proven by the German mathematician Johann Carl Friedrich Gauss in 1827 in his famous "Theorema Egregium" (Latin for"remarkable theorem") [4]. As such, the study of map projections is not only about minimising the distortions, but also about deciding what properties are important for the particular application of said map. In this paper, the assumption will be made that the Earth is a perfect sphere with radius R where $R \in \mathbb{R}_{>0}$ in order to simplify the problem. In reality, Earth has more of an ellipsoidal shape.

2.3 Classification of map projections

We can roughly subdivide map projections into the following categories [5]:

1. **Equal-area maps**. These maps preserve the size of areas. If one would put a coin on the sphere, it would have the same area on the projection. This, however, often comes at the cost of the shapes on the map; the image of the coin would likely not be a perfect circle.

2. **Conformal maps**. A map is said to be conformal if any angle between two curves on the sphere is preserved on the map. Hence, these maps preserve shape locally, which results in roughly accurate continent shapes.

3. **Conventional maps**. These maps are neither equal area nor conformal. Rather, they are often created to serve a certain application, and can thus have both some distortion in area as well as some angular distortion.

Besides maps being equal-area or conformal, there exist some other special characteristics that map projections can have [12]:

1. **Scale:** Even though no map projections portray scale (see Section 2.7) correctly throughout the whole map, most map projections generally have one or more lines

along which scale is preserved. These lines can often be chosen to one's liking to minimise scale errors elsewhere on the map. If a projection preserves scale between a certain point and every other point or along every meridian, it is called equidistant.

2. **Direction:** Besides conformal maps, on which the local relative directions are correct, there also exist map projections called azimuthal, on which all points are at the correct direction with respect to the center. This means that the angle between the center and any point is preserved by the projection.

3. **Shortest route:** On (only) the Gnomonic projection (see Section 3.3.3), the great circles (see Section 2.5), and thus the route between two points on the sphere with the shortest distance, are portrayed as straight lines.

A different way of classifying some map projections is by the surface on which they are projected. The idea is that the surface, specifically one which can be unrolled into a plane without introducing distortion, is placed in contact with the Earth, after which the features of the Earth are transferred to the surface, which is then folded out to get the map. The most common ones are (Figure 3):

1. **Cylindrical projections**: These projections feature a surface that is wrapped around the Earth to form a cylinder.

2. **Conic projections**: Conic projections include projections which have a surface wrapped around the Earth to form a cone.

3. **Planar projections (azimuthal)**: Planar projections involve a flat plane onto which the Earth's features are projected.

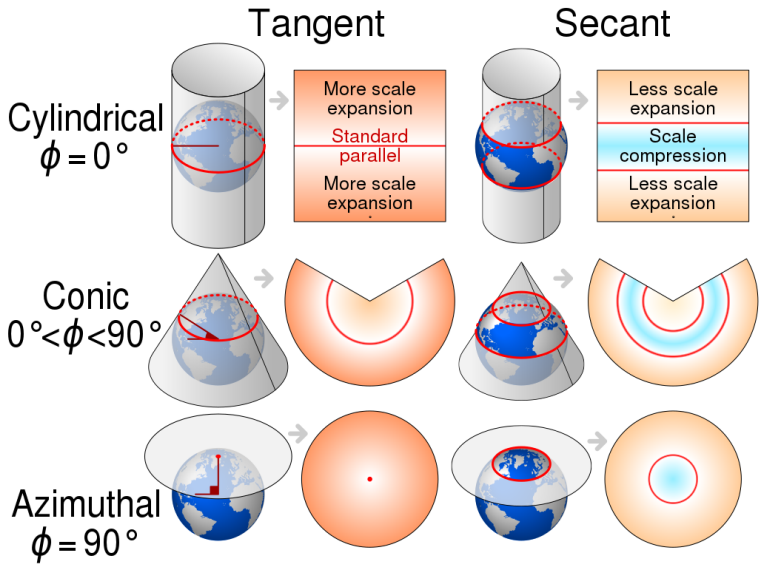

Figure 3: Three common projection surfaces: cylindrical, conic and planar (azimuthal). Furthermore, the difference between tangent and secant is displayed [1].

Figure 3 shows the distinction between surfaces that are tangent and secant to the sphere. The surface is said to be tangent to the sphere if it touches it, but does not intersect it. On the other hand, secant means that the surface does intersect the sphere. Tangent and secant lines, also called standard lines, are always undistorted, as the scale along these lines is preserved (equal to one). When these lines are parallels, they are called standard parallels, which are common in conic projections.

A critique of this way of classification, however, is that many map projections do not (neatly) fall in any of these categories. Hence, other categories have also been described in literature. Examples of these include pseudoconic, pseudocylindrical, pseudoazimuthal, retroazimuthal and polyconic [12]. Still, these categories provide useful geometrical insight in the workings of the projection and may benefit the visual learner. In the next section, some examples of map projections are discussed.

2.4 Examples of map projections

To illustrate the concept of map projections, we discuss three projections, one of each of the three main groups: cylindrical, conic and azimuthal projections. We will commence with an intuitive cylindrical projection which happens to have a geometric interpretation. Imagine taking a rectangular piece of paper on which we want to draw the map, and we fold it around the Earth so that it forms a cylinder, as seen in Figure 4a. For simplicity, we will assume the width of the map to be exactly $2\pi R$, where $R \in \mathbb{R}_{>0}$ represents the radius of the globe. As such, the cylinder fits perfectly around the latter. Now place a light bulb at the centre

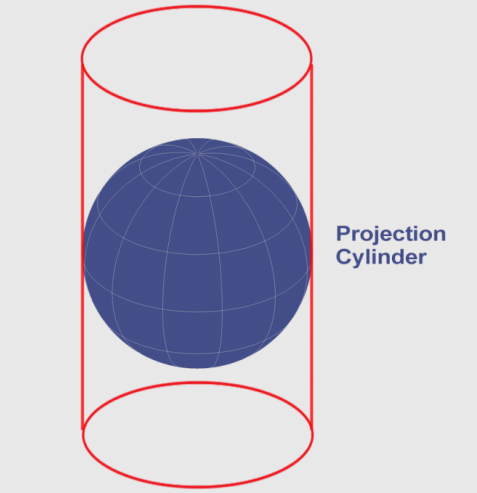

(a) A surface wrapped around the sphere to form the projection cylinder.

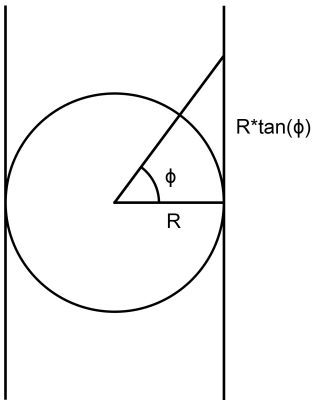

(b) Side view of the Central cylindrical projection. This figure displays a side view of the central cylindrical projection. It illustrates why the y-coordinate is $R\tan\phi$.

Figure 4: Geometrical view of a cylinder wrapped around the sphere used in the construction of the Central cylindrical projection.

of the globe and define the projection as follows: the point on the globe where a certain ray intersects the globe will be projected on the point on the cylinder where said ray intersects the cylinder. Unfolding the cylinder then provides us with our map. The x-coordinate on the map is rather simple; all the meridians simply become vertical lines on the map, and hence we can take x to be equal to $R\lambda$. For the y-coordinate, we examine Figure 4b. By the geometry of right-angled triangles, we find that the y-coordinate is $R\tan(\phi)$.

Thus, our projection, known as the Central cylindrical projection, is defined as follows:

$$x(\phi, \lambda) = R\lambda, \tag{2.4.0.1}$$
$$y(\phi, \lambda) = R\tan(\phi), \tag{2.4.0.2}$$
$$T(\phi, \lambda) \in \{(x, y) |\ x \in [-\pi R, \pi R),\ y \in \mathbb{R}\} \tag{2.4.0.3}$$

Plotting this map projection, we obtain Figure 5. One notices that the map looks somewhat odd, with the poles being considerably stretched out. As one intuitively may feel, this map is neither conformal nor equal-area (this will be treated in the next section). Because the distortion increases significantly as one travels further from the Equator, this projection is not often used in practice, but it does serve as a convenient example to obtain a feeling for map projections.

In general, cylindrical projections are given by the following transformation [5]:

$$x(\phi, \lambda) = R\lambda, \tag{2.4.0.4}$$
$$y(\phi, \lambda) = f(\phi), \tag{2.4.0.5}$$
$$T(\phi, \lambda) \in \{(x, y) |\ x \in (-\pi R, \pi R),\ y \in \mathbb{R}\}. \tag{2.4.0.6}$$

The intuition behind this, is that for any projection where the map is wrapped around the globe as a cylinder (hence a cylindrical projection), the meridians will be projected as vertical lines on the map. Hence, the x-coordinate of the map will be equal to the longitude. Furthermore, to produce a map without jumps or gaps, we define $f(\phi)$ to be continuous.

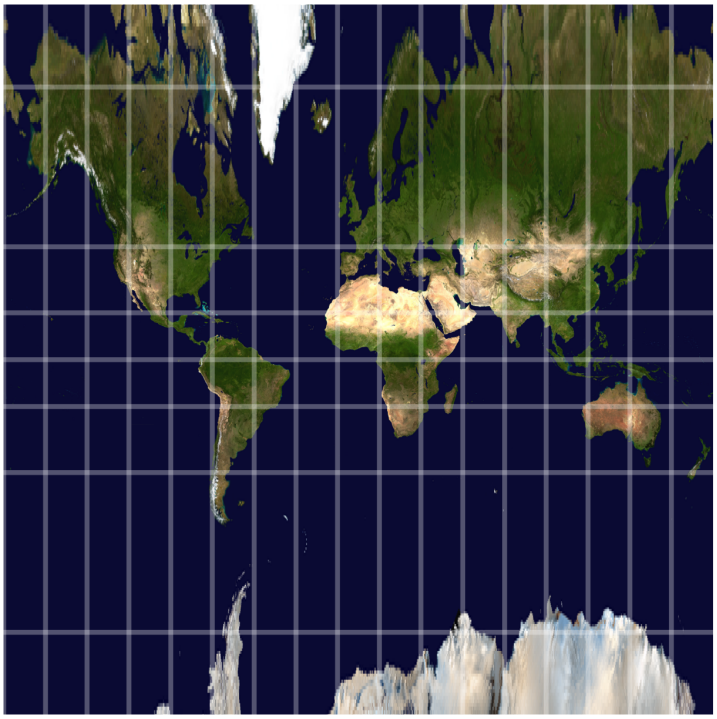

Figure 5: Central cylindrical projection. The projection is given by equations (2.4.0.1) to (2.4.0.3). The map is rather accurate near the Equator, but as one moves towards the poles, distortion increases rapidly.

Besides cylindrical projections, conic projections are also a prominent group of map projections. Geometrically, (the more elementary) conic projections arise from placing a cone over the sphere, projecting the sphere's features onto the cone, after which it is cut along a meridian and unfolded to lie flat. Contrary to cylindrical projections, the conic projections have no general form, but are often defined to be any projection in which the parallels are arcs of concentric circles and the meridians equally spaced straight radial lines of these circles. Unfortunately, contrary to cylindrical projections, these projections have no simple and intuitive example and hence take more time to understand geometrically. An example of a conic projection is Lambert's equal-area conic projection, which can be seen in Figure 6. The equations are more complicated than those of the cylindrical projections, but are worth listing here to get a feel for conic projections. Thinking in terms of polar coordinates will aid in this regard. The projection is given by:

$$x(\phi, \lambda) = \rho \sin(\theta), \tag{2.4.0.7}$$
$$y(\phi, \lambda) = \rho_0 - \rho \cos(\theta), \tag{2.4.0.8}$$

where

$$n = \frac{1}{2}\Big(\sin(\phi_1) + \sin(\phi_2)\Big), \ n \neq 0, \tag{2.4.0.9}$$
$$\theta = n\lambda, \tag{2.4.0.10}$$
$$C = \cos^2(\phi_1) + 2n\sin(\phi_1), \tag{2.4.0.11}$$
$$\rho = R\frac{\sqrt{C - 2n\sin(\phi)}}{n}, \tag{2.4.0.12}$$
$$\rho_0 = R\frac{\sqrt{C}}{n}. \tag{2.4.0.13}$$

Here, the ϕ_1 and ϕ_2 are the standard parallels. For an analysis of this projection, the reader is referred to Chapter 3, specifically Section (3.2.1).

As mentioned before, the azimuthal projections are created by placing a plane tangent to the sphere at one of the poles, the Equator or any point in between, after which the continents are projected onto the plane, resulting in a map. An important feature of

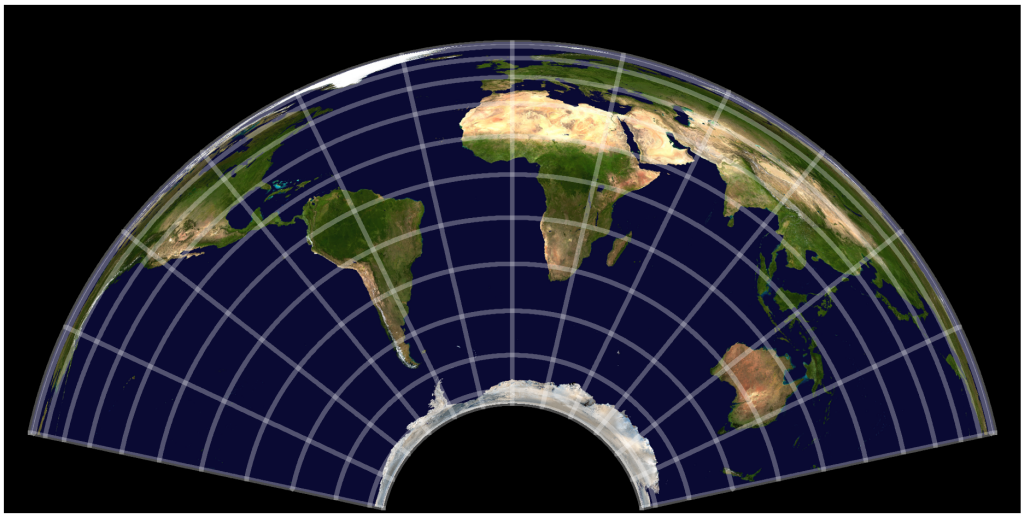

Figure 6: Albers equal-area conic projection. Local angles are not preserved, causing certain continents to take incorrect shapes. Nonetheless, it is equal-area, meaning the area sizes of the continents are correct with respect to one another. The standard parallels used in this figure are 0 and $\pi/3$, in between which there is the least distortion.

azimuthal projections is that the direction relative to the center of the projection is shown correctly. Furthermore, the shortest route between the center and any point is shown as a straight line. One example of an azimuthal projection is the Orthographic projection. As is shown in Figure 7, the point of perspective is at infinity, which causes all meridians and parallels to become ellipses, circles or straight lines. This also results in a close resemblance to a globe. A downside of this projection is that it can only show one hemisphere. The

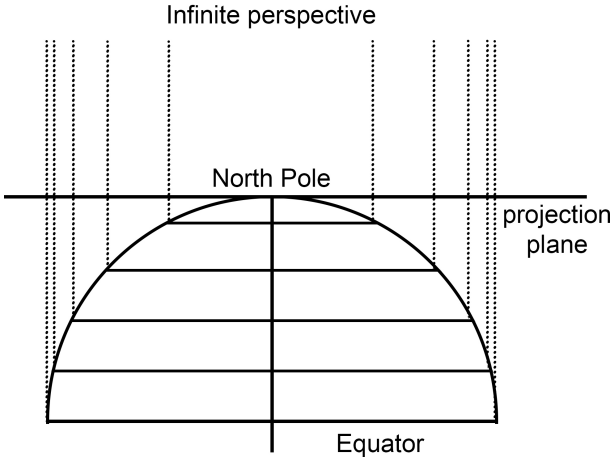

Figure 7: Geometric interpretation of the Orthographic projection. The point of perspective is placed at an infinite distance. Here, the plane is placed tangent to the North Pole.

equations for the Orthographic projection are:

$$x(\phi, \lambda) = R\cos(\phi)\sin(\lambda), \tag{2.4.0.14}$$

$$y(\phi, \lambda) = R\Big(\cos(\phi_1)\sin(\phi) - \sin(\phi_1)\cos(\phi)\cos(\lambda)\Big). \tag{2.4.0.15}$$

Here $(\phi_1, 0)$ is the center point of the projection. Once more, Chapter 3 covers this projection more in depth.

2.5 Great circle distance

Before continuing to the distortion analysis, it is advantageous to first discuss great circles, especially for the azimuthal projections discussed in Chapter 3. On a sphere, great circles

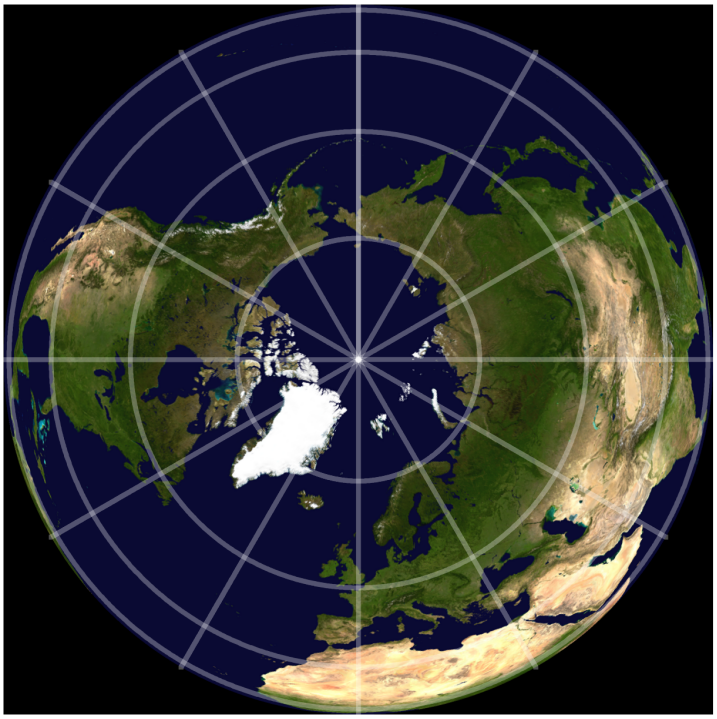

Figure 8: North Polar Orthographic projection. As the Orthographic projection is a parallel projection with its point of perspective at an infinite distance, this projection resembles the sphere with the North Pole at the center. Because of this point of perspective, the Orthographic projection can only display one hemisphere at once.

are defined to be any circle that cuts the sphere into two equal hemispheres. Obviously, the Equator is a great circle and all meridians are also arcs of great circles. Furthermore, any arc of a great circle between two points on the sphere happens to be the route between said two points with the smallest distance, also mathematically referred to as geodesics. Especially when studying the azimuthal projections, it can be useful to find a formula for the great circle distance between two points. In Figure 9, a spherical triangle is drawn with three points having the angles A, B and C, connected by three arcs of great circles with arc lengths a, b and c. By the spherical law of cosines, we have

$$\cos(c) = \cos(b)\cos(a) + \sin(b)\sin(a)\cos(C). \tag{2.5.0.1}$$

We take A and B to be at the latitudes and longitudes (ϕ_1, λ_1) and (ϕ, λ) respectively. Taking C to be at the North Pole, we find that C is simply the angle between the two meridians on which A and B lie: $C = \lambda - \lambda_1$. Furthermore, as a and b are arcs of meridians, they have the values $\frac{\pi}{2} - \phi$ and $\frac{\pi}{2} - \phi_1$, respectively. Combining this with equation (2.5.0.1) and using the trigonometric reflection and shift identities, we obtain the following equation for the angular great circle distance c between two points (ϕ_1, λ_1) and (ϕ, λ):

$$\cos(c) = \sin(\phi_1)\sin(\phi) + \cos(\phi_1)\cos(\phi)\cos(\lambda - \lambda_1). \tag{2.5.0.2}$$

This equation can be useful in determining what points are to be projected for azimuthal projections, as some map projections cannot project the entire sphere at once.

2.6 Four-quadrant inverse tangent

The four-quadrant inverse tangent, more commonly known as the 2-argument arctangent, or even simpler, the atan2 function, is a version of the arctangent that takes y and x as arguments and considers the quadrant the point (x, y) is in. It is defined as the angle between the positive x-axis and the line from the origin to the point (x, y) in the Cartesian plane. Furthermore, rather than taking values in $(-\pi/2, \pi/2)$ like the ordinary arctangent, atan2 takes values in the interval $(-\pi, \pi]$. The motivation for this function is that diametrically

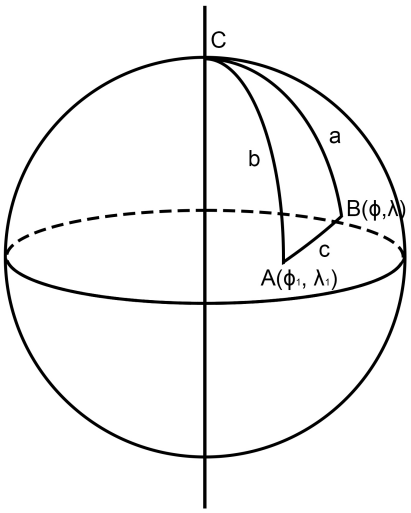

Figure 9: Spherical triangle with three points having the angles A, B and C respectively. They are connected by three great circle arcs with arc lengths a, b and c. The point with angle C is chosen to be at the North Pole, whereas the points with angles A and B have the latitudes and longitudes (ϕ_1, λ_1) and (ϕ, λ), respectively.

opposite angles have the same tangent, as $\frac{y}{x} = \frac{(-y)}{(-x)}$, and hence the ordinary arctangent is not sufficient for uniquely determining angles in all four quadrants of the Cartesian plane, a functionality that would be useful in some map projections. Hence, by considering the signs of x and y, $\pm\pi$ may be added to correct for the quadrant of the point. It is defined as follows:

$$\operatorname{atan2}(y,x) = \begin{cases} \arctan(\frac{y}{x}) & \text{if } x > 0, \\ \arctan(\frac{y}{x}) + \pi & \text{if } x < 0 \text{ and } y \geq 0, \\ \arctan(\frac{y}{x}) - \pi & \text{if } x < 0 \text{ and } y < 0, \\ +\frac{\pi}{2} & \text{if } x = 0 \text{ and } y > 0, \\ -\frac{\pi}{2} & \text{if } x = 0 \text{ and } y < 0, \\ \text{undefined} & \text{if } x = 0 \text{ and } y = 0. \end{cases} \tag{2.6.0.1}$$

For $x > 0$, $\operatorname{atan2}(x, y)$ is simply the arctangent of $\frac{y}{x}$. For $x < 0$, however, a half turn is added or subtracted to correct for the quadrant. The case that $x = 0$ would also be problematic for the ordinary arctangent, but is also handled by the atan2 function. As this functionality is required for some map projections discussed in this paper, the atan2 function will be useful.

2.7 Scale factors

To understand whether or not a projection is equal-area or conformal requires us to examine scale factors. When one walks from a point to another point on the globe, a certain distance on the sphere is travelled. Consequently, the projection of this path can also be walked on the map, leading to a (different) distance travelled on the map as compared to the distance travelled on the globe. A scale factor is defined as the infinitesimal distance travelled on the map divided by the infinitesimal distance travelled on the sphere. Hence, a scale factor is a function of ϕ and λ that takes values in $[0, \infty)$ if the projection is continuous. For a given point, in every direction the map is scaled by a different scale factor, which can be visualised as an ellipse around it. In general, however, we are interested in the scaling factors along the meridians and parallels, henceforth denoted by h and k respectively. If dealing with azimuthal projections however, we use h' and k' instead: h' is the scale factor in the

direction of a straight line radiating from the center of the projection and k' is the scale factor in the direction perpendicular to such a radiating line.

2.7.1 Scale factors of cylindrical projections

To understand how scale factors play a role in the properties of maps, we continue with cylindrical projections and examine a very simple example which generalises well to other map projections later on. We examine the transformation of a rectangle (see Figure 10). We want the transformation of the rectangle to be conformal (thus angle preserving). To achieve this, both sides of the rectangle must be multiplied by the same scale factor $M \neq 0$.

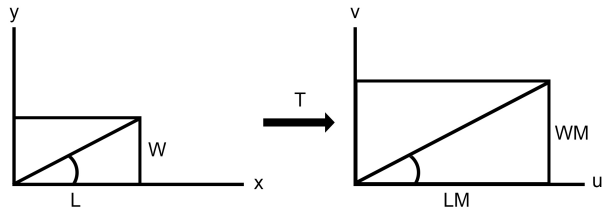

Figure 10: Conformality demonstrated using a rectangle with sides L and W. This figure depicts a transformation in which the triangles retain their angles by scaling both sides with the same factor $M \neq 0$.

If, however, we aim to preserve the area of our rectangle, we must do the opposite. If we scale one side with factor M, we need to scale the other side with factor $\frac{1}{M}$ in order to preserve the area of our rectangle (see Figure 11). Hence, the horizontal and vertical scale factors must be reciprocals of each other. This example demonstrates the intuition that we cannot have both area and angular preservation in a point, unless there is no scaling ($M = 1$). Before we can apply our ideas to the projections, we must first calculate these

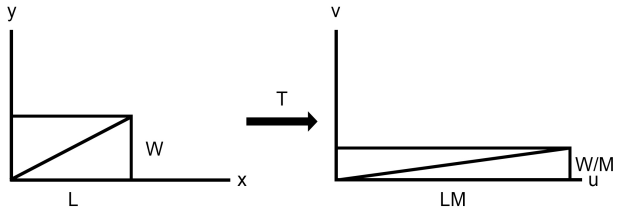

Figure 11: Area preservation of a rectangle with sides L and W. This figure depicts a transformation in which the rectangle retains its area by scaling the sides with a scale factor $M \neq 0$ and the other with its reciprocal $\frac{1}{M}$.

scale factors. We will assume to be working with an arbitrary cylindrical projection, the transformation of which is given by equations (2.4.0.4) and (2.4.0.5):

$$x(\phi, \lambda) = R\lambda,$$
$$y(\phi, \lambda) = f(\phi).$$

Then, the scale factors are given by

$$h = \frac{1}{R}\frac{\partial y}{\partial \phi}, \tag{2.7.1.1}$$

$$k = \frac{1}{R\cos(\phi))}\frac{\partial x}{\partial \lambda},\ \phi \neq \pm\frac{\pi}{2}. \tag{2.7.1.2}$$

Here, $\frac{\partial y}{\partial \phi}$ denotes the partial derivative of y with respect to ϕ etc. As we approach the poles, ϕ approaches $\pm\frac{\pi}{2}$ and hence $\cos(\phi)$ goes to zero. This causes the scale factor along the parallels k to approach infinity. Geometrically, this is the result of trying to stretch a

point (the poles) into a line on the map, which is nonsensical. Continuing, imagine a very small rectangle on the sphere, which we will denote by $PMQK$. We will define point P to have latitude ϕ and longitude λ and consequently, the point Q will have latitude $\phi + d\phi$ and longitude $\lambda + d\lambda$. As the lines PK and MQ lie on meridians, they have arc lengths of $Rd\phi$. The lines KQ and PM lie on parallels with radius $R\cos(\phi)$ and hence have arc lengths $R\cos(\phi)d\lambda$. Given that we are working with cylindrical projections, the rectangle $PMQK$ on the globe is projected to a rectangle $P'M'Q'K'$ on the map, as depicted by Figure 12. The sides of $P'M'Q'K'$ have the lengths dy and $dx = Rd\lambda$ by our definition of cylindrical projections. Hence, using the fact that x and y are functions of only λ and ϕ respectively,

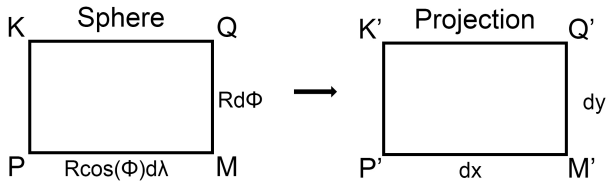

Figure 12: The cylindrical projection of a rectangle with infinitesimal sides from the sphere to the plane.

the scale factors for the general case of cylindrical projections can be computed:

$$k = \frac{1}{R\cos(\phi)}\frac{\partial x}{\partial \lambda} = \frac{1}{R\cos(\phi)}\frac{dx}{d\lambda} = \frac{1}{R\cos(\phi)}\frac{Rd\lambda}{d\lambda} = \frac{1}{\cos(\phi)},\ \phi \neq \pm\frac{\pi}{2} \tag{2.7.1.3}$$

$$h = \frac{1}{R}\frac{\partial y}{\partial \phi} = \frac{1}{R}\frac{dy}{d\phi} = \frac{y'(\phi)}{R}. \tag{2.7.1.4}$$

In the next section, these results will be applied to obtain equal-area and conformal cylindrical projections.

2.7.2 Cylindrical equal-area projection and Mercator projection

Applying the ideas of the previous section, one can obtain a cylindrical equal-area projection by having the scale factors along the meridians and parallels be reciprocals of one another. This is the case for $h = \frac{1}{k}$ and hence we have $\frac{y'(\phi)}{R} = \cos(\phi)$. Integrating and setting the integration coefficient to be equal to 0, we obtain

$$y(\phi) = R\sin(\phi). \tag{2.7.2.1}$$

This gives the Cylindrical equal-area projection, plotted in Figure 13. Conversely, if we

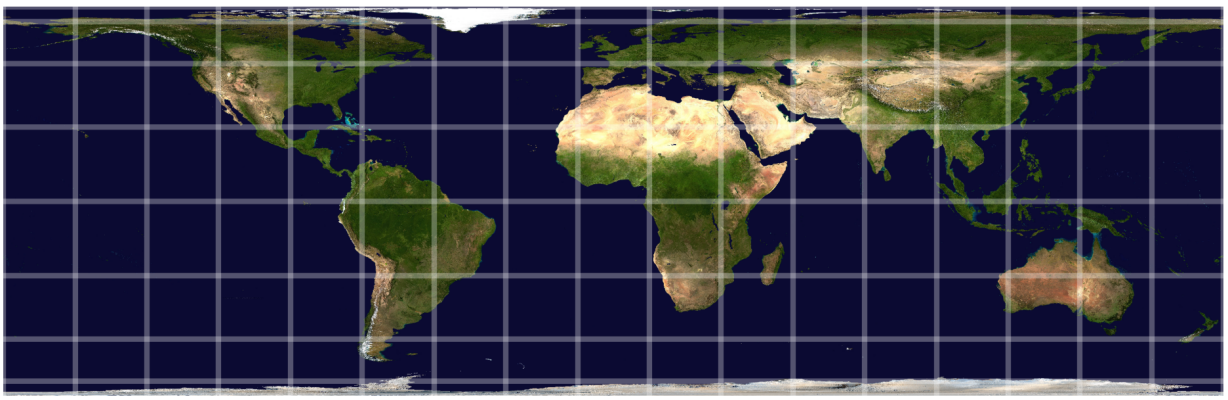

Figure 13: Cylindrical equal area projection. The choice of the y-coordinate is given by equation (2.7.2.1). As its name indicates, the areas of the continents are preserved by the projection. The angles (and thus shapes of the countries) however are not, hence giving it a squished feeling. It has a 1 to π aspect ratio.

would want to preserve angles, one must set the scaling factors equal to each other. Setting $h = k$, we get $\dfrac{y'(\phi)}{R} = \dfrac{1}{\cos(\phi)}$. Again, integrating and setting the integration coefficient to be equal to 0, we obtain

$$y(\phi) = R \ln\left(\frac{1}{\cos(\phi)} + \tan(\phi)\right). \tag{2.7.2.2}$$

This choice of the y-coordinate gives us the Mercator projection, named after its creator Gerardus Mercator (1569) [12] and is plotted in Figure 14. As the angles are preserved locally, so are (roughly) the shapes of the countries. This, however, comes at the cost of the area preservation; the area gets increasingly more distorted as one moves further away from the Equator.

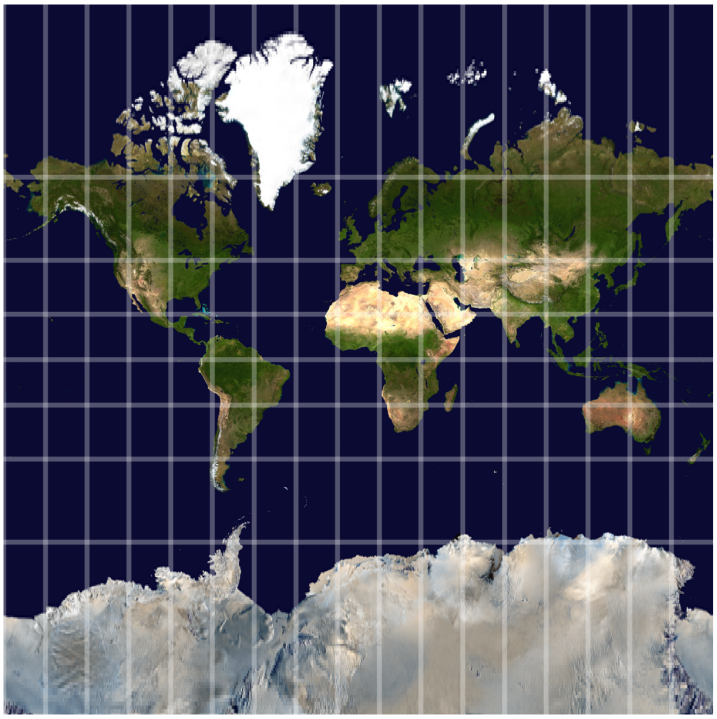

Figure 14: Mercator projection. The choice of the y-coordinate is given by equation (2.7.2.2). It is a cylindrical projection which locally preserves angles, and thus roughly the shapes of the continents. As such, it has uses in navigation. Note that areas get more distorted as one travels further away from the Equator.

We can generalise these results for all map projections which have their parallels and meridians intersecting at right angles, among which all cylindrical projections and many conic projections fall: any point (ϕ, λ) for which $h = k$ will display no angular distortion on the map around this point. If this holds for all points, the map projection will have no local angular distortion and hence be classified as conformal. Furthermore, if $h = 1/k$, then the projection is equal-area. Later on, the case for which the parallels and meridians do not intersect at right angles will be discussed.

2.8 Measuring the distortion of area

Naturally, we seek to quantify both the area and angular distortion. Starting with the area, mathematical analysis has provided us with a neat way of calculating the area distortion: the Jacobian determinant. Given a transformation, simply put, the Jacobian determinant measures how much the area of a very small rectangle changes as it is transformed. It is given by:

$$J_T(\phi, \lambda) = \begin{vmatrix} \dfrac{\partial x}{\partial \lambda} & \dfrac{\partial x}{\partial \phi} \\ \dfrac{\partial y}{\partial \lambda} & \dfrac{\partial y}{\partial \phi} \end{vmatrix}. \tag{2.8.0.1}$$

This Jacobian, however, measures the area inflation or deflation from the (cylindrical) Equirectangular transformation $T_1(\phi, \lambda) = (R\lambda, R\phi)$ to our transformation $T(\phi, \lambda) = (x, y)$, rather than from the sphere. As such, we must incorporate the area distortion from the sphere to the Equirectangular projection, which follows from Section (2.7) to be the multiplication of the scaling factors $hk = \dfrac{1}{R^2\cos(\phi)}$. Hence, the area distortion s is given by

$$s = \frac{1}{R^2\cos(\phi)} \begin{vmatrix} \dfrac{\partial x}{\partial \lambda} & \dfrac{\partial x}{\partial \phi} \\ \dfrac{\partial y}{\partial \lambda} & \dfrac{\partial y}{\partial \phi} \end{vmatrix} = \frac{1}{R^2\cos(\phi)} \left(\frac{\partial x}{\partial \lambda}\frac{\partial y}{\partial \phi} - \frac{\partial y}{\partial \lambda}\frac{\partial x}{\partial \phi} \right). \tag{2.8.0.2}$$

Example
If we apply this to the Cylindrical equal-area projection, we get:

$$\begin{aligned} s =& \frac{1}{R^2\cos(\phi)} \left(\frac{\partial x}{\partial \lambda}\frac{\partial y}{\partial \phi} - \frac{\partial y}{\partial \lambda}\frac{\partial x}{\partial \phi} \right) && (2.8.0.3)\\ =& \frac{1}{R^2\cos(\phi)} R\cos(\phi)R && (2.8.0.4)\\ =& 1 && (2.8.0.5) \end{aligned}$$

Thus, as expected, the area is not distorted. On the other hand, if we examine the area distortion of the Mercator projection, we get:

$$\begin{aligned} s =& \frac{1}{R^2\cos(\phi)} \left(\frac{\partial x}{\partial \lambda}\frac{\partial y}{\partial \phi} - \frac{\partial y}{\partial \lambda}\frac{\partial x}{\partial \phi} \right) && (2.8.0.6)\\ =& \frac{1}{R^2\cos(\phi)} R \frac{1}{\cos(\phi)} R && (2.8.0.7)\\ =& \frac{1}{\cos^2(\phi)}. && (2.8.0.8) \end{aligned}$$

As ϕ approaches $\pm\dfrac{\pi}{2}$, which represent the poles, the area distortion s goes to infinity. This means that the area gets infinitely inflated as one approaches the poles, whereas at the Equator ($\phi = 0$), we have that s equals 1 and hence the area is preserved.

2.9 Tissot's indicatrix

Before we continue with the angular distortion, we will first examine Tissot's indicatrix [12, 9]. To visualise both the angular and area distortion, the French mathematician Nicolas Auguste Tissot presented the Tissot's indicatrix in 1859 and 1881 [12]. Tissot proved that projecting a circle of infinitesimal radius from the globe onto a map results in an ellipse of infinitesimal size whose major and minor semi-axes show the maximum and minimum scale factors at that point, which are directly related to the angular distortion. Naturally, if the map is conformal (at least at that point), the resulting ellipse is a perfect circle. Otherwise, it being an ellipse indicates that some angular distortion has occurred. Similarly, as the area of all indicatrices are equal, having indicatrices with varying size on the map makes the area distortion evident. As a single indicatrix displays the distortion of only one point, it is common practice to place them all over the map, typically at the intersections of parallels and meridians.

2.9.1 Angular distortion

With the Tissot's Indicatrix in mind, we will first examine a simple case in determining the angular distortion [8]. Consider Figure 16. We will assume to have a projection where the maximum and minimum scale factors (and thus the major and minor semi axes of the ellipse) are in the direction of the x and y axes, as is the case with cylindrical projections. As can be seen in the figure, the angles made with the diagonal are α and β respectively. If the sides of the rectangle on the sphere have the infinitesimal lengths $d\lambda$ and $d\phi$ respectively, then using the scale factors as defined earlier, the sides of the rectangle on the projection

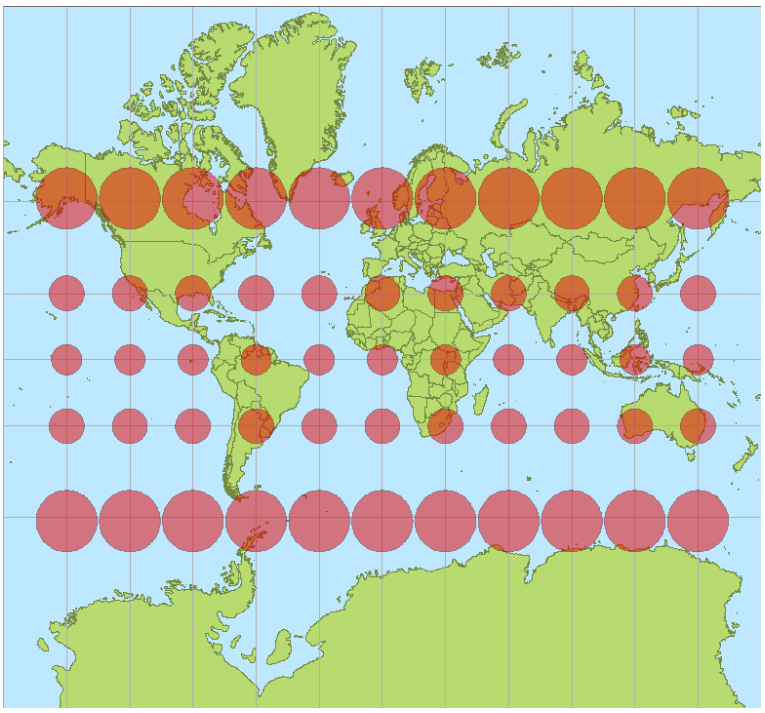

Figure 15: Tissot's Indicatrix on the Mercator projection [7]. As the Mercator projection is conformal, there is no angular distortion and hence all indicatrices are circles. As indicated by the different sizes of the indicatrices, the area distortion increases sharply as one approaches the poles.

have lengths $kd\lambda$ and $hd\phi$ respectively. Using the geometry of right-angled triangles, we get

$$\tan(\alpha) = \frac{d\phi}{d\lambda}, \tag{2.9.1.1}$$

$$\tan(\beta) = \frac{h}{k}\frac{d\phi}{d\lambda}. \tag{2.9.1.2}$$

Hence, α and β are related by the following equation:

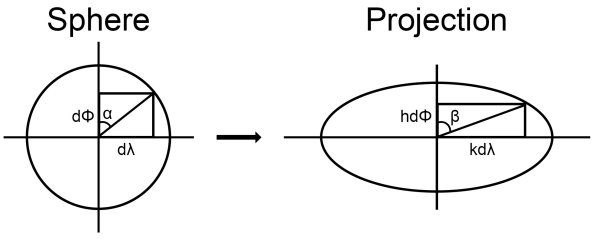

Figure 16: The projection of a circle of infinitesimal radius on the sphere to an ellipse in the plane. The circle on the sphere has a rectangle divided into two right-angled triangles drawn inside of it. They have sides $d\lambda$ and $d\phi$ and α is the angle made with the ϕ axis. Similarly, the projected ellipse has sides $kd\lambda$ and $hd\phi$ and angle β.

$$\tan(\beta) = \frac{h}{k}\tan(\alpha). \tag{2.9.1.3}$$

We now assume β to be dependent on the original angle α, differentiate the change in the angle angle $\beta - \alpha$ with respect to α and equate it to 0 to obtain an extreme.

$$\begin{gathered}\frac{d(\beta-\alpha)}{d\alpha} = 0 \\ \Longleftrightarrow \\ \frac{d\beta}{d\alpha} = 1.\end{gathered} \tag{2.9.1.4}$$

Now differentiating equation (2.9.1.3) and substituting equation (2.9.1.4) into it, we get

$$\frac{1}{\cos^2(\beta)} = \frac{h}{k}\frac{1}{\cos^2(\alpha)} \tag{2.9.1.5}$$

$$\iff \tag{2.9.1.6}$$

$$1 + \tan^2(\beta) = \frac{h}{k}(1 + \tan^2(\alpha)). \tag{2.9.1.7}$$

Using $\tan(\beta)$ from equation (2.9.1.3), solving for $\tan(\alpha)$ gives

$$\tan(\alpha) = \sqrt{\frac{k}{h}}. \tag{2.9.1.8}$$

Consequently, $\tan(\beta)$ can then be deduced from equation (2.9.1.3):

$$\tan(\beta) = \sqrt{\frac{h}{k}}. \tag{2.9.1.9}$$

We will calculate the change in the angle $\beta - \alpha$ using the trigonometric identity

$$\sin(\beta - \alpha) = \sin(\beta)\cos(\alpha) - \sin(\alpha)\cos(\beta). \tag{2.9.1.10}$$

From equations (2.9.1.8) and (2.9.1.9), we have by the geometry of right-angled triangles:

$$\sin(\beta) = \sqrt{\frac{h}{k+h}} = \cos(\alpha), \tag{2.9.1.11}$$

$$\sin(\alpha) = \sqrt{\frac{k}{k+h}} = \cos(\beta). \tag{2.9.1.12}$$

Hence, equation (2.9.1.10) gives us

$$\sin(\beta - \alpha) = \frac{h}{k+h} - \frac{k}{k+h} = \frac{h-k}{k+h}, \tag{2.9.1.13}$$

$$\sin(\alpha - \beta) = \frac{k}{k+h} - \frac{h}{k+h} = \frac{k-h}{k+h}. \tag{2.9.1.14}$$

Because in distortion analysis the orientation is of less importance than the size of the angular distortion, we define the maximum angular deformation ω to be double the absolute value of change in the angle $|\beta - \alpha|$:

$$\omega = 2|\beta - \alpha|. \tag{2.9.1.15}$$

Hence, the maximum angular deformation ω can be calculated from:

$$\sin\left(\frac{\omega}{2}\right) = \frac{|k-h|}{k+h}, \quad 0 \leq \omega \leq \pi, \tag{2.9.1.16}$$

if and only if the parallels and meridians intersect at right angles. In general, however, this may not be so, in which case we examine the ellipse that is the Tissot's Indicatrix: if we know the major and minor semi-axes a and b, respectively, which are also the maximum and minimum scale factors in that point, the maximum angular deformation ω is given by [9]:

$$\sin\left(\frac{\omega}{2}\right) = \frac{|a-b|}{a+b}. \tag{2.9.1.17}$$

The next section will use this equation to describe angular deformation for projections that do not have their parallels and meridians intersect at right angles.

2.9.2 The general case for measuring distortion

The general case, where we only require the map projections to be differentiable and continuous, gets a bit more complicated and is derived with the Tissot's Indicatrix in mind.

As the x and y coordinates are functions of both ϕ and λ, the scale factors k and h along the parallels and meridians, respectively, are calculated as [12]:

$$h = \frac{1}{R}\sqrt{\left(\frac{\partial x}{\partial \phi}\right)^2 + \left(\frac{\partial y}{\partial \phi}\right)^2}, \tag{2.9.2.1}$$

$$k = \frac{1}{R\cos(\phi)}\sqrt{\left(\frac{\partial x}{\partial \lambda}\right)^2 + \left(\frac{\partial y}{\partial \lambda}\right)^2}. \tag{2.9.2.2}$$

If we define a and b to be the maximum and minimum scale factors in a point, respectively, (or the factor with which the major and minor semi-axes of the Tissot's Indicatrix are scaled), the First Theorem of Apollonius [9] states that

$$h^2 + k^2 = a^2 + b^2. \tag{2.9.2.3}$$

Furthermore, if we define ϑ to be the angle between a given parallel and meridian on the map, the Second Theorem of Apollonius [9] gives:

$$ab = hk\sin(\vartheta). \tag{2.9.2.4}$$

Combining these theorems and defining the following two terms for notational simplicity,

$$a' = \sqrt{k^2 + h^2 + 2hk\sin(\vartheta)}, \tag{2.9.2.5}$$

$$b' = \sqrt{k^2 + h^2 - 2hk\sin(\vartheta)}, \tag{2.9.2.6}$$

basic algebra reveals that the values for a and b are given by

$$a = \frac{a' + b'}{2}, \tag{2.9.2.7}$$

$$b = \frac{a' - b'}{2}. \tag{2.9.2.8}$$

The maximum angular deformation ω derived in Section (2.9.1) is then calculated using

$$\sin\left(\frac{\omega}{2}\right) = \frac{|a-b|}{a+b} = \frac{b'}{a'} \text{ for } a' \neq 0. \tag{2.9.2.9}$$

The area scale factor s derived in section (2.8) is repeated here for convenience:

$$s = \frac{1}{R^2\cos(\phi)}\left(\frac{\partial x}{\partial \lambda}\frac{\partial y}{\partial \phi} - \frac{\partial y}{\partial \lambda}\frac{\partial x}{\partial \phi}\right).$$

The Tissot's Indicatrix also provides us with a different way of calculating the distortion in area. By the geometry of ellipses [9] we have

$$s = ab. \tag{2.9.2.10}$$

Furthermore, substituting equation (2.9.2.4) gives

$$s = hk\sin(\vartheta). \tag{2.9.2.11}$$

If $\vartheta = \dfrac{\pi}{2}$, this simplifies to $s = hk$.

Checking for conformality can be done quite easily by using the Cauchy-Riemann equations [12], which are given by

$$\frac{\partial y}{\partial \phi} = \frac{1}{\cos(\phi)}\frac{\partial x}{\partial \lambda}, \tag{2.9.2.12}$$

$$\frac{\partial x}{\partial \phi} = -\frac{1}{\cos(\phi)}\frac{\partial y}{\partial \lambda}. \tag{2.9.2.13}$$

If and only if a map projection satisfies these equations, it is conformal. Conformality can also be checked using the same logic used in Section (2.7.1), but using a and b instead of k and h. A map is conformal if and only if for the maximum and minimum scale factor a and b, respectively, in a point [9], we have that

$$a = b. \tag{2.9.2.14}$$

We can also derive a sufficient and necessary condition for map projections being equal-area [12], namely:

$$\left(\frac{\partial x}{\partial \lambda}\frac{\partial y}{\partial \phi} - \frac{\partial y}{\partial \lambda}\frac{\partial x}{\partial \phi}\right) = R^2\cos(\phi). \tag{2.9.2.15}$$

This results can also be given in terms of a and b. A map is equal-area if and only if for the maximum and minimum scale factor a and b, respectively, in a point, we have that a and b are nonzero and are reciprocals of one another [9], that is,

$$ab = 1. \tag{2.9.2.16}$$

Example
The sinusoidal projection is given by

$$x(\phi, \lambda) = R\lambda\cos(\phi), \tag{2.9.2.17}$$
$$y(\phi, \lambda) = R\phi, \tag{2.9.2.18}$$

where the range of the transformation is $\{(x, y)|\ x \in (-\pi R, \pi R),\ y \in (-\pi R/2, \pi R/2)\}$. The scale factors are then given by

$$h = \sqrt{\lambda^2\sin(\phi)^2 + 1}, \tag{2.9.2.19}$$
$$k = 1. \tag{2.9.2.20}$$
$$\tag{2.9.2.21}$$

The area inflation s can be calculated from equation (2.8.0.2):

$$s = \frac{1}{\cos(\phi)}\cos(\phi) = 1. \tag{2.9.2.22}$$

Hence, the projection is equal-area. As $s = hk\sin(\vartheta) = 1$, the values for a' and b' are given by

$$a' = \sqrt{h^2 + k^2 + 2s} = \sqrt{\lambda^2\sin(\phi)^2 + 4}, \tag{2.9.2.23}$$
$$b' = \sqrt{h^2 + k^2 - 2s} = \sqrt{\lambda^2\sin(\phi)^2}. \tag{2.9.2.24}$$

The maximum angular deformation ω is then calculated from equation (2.9.2.9):

$$\sin\left(\frac{\omega}{2}\right) = \frac{\sqrt{\lambda^2\sin(\phi)^2}}{\sqrt{\lambda^2\sin(\phi)^2 + 4}}, \tag{2.9.2.25}$$

or

$$\omega = 2\arctan\left|\frac{1}{2}\lambda\sin(\phi)\right|. \tag{2.9.2.26}$$

2.9.3 First fundamental form and singular value decomposition

A different, more elegant way of describing the Tissot's Indicatrix is using differential geometry and singular value decomposition [11]. We will first determine the first fundamental form of the sphere, which completely describes its metric properties. Later, we will use this to define the transformation that represents the Tissot's Indicatrix. The length element ds, informally thought of as the element of distance, may be expressed as [5]:

$$ds^2 = Ed\phi^2 + 2Fd\phi d\lambda + Gd\lambda^2, \tag{2.9.3.1}$$

where E, F and G are given by

$$E = X_\phi \cdot X_\phi, \tag{2.9.3.2}$$
$$F = X_\phi \cdot X_\lambda, \tag{2.9.3.3}$$
$$G = X_\lambda \cdot X_\lambda. \tag{2.9.3.4}$$

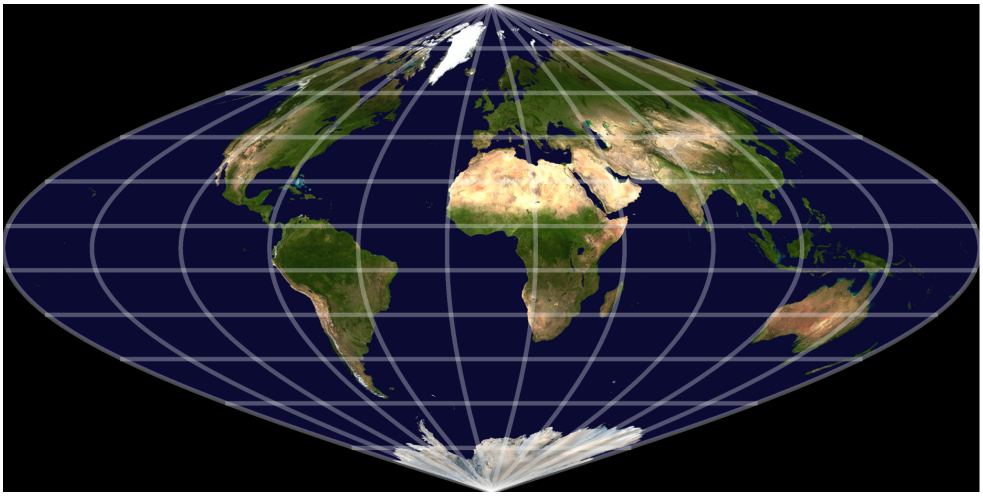

Figure 17: Sinusoidal projection. The equations are given by equations (2.9.2.17) and (2.9.2.18). It is equal-area, but it does feature a lot of angular distortion, which increases as one moves away from the Central Meridian and Equator. The poles are represented as points.

Here $X(\phi, \lambda)$ is a parameterisation of the sphere in $\mathbb{R}^3$, $\cdot$ represents the dot product and X_ϕ is the partial derivative of X with respect to ϕ etc. We will use the standard parameterisation

$$X(\phi, \lambda) = \begin{bmatrix} R\cos(\phi)\cos(\lambda) \\ R\cos(\phi)\sin(\lambda) \\ R\sin(\phi) \end{bmatrix}, \ (\phi, \lambda) \in [-\pi/2, \pi/2] \times [-\pi, \pi). \tag{2.9.3.5}$$

Hence, the partial derivatives of X with respect to ϕ and λ are

$$X_\phi = \begin{bmatrix} -R\sin(\phi)\cos(\lambda) \\ -R\sin(\phi)\sin(\lambda) \\ R\cos(\phi) \end{bmatrix}, \quad X_\lambda = \begin{bmatrix} -R\cos(\phi)\sin(\lambda) \\ R\cos(\phi)\cos(\lambda) \\ 0 \end{bmatrix}. \tag{2.9.3.6}$$

The functions E, F and G are then computed to be

$$E = R^2\sin(\phi)^2\cos(\lambda)^2 + R^2\sin(\phi)^2\sin(\lambda)^2 + R^2\cos(\phi)^2 = R^2 \tag{2.9.3.7}$$

$$F = R^2\sin(\phi)\cos(\phi)\sin(\lambda)\cos(\lambda) - R^2\sin(\phi)\sin(\lambda)\cos(\phi)\cos(\lambda) = 0 \tag{2.9.3.8}$$

$$G = R^2\cos(\phi)^2\sin(\lambda)^2 + R^2\cos(\phi)^2\cos(\lambda)^2 = R^2\cos(\phi)^2. \tag{2.9.3.9}$$

Thus, the first fundamental form in a spherical model is given by [5]:

$$ds^2 = R^2 d\phi^2 + R^2\cos(\phi)^2 d\lambda^2. \tag{2.9.3.10}$$

Now, we combine this with the Tissot's Indicatrix. Since a Tissot's Indicatrix relates distances on the map to those on the sphere, specifically those along the parallels and meridians, we seek for a transformation matrix $\mathcal{T}$ that satisfies the equation

$$\begin{bmatrix} dx \\ dy \end{bmatrix} = \mathcal{T} \begin{bmatrix} ds(0, \lambda) \\ ds(\phi, 0) \end{bmatrix}, \tag{2.9.3.11}$$

where $ds(0, \lambda)$ and $ds(\phi, 0)$ is the computation of ds along the parallels and meridians respectively. From equation (2.9.3.10), $ds(0, \lambda)$ and $ds(\phi, 0)$ are related to ϕ and λ by

$$\begin{bmatrix} d\lambda \\ d\phi \end{bmatrix} = K \begin{bmatrix} ds(0, \lambda) \\ ds(\phi, 0) \end{bmatrix}, \ K = \begin{bmatrix} \frac{1}{R\cos(\phi)} & 0 \\ 0 & \frac{1}{R} \end{bmatrix}. \tag{2.9.3.12}$$

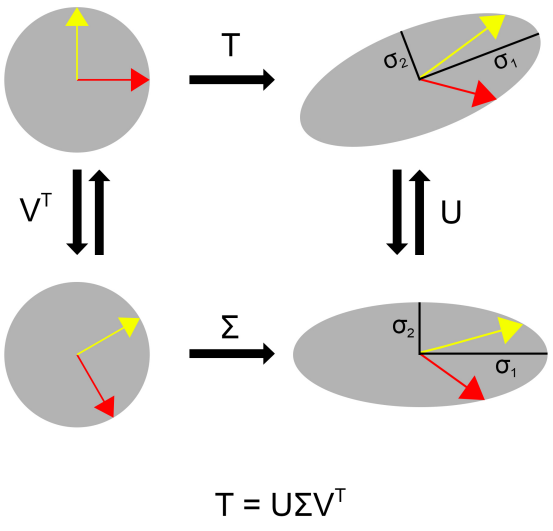

Figure 18: Singular value decomposition visualised starting with a circle. The linear transformation $\mathcal{T}$ in a point (ϕ, λ) can be decomposed into a rotation on the sphere V^T, followed by a coordinate scaling Σ and concluding with another rotation U. The red and yellow arrows give geometric insight into the transformation. The singular values σ_1 and σ_2 represent the maximum and minimum scale factors at the point.

Furthermore, distances on the sphere are related to the distances on the plane by the Jacobian matrix J:

$$\begin{bmatrix} dx \\ dy \end{bmatrix} = J \begin{bmatrix} d\lambda \\ d\phi \end{bmatrix}, \; J = \begin{bmatrix} \frac{\partial x}{\partial \lambda} & \frac{\partial x}{\partial \phi} \\ \frac{\partial y}{\partial \lambda} & \frac{\partial y}{\partial \phi} \end{bmatrix}. \tag{2.9.3.13}$$

We substitute equation (2.9.3.12) into equation (2.9.3.13) to obtain

$$\begin{bmatrix} dx \\ dy \end{bmatrix} = JK \begin{bmatrix} ds(0, \lambda) \\ ds(\phi, 0) \end{bmatrix}. \tag{2.9.3.14}$$

Hence, we find

$$\mathcal{T} = JK = \begin{bmatrix} \frac{\partial x}{\partial \lambda} \cdot \frac{1}{R\cos(\phi)} & \frac{\partial x}{\partial \phi} \cdot \frac{1}{R} \\ \frac{\partial y}{\partial \lambda} \cdot \frac{1}{R\cos(\phi)} & \frac{\partial y}{\partial \phi} \cdot \frac{1}{R} \end{bmatrix}. \tag{2.9.3.15}$$

Applying singular value decomposition on $\mathcal{T}$ will allow us to extract important components of the local transformation. As $\mathcal{T}$ is a real matrix, we have

$$\mathcal{T} = U\Sigma V^T. \tag{2.9.3.16}$$

As shown in Figure 18, $\mathcal{T}$ is decomposed into a rotation on the sphere V^T, followed by a coordinate scaling Σ and concluding with another rotation (but now in the (x, y)-plane) U. In Figure 18, we see that Σ scales the circle along the two axes, causing it to take the form of an ellipse. Hence, we find that the singular values σ_1 and σ_2 are the maximal and minimal scale factors in a point, previously denoted by a and b, respectively. As σ_1 and σ_2 are the semi-major and semi-minor axes of the ellipse, we can compute the area distortion s using equation (2.9.2.10) as

$$s = \sigma_1 \sigma_2. \tag{2.9.3.17}$$

The maximum angular deformation ω can be found from substituting σ_1 and σ_2 for a and b, respectively, into the familiar equation (2.9.2.9):

$$\sin\left(\frac{\omega}{2}\right) = \frac{|\sigma_1 - \sigma_2|}{\sigma_1 + \sigma_2}, \quad 0 \leq \omega \leq \pi. \tag{2.9.3.18}$$

As some projections feature scale factors that contain partial derivatives that are rather tedious to calculate, one can also numerically approximate these derivatives using central differences [14], which we will do for, for example, the Van der Grinten projection (see Section (3.4.5).

3 Analysis of map projections

In this chapter we present a list of map projections and their respective distortions. It covers the scale factors, the angular and area distortion of these projections and includes figures of the map projections. As this chapter is structured as a list, one need not read it in order. It is subdivided in cylindrical, conic, azimuthal and miscellaneous projections.

Besides figures of the map projections itself, this chapter also includes heatmaps that overlay the map projections with the purpose of visualising the distortions. For the angular distortion, the amount of distortion (which ranges from 0 to π) in a given point will be expressed by a certain colour, which is indicated by the legend. The colour scheme starts with grey shades, depicts medium values with red and ends with a yellow/white hue. In a separate figure, the area distortion is also visualised using a heatmap, employing a colour scheme that ranges from white to purple. Given that it is a factor, the area distortion may tend to infinity in some points, and hence for some projections the legend is capped at a certain value in order to produce a coherent heatmap, which is stated in the figure captions.

3.1 Cylindrical projections

Cylindrical projections feature the projection surface wrapped around the Earth in the shape of a cylinder, after which the Earth's features are transferred to the surface. As such, the meridians are presented as straight vertical equidistant lines which intersect the straight horizontal (but often not equidistant) parallels at a right angle. As is the case for the transverse Mercator projection, the surface can also be wrapped around the Earth to form a cylinder lying on its side, which results in the meridians and parallels often not being straight lines. The following projections are treated:

- Central cylindrical projection
- Mercator projection
- Transverse Mercator projection
- Cylindrical equal-area projection.

3.1.1 Central cylindrical projection

The Central Cylindrical projection is one of few projections that has a direct geometric interpretation (see Section (2.4)). It is constructed by wrapping the projection surface around the Earth like a cylinder and placing a light bulb at the center of the Earth. The point where a ray of light intersects the Earth is to be projected on the cylinder where that same ray intersects it. It is neither conformal nor equal-area and is mainly used as a simple example of map projections. The meridians are equidistant vertical straight lines which intersect the horizontal straight parallels at a right angle. The parallels are spaced increasingly further apart as they move away from the Equator. Both the angular and area distortion increase rapidly towards the poles. The formulas are given by:

$$x(\phi, \lambda) = R\lambda \tag{3.1.1.1}$$

$$y(\phi, \lambda) = R\tan(\phi). \tag{3.1.1.2}$$

The range of the transformation is $\{(x, y)|\ x \in (-\pi R, \pi R),\ y \in \mathbb{R}\}$. As the y-coordinate goes to infinity as one approaches the poles at $\pm\frac{\pi}{2}$, the map cannot fully show the poles and any finite/bounded map must have the domain truncated at some latitude ϕ. The inverse formulas of the Central cylindrical projection are:

$$\lambda(x, y) = \frac{x}{R} \tag{3.1.1.3}$$

$$\phi(x, y) = R\arctan(y). \tag{3.1.1.4}$$

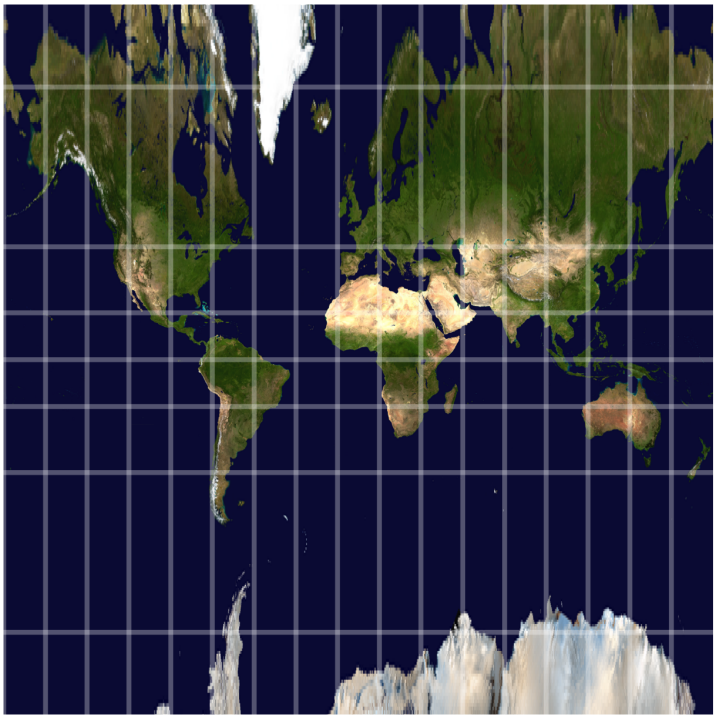

Figure 19: Central cylindrical projection. The equations are given by (3.1.1.1) and (3.1.1.2). The map is somewhat accurate near the Equator, but as one moves towards the poles the distortion increases rapidly. As the y-coordinate goes to infinity as one approaches the poles at $\pm\frac{\pi}{2}$, the map cannot fully show the poles. Furthermore, the parallels and meridians intersect at right angles.

The scale factors and distortions are given by

$$k = \frac{1}{\cos(\phi)}, \tag{3.1.1.5}$$

$$h = \frac{1}{\cos^2(\phi)}, \tag{3.1.1.6}$$

$$\omega = 2\arcsin\left(\frac{\left|\frac{1}{\cos(\phi)} - \frac{1}{\cos^2(\phi)}\right|}{\frac{1}{\cos(\phi)} + \frac{1}{\cos^2(\phi)}}\right) \tag{3.1.1.7}$$

$$s = \frac{1}{\cos^3(\phi)}. \tag{3.1.1.8}$$

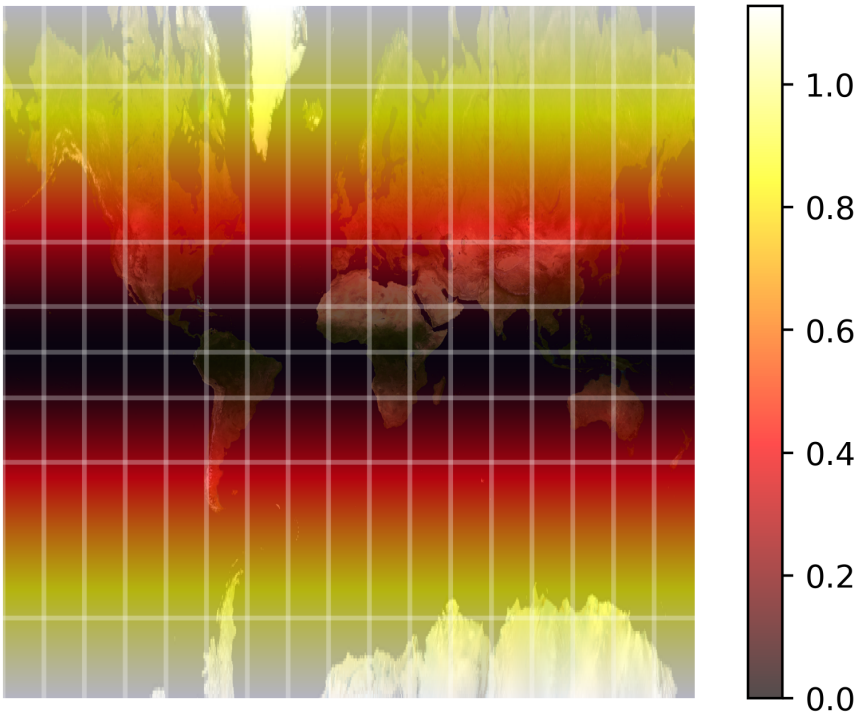

Figure 20: A heat map overlaid on the Central cylindrical projection, showing where the distortion in angle is the biggest. As ϕ approaches the poles at $\pm\frac{\pi}{2}$, the angular distortion ω goes to π. As the map has been truncated, this figure only displays the points with angular distortion up to a bit over 1.0, as indicated in the legend.

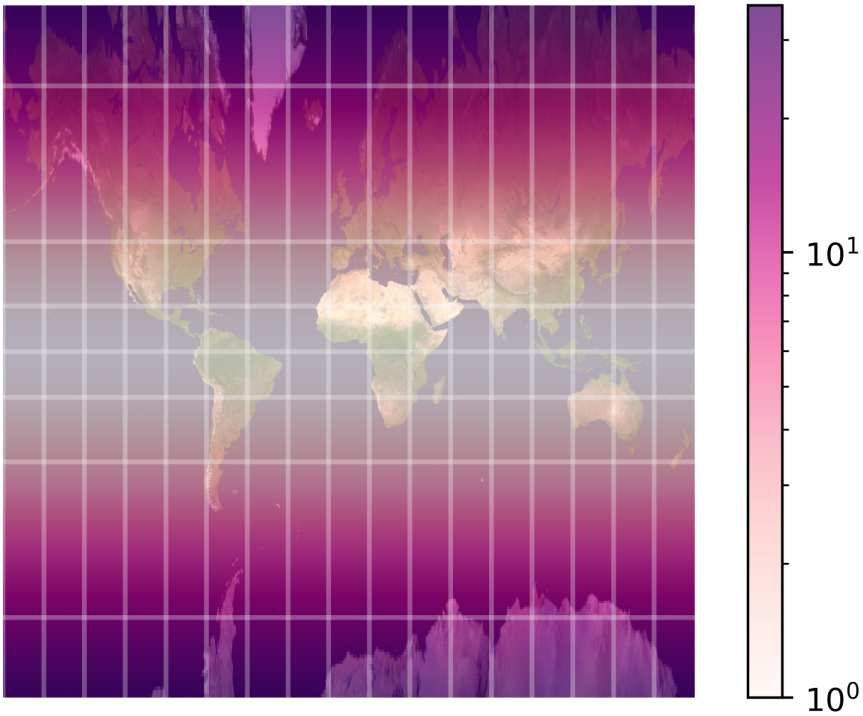

Figure 21: A heat map overlaid on the central cylindrical projection, showing where the distortion in area is the biggest. From equation (3.1.1.8), we see that the area distortion tends to infinity as one approaches the poles.

3.1.2 Mercator projection

The Mercator projection is likely the most well-known map projection [12]. Similar to the Central cylindrical projection, the meridians are drawn as equidistant vertical straight lines. They cross the increasingly further spaced horizontal straight parallels at a right angle. In contrast to the the Central cylindrical projection, however, the Mercator projection is conformal. Hence, angles are locally preserved, which translates to recognisable continent shapes. This, however, comes at the cost of the area distortion, which increases rapidly as one moves away from the Equator. Another, more historically interesting feature is that the Mercator projection maps rhumb lines, arcs which intersect all meridians at a constant angle, to straight lines. Hence, in marine navigation, one can measure the angle to the destination on the Mercator projection and consequently follow said angle on a compass to arrive at the mentioned destination. This, however, is not the shortest path. The equations

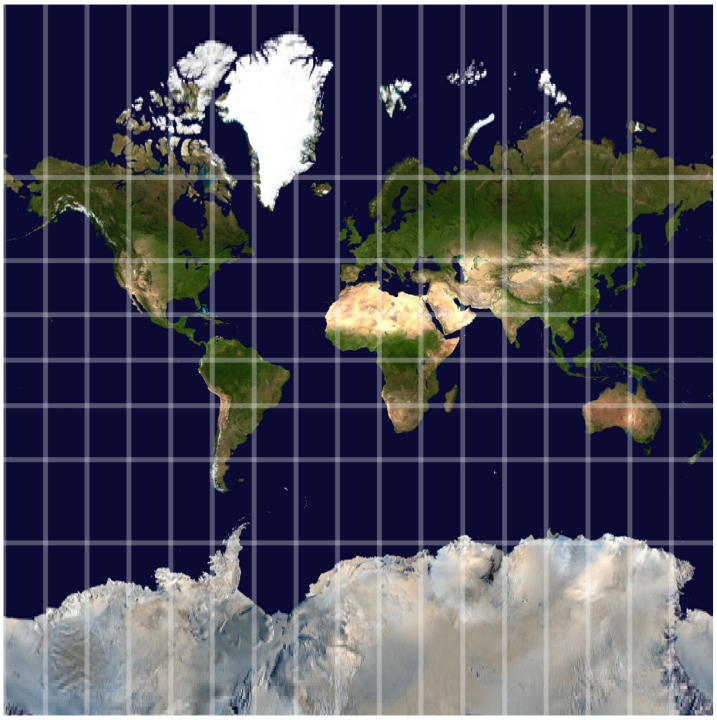

Figure 22: Mercator projection. The equations are given by (3.1.2.1) and (3.1.2.2). It is conformal and hence has roughly correct continent shapes, but the area distortion increases quickly as one approaches the poles. The meridians and parallels intersect at right angles.

for the Mercator projection are given by:

$$x(\phi, \lambda) = R\lambda, \tag{3.1.2.1}$$

$$y(\phi, \lambda) = R \ln\left(\tan(\phi) + \frac{1}{\cos(\phi)}\right). \tag{3.1.2.2}$$

The range of the transformation is $\{(x, y) |\ x \in (-\pi R, \pi R),\ y \in \mathbb{R}\}$. As is the case with the Central cylindrical projection, the Mercator projection is truncated at a certain latitude and hence cannot fully show the poles. The inverse formulas are given by:

$$\lambda(x, y) = \frac{x}{R}, \tag{3.1.2.3}$$

$$\phi(x, y) = 2 \arctan(e^{y/R}) - \frac{1}{2}\pi \tag{3.1.2.4}$$

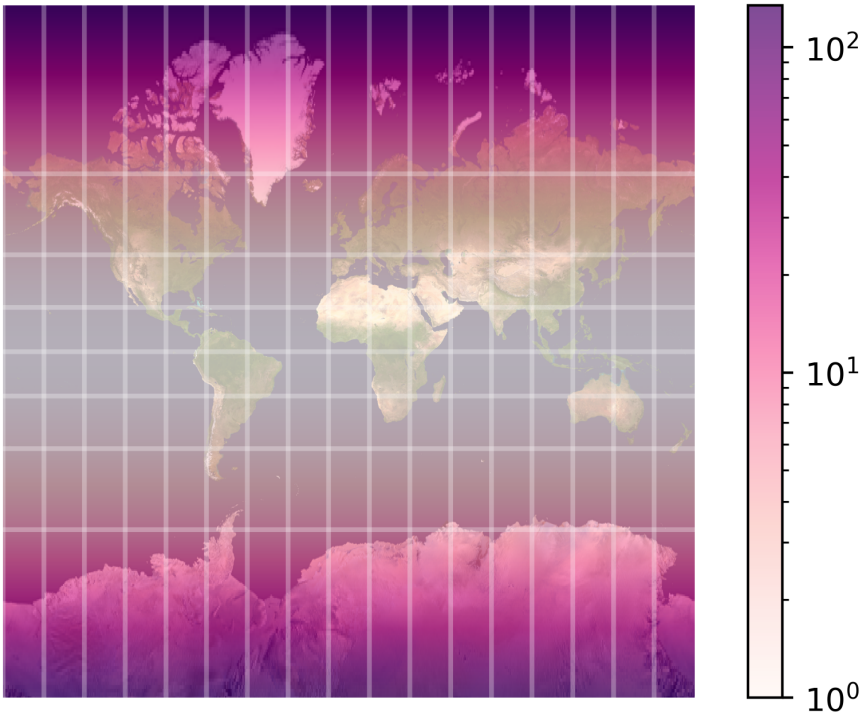

Figure 23: A heat map overlaid on the Mercator projection, showing where the distortion in area is the biggest. Conforming with s given by equation (3.1.2.7), the figure displays the area distortion going to infinity as one approaches the poles.

The scale factors and distortions are given by

$$k = h = \frac{1}{\cos(\phi)}, \tag{3.1.2.5}$$

$$\omega = 2\arcsin(0) = 0, \tag{3.1.2.6}$$

$$s = \frac{1}{\cos^2(\phi)} \tag{3.1.2.7}$$

3.1.3 Transverse Mercator projection

The transverse Mercator projections is an example of a transverse cylindrical projection, which means that the cylinder is wrapped around the Earth so that it makes a right angle with the Earth's axis. The meridians are complex curves, except for the Central Meridian, the meridian π radians from the Central Meridian and both meridians $\frac{\pi}{2}$ from the Central Meridian, which are drawn as straight lines. Similarly, the parallels are also complex curves, with the exception of the Equator, which, likewise, is a straight line. As is the case with the regular Mercator projection, this projection is conformal and thus roughly preserves the shapes of the continents. Along the central meridian, the scale is preserved. The equations are given by:

$$x(\phi, \lambda) = \frac{1}{2} R \ln\left(\frac{1 + \cos(\phi)\sin(\lambda)}{1 - \cos(\phi)\sin(\lambda)}\right), \tag{3.1.3.1}$$

$$y(\phi, \lambda) = R\,\mathrm{atan2}\left(\tan(\phi), \cos(\lambda)\right), \tag{3.1.3.2}$$

where we use the atan2 function defined in Section (2.6). Notice that when $\cos(\phi)\sin(\lambda)$ approaches ± 1, we have that x goes to $\pm\infty$. As λ approaches $\pm\frac{\pi}{2}$, $\cos(\lambda)$ goes to zero, causing y to become a straight line $y = \pm\frac{\pi}{2}$. The range of the transformation is $\{(x, y) |\ x \in$

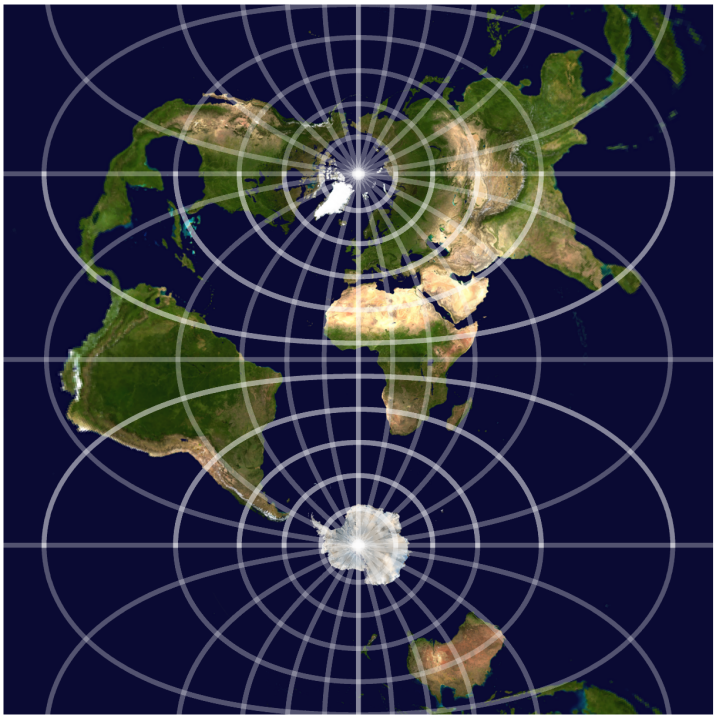

Figure 24: Transverse Mercator projection. The equations are given by (3.1.3.1) and (3.1.3.2). Just like the Mercator projection, it is conformal and hence has roughly correct continent shapes. The parallels are ellipes, except for the Equator, which is a straight line. The meridians are sinusoidal-like curves, except for the Central Meridian, the meridian π radians from the Central Meridian and both meridians $\frac{\pi}{2}$ radians from the Central Meridian.

$\mathbb{R},\ y \in (-R\pi, R\pi]\}$. The inverse equations are:

$$\lambda(x,y) = \operatorname{atan2}\left(\sinh(x/R), \cos(y/R)\right), \tag{3.1.3.3}$$

$$\phi(x,y) = \arcsin\left(\frac{\sin(y/R)}{\cosh(x/R)}\right). \tag{3.1.3.4}$$

The scale factors and distortions are given by

$$k = h = \frac{1}{\sqrt{1-\cos^2(\phi)\sin^2(\lambda)}}, \tag{3.1.3.5}$$

$$\omega = 2\arcsin(0) = 0, \tag{3.1.3.6}$$

$$s = \frac{1}{(1-\cos^2(\phi)\sin^2(\lambda))}. \tag{3.1.3.7}$$

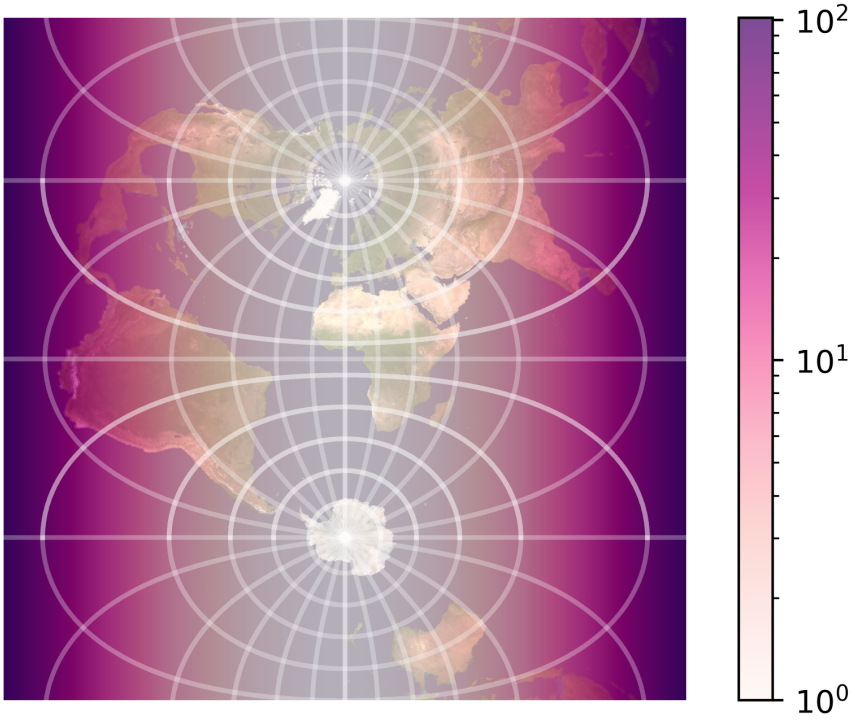

Figure 25: Transverse Mercator projection area heatmap. The area distortion is greatest towards the sides of the map, which is essentially the same as for the Mercator projection.

3.1.4 Cylindrical equal-area projection

The two most important features of the Cylindrical equal-area projection can be found in the name: it is a cylindrical projection and has no area distortion. Again, the meridians are equally-spaced straight lines. The parallels, on the other hand, are not equally-spaced, being furthest apart near the Equator, and cross the meridians at right angles. Being equal-area, however, the Cylindrical equal-area projection exhibits quite a bit of angular deformation, particularly near the poles. Its equations are given by:

$$x(\phi, \lambda) = R\lambda, \tag{3.1.4.1}$$
$$y(\phi, \lambda) = R\sin(\phi). \tag{3.1.4.2}$$

The range of the transformation is $\{(x, y)|\ x \in [-\pi R, \pi R),\ y \in [-R, R]\}$. For the inverse

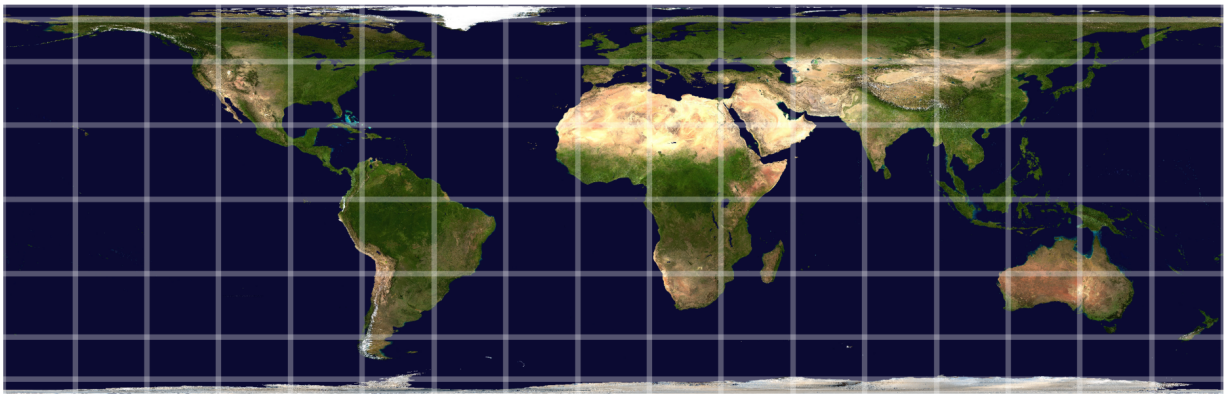

Figure 26: Cylindrical equal area projection. The equations are given by (3.1.4.1) and (3.1.4.2). As the name indicates, the areas of the continents are preserved by the projection. The angles (and thus shapes of the continents) however, are not, giving it a squished feeling. Furthermore, the parallels and meridians intersect at right angles.

equations we have:

$$\lambda(x, y) = \frac{x}{R}, \tag{3.1.4.3}$$

$$\phi(x, y) = \arcsin\left(\frac{y}{R}\right). \tag{3.1.4.4}$$

The scale factors and distortions are given by

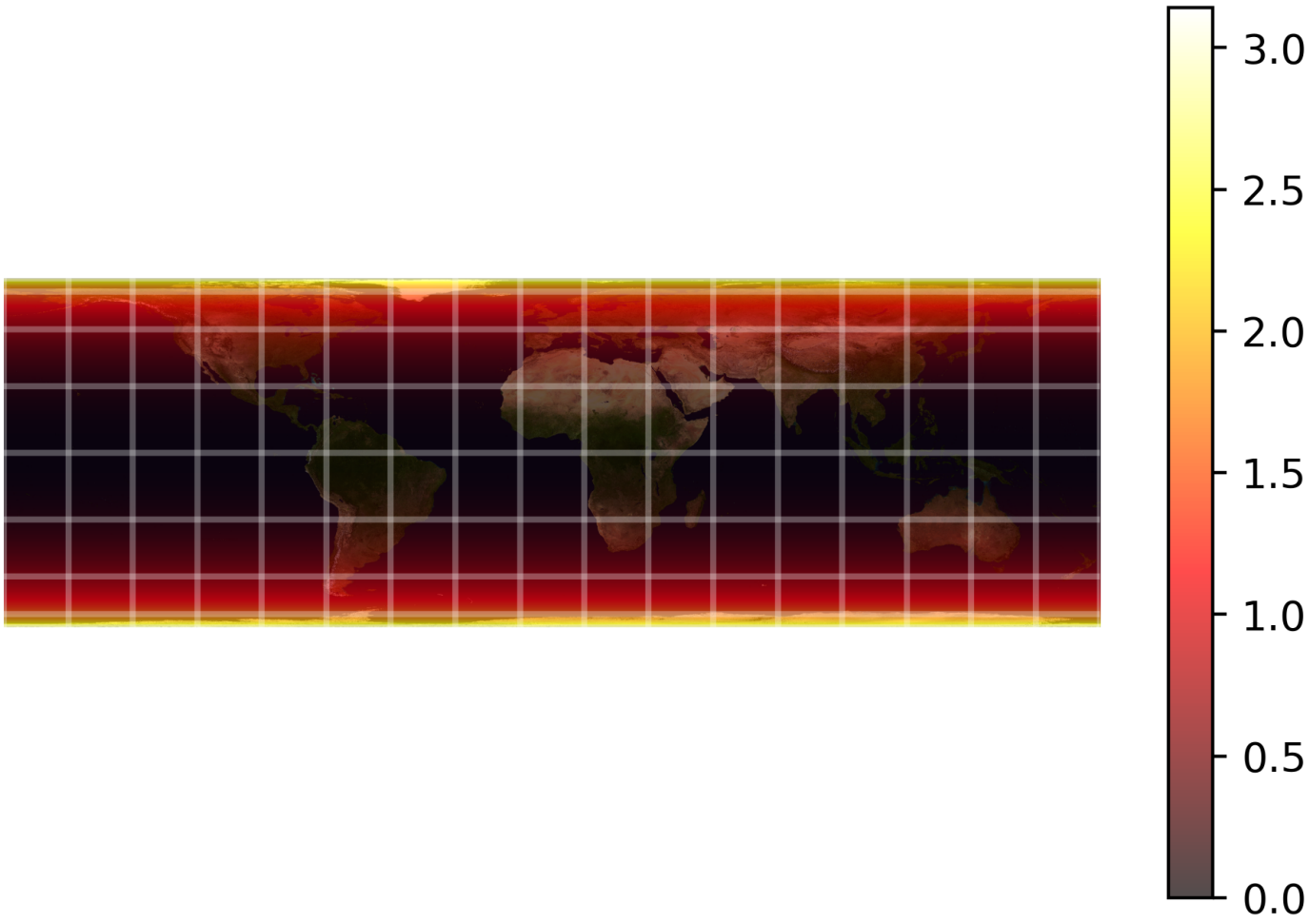

Figure 27: Cylindrical equal-area projection angle distortion heat map. While low at the Equator, the angular distortion is rather high at the poles, up to and including 3.0.

$$k = \frac{1}{\cos(\phi)}, \tag{3.1.4.5}$$

$$h = \cos(\phi), \tag{3.1.4.6}$$

$$\omega = 2\arcsin\left(\frac{\left|\frac{1}{\cos(\phi)} - \cos(\phi)\right|}{\frac{1}{\cos(\phi)} + \cos(\phi)}\right), \tag{3.1.4.7}$$

$$s = \frac{1}{\cos(\phi)}\cos(\phi) = 1. \tag{3.1.4.8}$$

3.2 Conic projections

As is the case with the cylindrical projections, the name for the group of conic projections emerged from the shape of the projection surface onto which the globe is projected. Geometrically, for the more elementary conic projections, this can be interpreted as placing a cone on top of the globe and lining the cone's tip up with the globe's axis. The sides of the cone touch the globe at a chosen standard latitude (or two, in which case it is a secant

conic projection), along which the scale is preserved. The cone is then cut along a meridian and laid flat, resulting in a map. As mentioned before, for the more complicated conic projections, this geometric interpretation does not hold. The following conic projections will be discussed:

- Albers equal-area Conic projection
- Lambert conformal conic projection
- Bonne projection

3.2.1 Albers equal-area conic projection

The Albers equal-area conic projection is a conic projection that incorporates the equal-area property. Although one standard parallel is possible, it nearly always includes two standard parallels, along which the scale is preserved and the shape is undistorted. As per usual, the meridians are equally spaced radii and the parallels are concentric arcs of circles; they are spaced farthest apart in the latitudes enclosed by the standard parallels and are closer together as one moves from the standard parallels towards the poles. Contrary to what one might expect, the pole is not the center of these circles, but is an arc itself as well. The meridians and parallels intersect at right angles. The equations are given by:

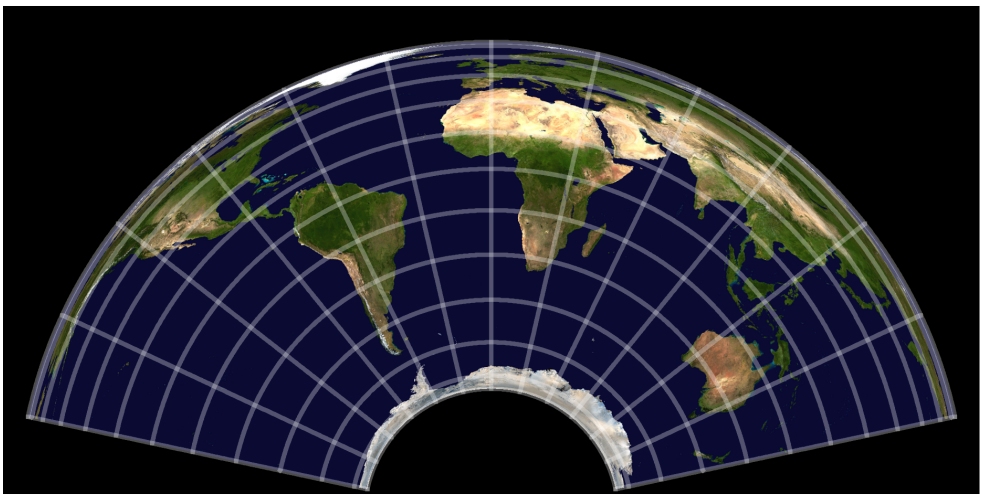

Figure 28: This projection is Albers equal-area conic Projection. The equations are given by (3.2.1.1) to (3.2.1.7). Even though it is not conformal, it is equal-area. The standard parallels are $\phi_1 = 0$ and $\phi_1 = -\pi/3$.

$$x(\phi, \lambda) = \rho \sin(\theta), \tag{3.2.1.1}$$

$$y(\phi, \lambda) = \rho_0 - \rho \cos(\theta), \tag{3.2.1.2}$$

$$n = \frac{1}{2}\Big(\sin(\phi_1) + \sin(\phi_2)\Big), \; n \neq 0, \tag{3.2.1.3}$$

$$\theta = n\lambda, \tag{3.2.1.4}$$

$$C = \cos^2(\phi_1) + 2n \sin(\phi_1), \tag{3.2.1.5}$$

$$\rho = R\frac{\sqrt{C - 2n \sin(\phi)}}{n}, \tag{3.2.1.6}$$

$$\rho_0 = R\frac{\sqrt{C}}{n}. \tag{3.2.1.7}$$

Here, the ϕ_1 and ϕ_2 are the standard parallels. If only one standard parallel is desired, $\phi_1 = \phi_2$ is chosen. The constants n, C and ρ_0 need only be calculated once. It is important to note that the standard parallels may not be chosen equidistant from the Equator, as this results in n being equal to 0. Furthermore, if only one standard parallel located at the one of

the poles is chosen, $n = 1$ and the projection simplifies to the Lambert azimuthal equal-area projection. If $0 < n < \frac{1}{2}$ or $\frac{1}{2} < n < 1$, the range of the transformation is

$$\left\{(x,y)\middle|\ \frac{C-2n}{n^2} \le x^2 + (\rho_0 - y)^2 \le \frac{C+2n}{n^2}\right\} \tag{3.2.1.8}$$

$$\cap \left\{(x,y)|\ y \le \rho_0 - \frac{x}{\tan(n\pi)}, y \le \rho_0 + \frac{x}{\tan(n\pi)}\right\}. \tag{3.2.1.9}$$

If $n = \frac{1}{2}$, this simplifies to

$$\left\{(x,y)\middle|\ \frac{C-2n}{n^2} \le x^2 + (\rho_0 - y)^2 \le \frac{C+2n}{n^2}\right\} \tag{3.2.1.10}$$

$$\cap \{(x,y)|\ y \le \rho_0\}. \tag{3.2.1.11}$$

If $-1 < n < -\frac{1}{2}$ or $-\frac{1}{2} < n < 0$, the range is

$$\left\{(x,y)\middle|\ \frac{C+2n}{n^2} \le x^2 + (\rho_0 - y)^2 \le \frac{C-2n}{n^2}\right\} \tag{3.2.1.12}$$

$$\cap \left(\left\{(x,y)|\ y \ge \rho_0 - \frac{x}{\tan(n\pi)}\right\} \cup \left\{(x,y)|\ y \ge \rho_0 + \frac{x}{\tan(n\pi)}\right\}\right). \tag{3.2.1.13}$$

If $n = -\frac{1}{2}$, this simplifies to

$$\left\{(x,y)\middle|\ \frac{C+2n}{n^2} \le x^2 + (\rho_0 - y)^2 \le \frac{C-2n}{n^2}\right\} \tag{3.2.1.14}$$

$$\cap \{(x,y)|\ y \ge \rho_0\} \tag{3.2.1.15}$$

The inverse equations are:

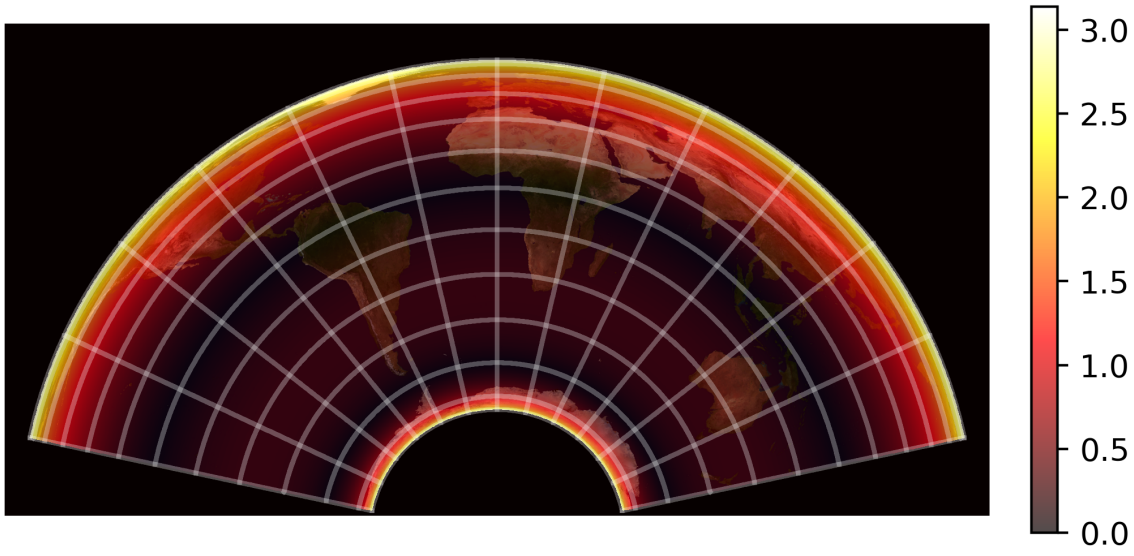

Figure 29: Albers equal-area conic projection angular distortion heatmap. The standard parallels are $\phi_1 = 0$ and $\phi_2 = -\pi/3$. The angular distortion is highest at the poles.

$$\lambda(x,y) = \frac{\theta}{n} \tag{3.2.1.16}$$

$$\phi(x,y) = \arcsin\left(\frac{C - \rho^2 n^2}{2n}\right) \tag{3.2.1.17}$$

$$\rho = \sqrt{x^2 + (\rho_0 - y)^2} \tag{3.2.1.18}$$

$$\theta = \arctan\left(\frac{x}{\rho_0 - y}\right). \tag{3.2.1.19}$$

The scale factors and distortions are given by

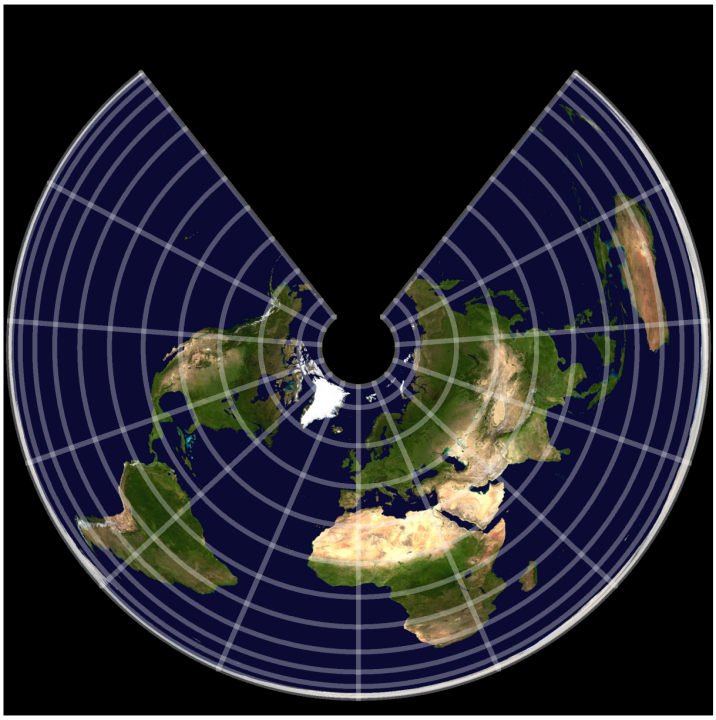

Figure 30: Albers equal-area conic projection. The equations are given by (3.2.1.1) to (3.2.1.7). Even though local angles are not preserved, it is equal-area. The standard parallels are $\phi_1 = \pi/4$ and $\phi_2 = \pi/3$.

$$k = \frac{\sqrt{C - 2n\sin(\phi)}}{\cos(\phi)} \tag{3.2.1.20}$$

$$h = \frac{\cos(\phi)}{\sqrt{C - 2n\sin(\phi)}} \tag{3.2.1.21}$$

$$\omega = 2\arcsin\left(\frac{|k-h|}{k+h}\right) \tag{3.2.1.22}$$

$$s = 1. \tag{3.2.1.23}$$

In between the standard parallels, the scale along the parallels k is too small, whereas outside these parallels, it is too large. For the meridians, it is just the opposite. In fact, as expected for an equal-area map, the scale factors k and h are reciprocals of one another. Furthermore, along any parallel, the scale is constant. The projection, however, does include some angular distortion, particularly near the poles. It is interesting to note that the distortions given by equations (3.2.1.20) to (3.2.1.23) are strictly functions of latitude.

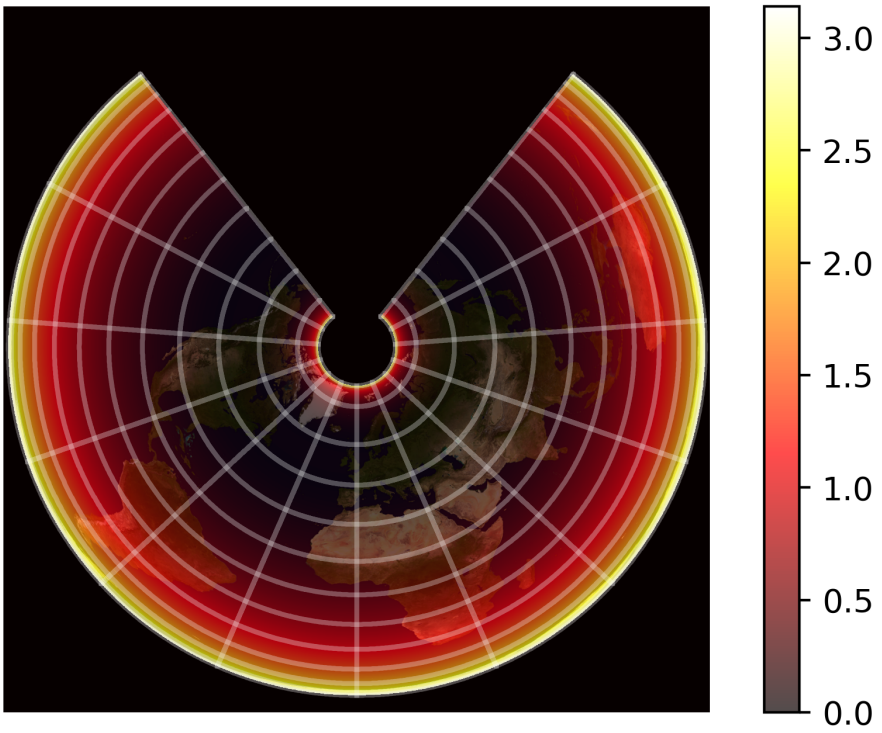

Figure 31: Albers equal-area conic projection angular distortion heatmap. The standard parallels are $\phi_1 = \pi/4$ and $\phi_2 = \pi/3$. The angular distortion is highest at the poles.

3.2.2 Lambert conformal conic projection

The Lambert conformal conic projection is a conformal map projection; it preserves angles locally and thus also roughly the shapes of the continents. The parallels are arcs of concentric circles, spaced more closely together near the center of the map. The meridians are again equally spaced radii of the mentioned circles, hence intersecting the parallels at right angles. Analogous to Albers equal-area conic projection, the scale is preserved along the two (or one) standard parallels. It is interesting to note that conformality fails at both poles, one of which is portrayed on the map as a point whereas the other is at infinity, depending on the choice of the standard parallels. The equations are given by:

$$x(\phi, \lambda) = \rho \sin(\theta), \tag{3.2.2.1}$$

$$y(\phi, \lambda) = \rho_0 - \rho \cos(\theta), \tag{3.2.2.2}$$

$$\rho = \frac{RF}{\tan(\pi/4 + \phi/2)^n}, \tag{3.2.2.3}$$

$$\theta = n\lambda, \tag{3.2.2.4}$$

$$\rho_0 = RF, \tag{3.2.2.5}$$

$$F = \frac{\cos(\phi_1)\tan(\pi/4 + \phi_1/2)^n)}{n}, \tag{3.2.2.6}$$

$$n = \frac{\ln\left(\dfrac{\cos(\phi_1)}{\cos(\phi_2)}\right)}{\ln\left(\dfrac{\tan(\pi/4 + \phi_2/2)}{\tan(\pi/4 + \phi_1/2)}\right)}, \; n \neq 0. \tag{3.2.2.7}$$

Here, the ϕ_1 and ϕ_2 are the standard parallels. Again, the constants n, F and ρ_0 need only be calculated once for the entire map. If the standard parallels are chosen equidistant to the Equator, n becomes 0, in which case it becomes the Mercator projection (After some rewriting). In the case of only one standard parallel, n is chosen to be $n = \sin(\phi_1)$. If this standard parallel is chosen to be the one of the poles, $n = 1$ and the polar Stereographic

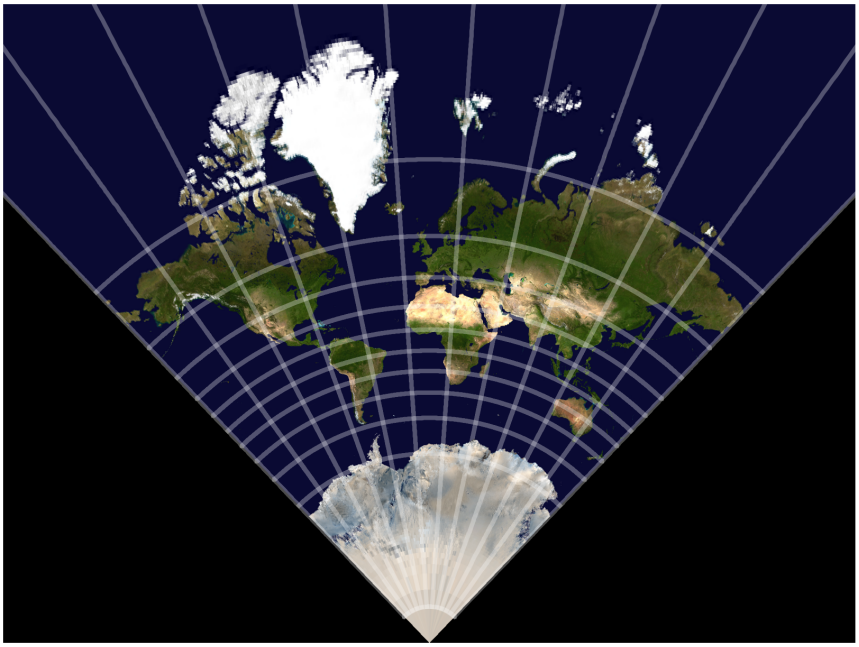

Figure 32: Lambert conformal conic projection. The equations are given by (3.2.2.1) to (3.2.2.7). It has the standard parallels $\phi_1 = \pi/5$ and $\phi_2 = -\pi/3$.

projection results. If $0 < n < \frac{1}{2}$ or $\frac{1}{2} < n < 1$, the range of the transformation is the area:

$$\{(x,y)|\ y \leq \rho_0 - \frac{x}{\tan(n\pi)}, y \leq \rho_0 + \frac{x}{\tan(n\pi)}\}.$$

If $n = \frac{1}{2}$, the range is

$$\{(x,y)|\ y \leq \rho_0)\}.$$

For $-1 < n < -\frac{1}{2}$ or $-\frac{1}{2} < n < 0$, the range is

$$\{(x,y)|\ y \geq \rho_0 - \frac{x}{\tan(n\pi)}\} \cup \{(x,y)|\ y \geq \rho_0 + \frac{x}{\tan(n\pi)}\}.$$

If $n = -\frac{1}{2}$, the range is

$$\{(x,y)|\ y \geq \rho_0)\}.$$

The inverse equations are given by:

$$\phi(x,y) = 2\arctan(RF/\rho)^{1/n} - \pi/2, \tag{3.2.2.8}$$

$$\lambda(x,y) = \text{atan2}(x, (\rho_0 - y))/n, \tag{3.2.2.9}$$

$$\rho = \text{sgn}(n)\sqrt{x^2 + (\rho_0 - y)^2}. \tag{3.2.2.10}$$

The scale factors and distortions are given by

$$k = h = \frac{\cos(\phi_1)\tan(\pi/4 + \phi_1/2)^n}{\cos(\phi)\tan(\pi/4 + \phi/2)^n}, \tag{3.2.2.11}$$

$$\omega = 2\arcsin\left(\frac{|k-h|}{k+h}\right) = 0, \tag{3.2.2.12}$$

$$s = \frac{\left(Fn\left(\frac{1}{\cos(\phi)}\right)\right)^2}{\tan(\pi/4 + \phi/2)^{2n}}. \tag{3.2.2.13}$$

Because the projection is conformal, $k = h$, resulting in the maximum angular distortion w to be equal to 0. The area distortion s is again only a function of the latitude and the area gets increasingly more distorted as one moves towards the poles.

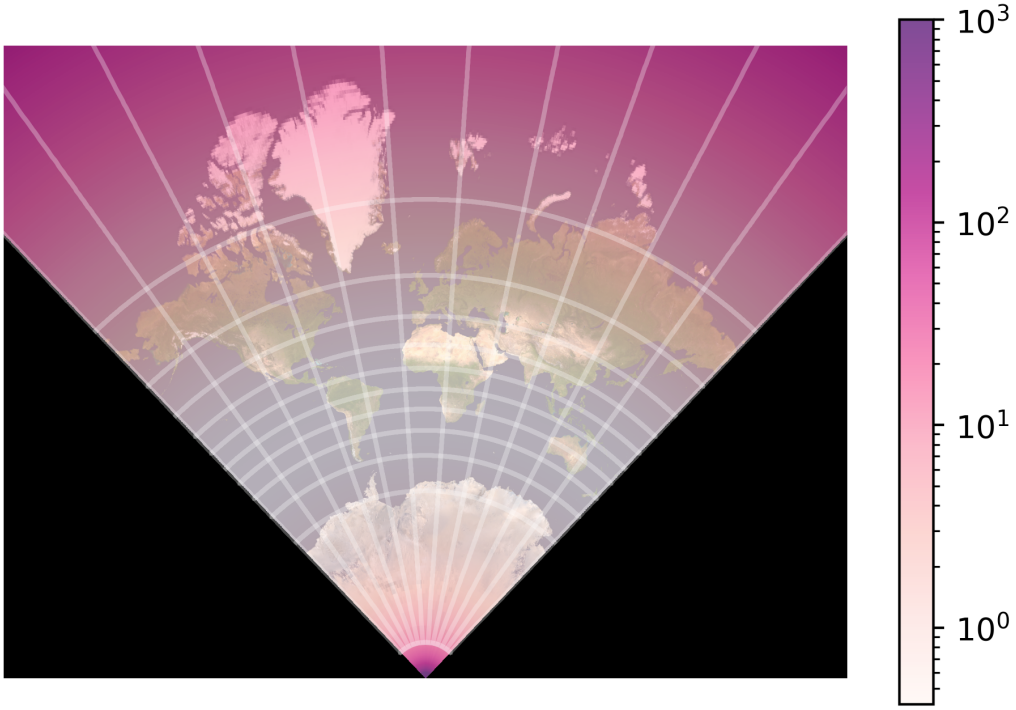

Figure 33: Lambert conformal conic projection area distortion heat map. As the area distortion tends to infinity at some places, in this case at the poles, the legend is capped at a factor of 10^3 in order to obtain a decent heatmap. It has the standard parallels $\phi_1 = \pi/5$ and $\phi_2 = -\pi/3$.

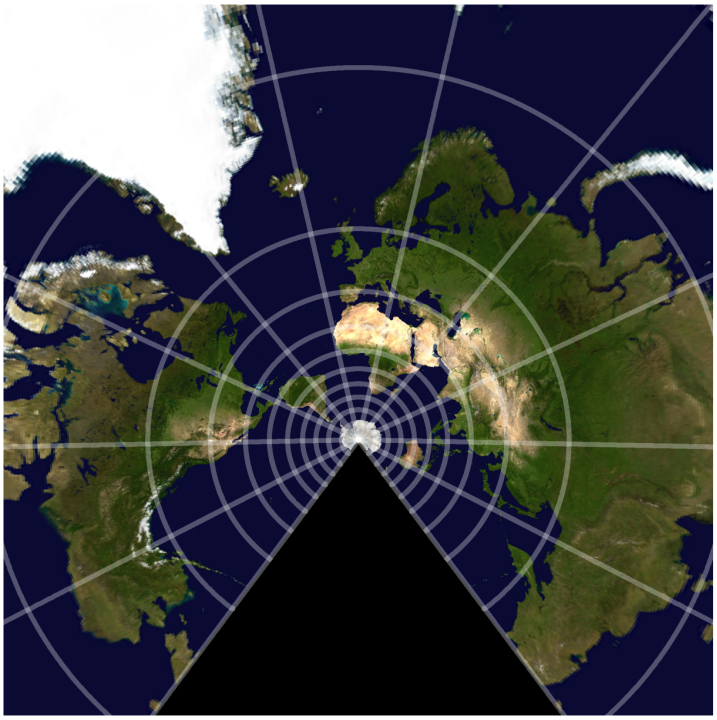

Figure 34: Lambert conformal conic projection. The equations are given by (3.2.2.1) - (3.2.2.7). It has the standard parallels $\phi_1 = -\pi/4$ and $\phi_2 = -\pi/3$.

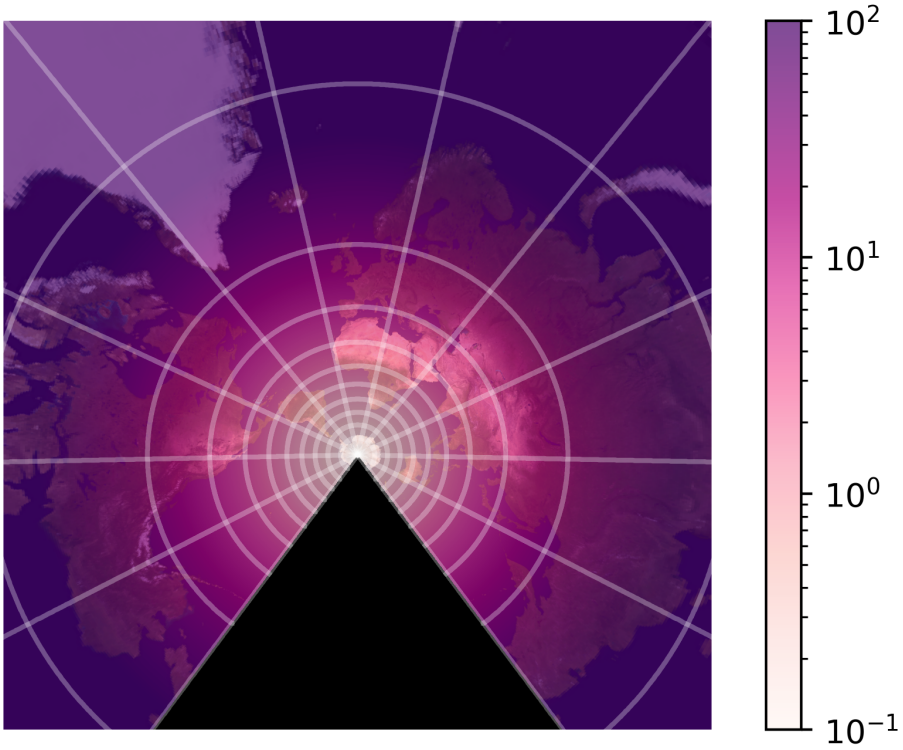

Figure 35: Lambert conformal conic projection area distortion heat map. As the area distortion tends to infinity at some places, the legend is capped at a factor of 10^2 in order to obtain a decent heatmap. As one moves towards the poles, the area distortions increases rapidly. It has the standard parallels $\phi_1 = -\pi/4$ and $\phi_2 = -\pi/3$.

3.2.3 Bonne projection

The Bonne projection is classified as a pseudoconical projection. This means that the parallels are equally spaced, concentric circular arcs, whereas the meridians are complex curves, except for the Central Meridian, which is a straight line. Along the Central Meridian and all parallels, the scale is preserved. Furthermore, both poles are represented as points and for the right choice of the standard parallel, the Bonne projection somewhat resembles the shape of a heart. With the projection being equal-area, only along the standard parallel and the central meridian is there no angular distortion; as one moves away from either of these curves, angular distortion increases rapidly. Contrary to the regular conic projections, the meridians and parallels do not intersect at right angles anywhere other than at the central meridian and standard parallel. The equations are given by:

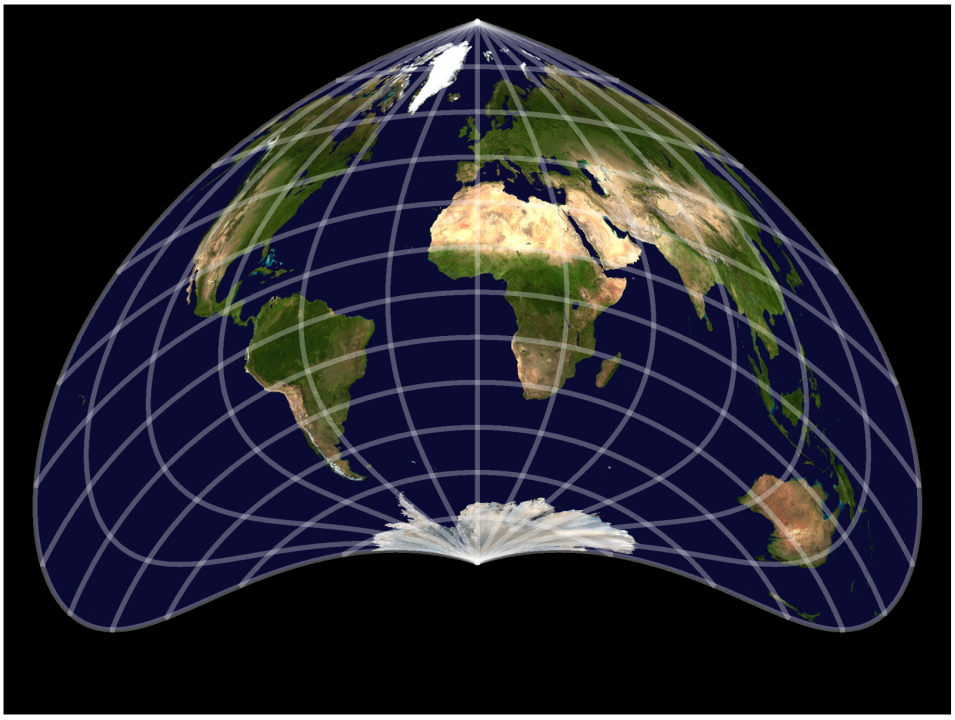

Figure 36: Bonne projection. The equations are given by equations (3.2.3.1 - 3.2.3.4). This projection has the standard parallel $\phi_1 = -\pi/8$. It is equal-area and for this particular choice of standard parallel, it somewhat resembles an upside down heart. The parallels are equally spaced, concentric circular arcs, whereas the meridians are complex curves (except for the Central Meridian).

$$x(\phi, \lambda) = \rho \sin(E), \tag{3.2.3.1}$$

$$y(\phi, \lambda) = R\frac{1}{\tan(\phi_1)} - \rho\cos(E), \tag{3.2.3.2}$$

$$\rho = R\left(\frac{1}{\tan(\phi_1)} + \phi_1 - \phi\right), \tag{3.2.3.3}$$

$$E = R\lambda\cos(\phi)/\rho. \tag{3.2.3.4}$$

Here, the ϕ_1 is the standard parallel. Unfortunately, the Bonne projection does not have an explicit form for its range. The inverse equations are given by:

$$\rho = \text{sgn}(\phi_1)\sqrt{x^2 + \left(R\frac{1}{\tan(\phi_1)} - y\right)^2}, \tag{3.2.3.5}$$

$$\phi(x, y) = \frac{1}{\tan(\phi_1)} + \phi_1 - \rho/R, \tag{3.2.3.6}$$

$$\lambda(x, y) = \frac{\rho}{R\cos(\phi)}\,\text{atan2}\left(x,\ R\frac{1}{\tan(\phi_1)} - y\right). \tag{3.2.3.7}$$

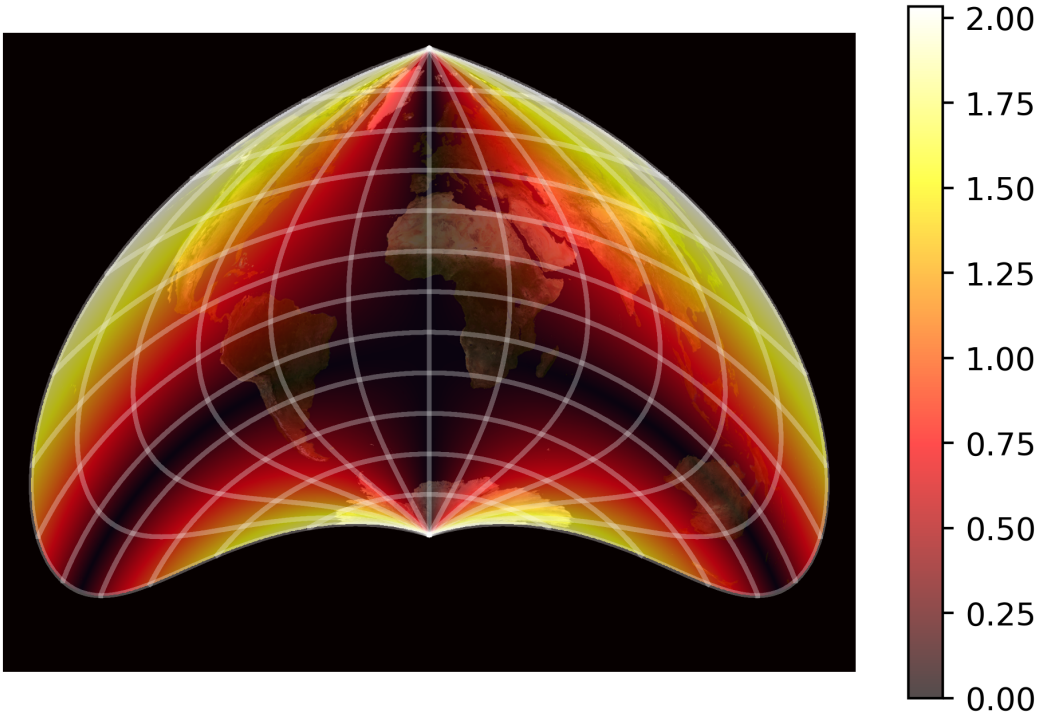

Figure 37: Bonne projection angular distortion heatmap. This projection has the standard parallel $\phi_1 = -\pi/8$. The angular distortion is lowest around the standard parallel and the Central Meridian and increases as one moves away from these.

The scale factors and distortions are given by

$$k = 1, \tag{3.2.3.8}$$

$$h = \sqrt{\frac{-2\sigma \sin\left(\frac{2\lambda\cos(\phi)}{\sigma}\right)\lambda\Big(\cos(\phi) - \sigma\sin(\phi)\Big) + \lambda\Big(\cos(\phi) - \sigma\sin(\phi)\Big)^2 + \sigma^2}{\sigma^2}}, \tag{3.2.3.9}$$

$$\sigma = \frac{1}{\tan(\phi_1)} + \phi_1 - \phi, \tag{3.2.3.10}$$

$$\omega = 2\arcsin\left(\frac{|k-h|}{k+h}\right), \tag{3.2.3.11}$$

$$s = 1. \tag{3.2.3.12}$$

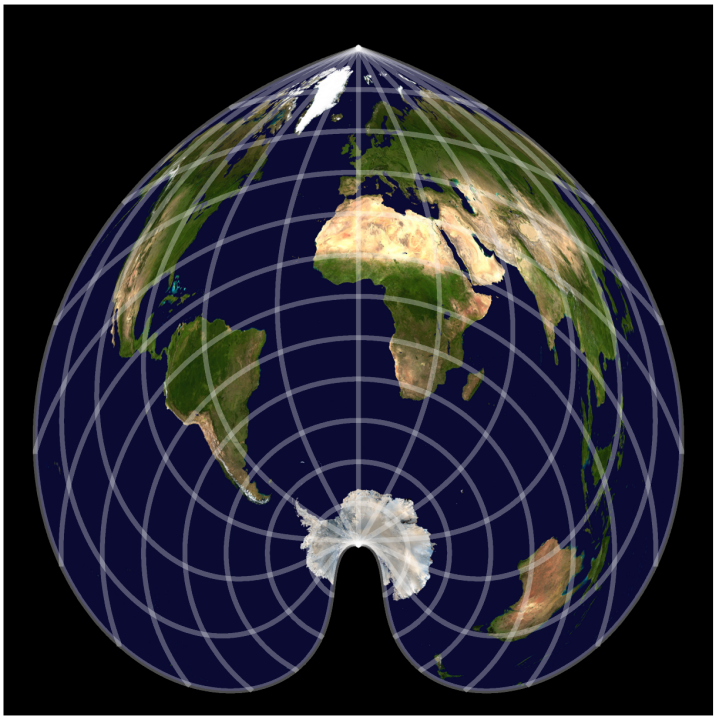

Figure 38: The equations are given by (3.2.3.1 - 3.2.3.4). This projection has the standard parallel $\phi_1 = -\pi/3$. It is equal-area and somewhat resembles an upside down heart.

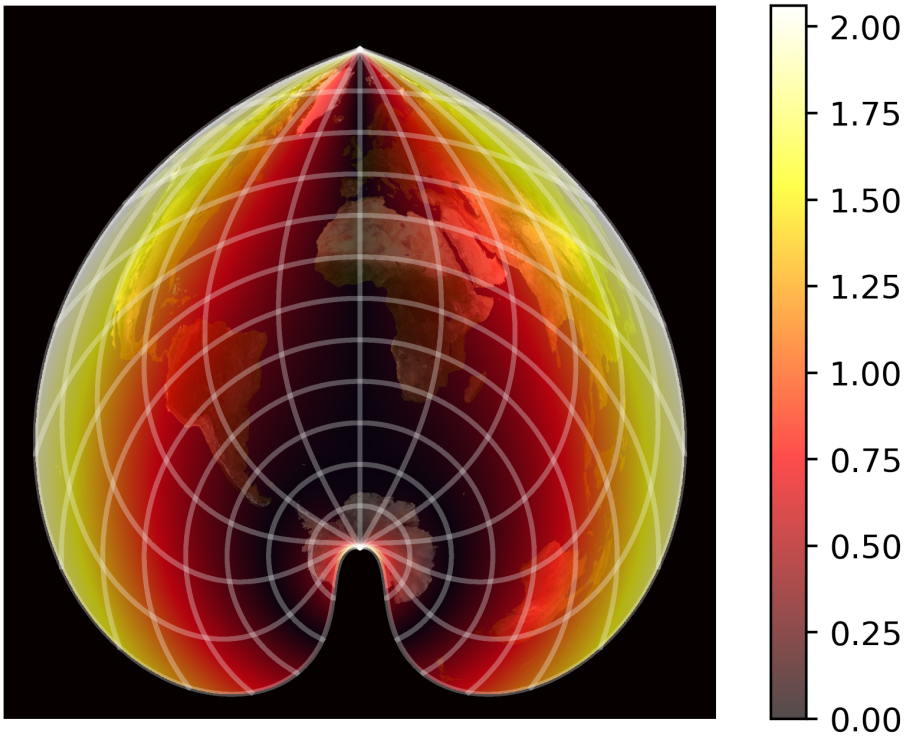

Figure 39: Bonne projection angular distortion heatmap. This projection has the standard parallel $\phi_1 = -\pi/3$. The angular distortion is lowest around the standard parallel and the Central meridian and increases as one moves away from these.

3.3 Azimuthal projections

Analogous to the cylindrical and conic projections, the azimuthal projections are also characterised by a single projection surface onto which they are projected. Instead of a cylinder or a cone, azimuthal projections are constructed using a plane tangent to the globe. This can be, for example, at the poles or the Equator. An important feature of the azimuthal projections is that the direction (or azimuth) from the center of a projection to every other point is preserved under the projection and hence portrayed correctly. On top of this, any great circle (the largest possible circle that can be drawn around a sphere) passing through the center of the map transforms into a straight line. Given that any arc of a great circle gives the shortest path between two points, azimuthal projections have the characteristic that the shortest path between any point and the center of the projection is a straight line. The following azimuthal projections will be treated:

- Orthographic projection
- Stereographic projection
- Gnomonic projection
- Lambert azimuthal equal-area projection

3.3.1 Orthographic projection

The Orthographic projection's point of perspective is at an infinite distance. Geometrically, this means that the projection lines are orthogonal to the tangent projection plane. Hence, all meridians and parallels are projected as either circles, ellipses or straight lines. This also causes a close resemblance in appearance to the globe, despite being one of the lesser useful projections due to its high amount of distortions. Furthermore, it is neither conformal nor equal-area and can only show half a hemisphere on a single map. Interestingly, however, the eye seems to be much more forgiving for this distortion than, for example, the distortions of the Mercator projection or the Cylindrical equal-area projection, likely due to its resemblance of the globe. The equations are given by:

Figure 40: Orthographic projection. The equations are given by (3.3.1.1) and (3.3.1.2). Here, $\phi_1 = 0$ such that the center of the map corresponds to the coordinates $(0, 0)$ on the sphere. The Orthographic projection corresponds to the Earth as viewed from infinity.

$$x(\phi, \lambda) = R\cos(\phi)\sin(\lambda), \tag{3.3.1.1}$$

$$y(\phi, \lambda) = R\Big(\cos(\phi_1)\sin(\phi) - \sin(\phi_1)\cos(\phi)\cos(\lambda)\Big). \tag{3.3.1.2}$$

Here, the center point of the map corresponds to the coordinates $(\phi_1, 0)$ on the sphere. Replacing all instances of λ with $\lambda - \lambda_1$ will result in the center being (ϕ_1, λ_1). As the

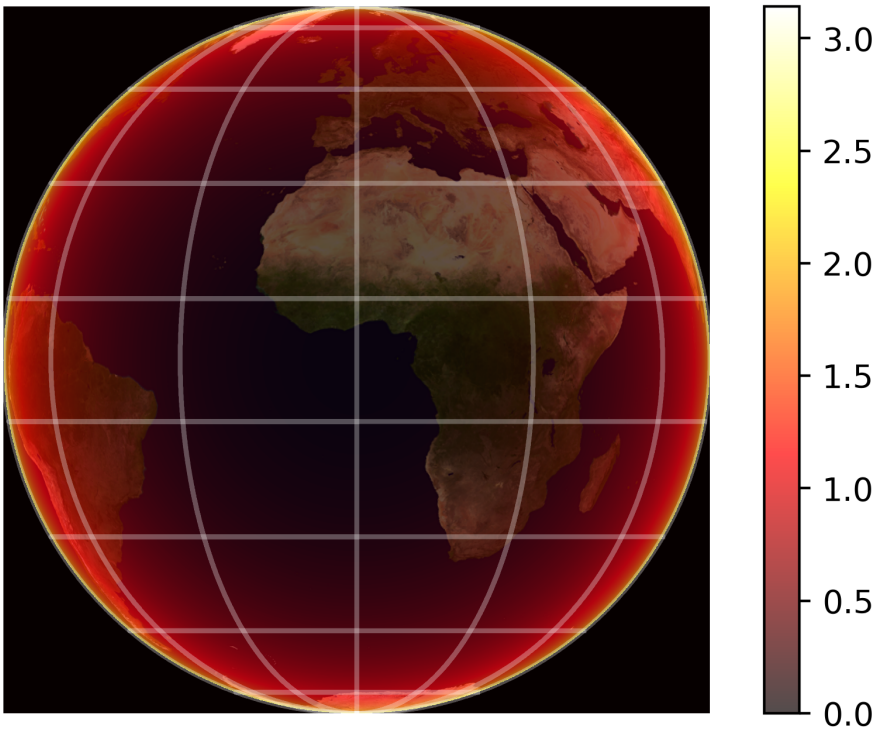

Figure 41: Orthographic projection angular distortion heatmap. Here, $\phi_1 = 0$ as in Figure 40. The angular distortion is highest at the edge of the map.

Orthographic projection can only show one hemisphere at a time, its domain is thus not the whole sphere. Instead, only the points with an angular distance c in radians less than $\frac{\pi}{2}$ to the center are projected. As all great circles passing through the center are represented as straight lines on azimuthal projections, we can use the great circle distance equation (2.5.0.2). Hence the domain is $\{(\phi, \lambda)|\ \cos(c) = \sin(\phi_1)\sin(\phi) + \cos(\phi_1)\cos(\phi)\cos(\lambda) \geq 0.)\}$. The range is simply a circle of radius R: $\{(x, y)|\ x^2 + y^2 \leq R^2\}$. The inverse equations are given by:

$$\phi(x, y) = \arcsin\left(\cos(c)\sin(\phi_1) + \frac{y\sin(c)\cos(\phi_1)}{\rho}\right), \tag{3.3.1.3}$$

$$\lambda(x, y) = \operatorname{atan2}\left(x\sin(c),\ \rho\cos(\phi_1)\cos(c) - y\sin(\phi_1)\sin(c)\right), \tag{3.3.1.4}$$

$$\rho = \sqrt{x^2 + y^2}, \tag{3.3.1.5}$$

$$c = \arcsin(\rho/R). \tag{3.3.1.6}$$

Here c is again the angular distance from the center of the projection, but now given in terms of x and y. If $\phi_1 = \pm\pi/2$, we have

$$\lambda(x, y) = \operatorname{atan2}\left(x,\ -\operatorname{sgn}(\phi_1)y\right). \tag{3.3.1.7}$$

Furthermore, if $x = 0$ and $y = 0$, we have $\phi(x, y) = \phi_1$ and $\lambda(x, y) = 0$. The scale and distortion factors are given by

$$k' = 1, \tag{3.3.1.8}$$

$$h' = \sin(\phi_1)\sin(\phi) + \cos(\phi_1)\cos(\phi)\cos(\lambda), \tag{3.3.1.9}$$

$$\omega = 2\arcsin\left(\frac{|h' - 1|}{h' + 1}\right), \tag{3.3.1.10}$$

$$s = h'. \tag{3.3.1.11}$$

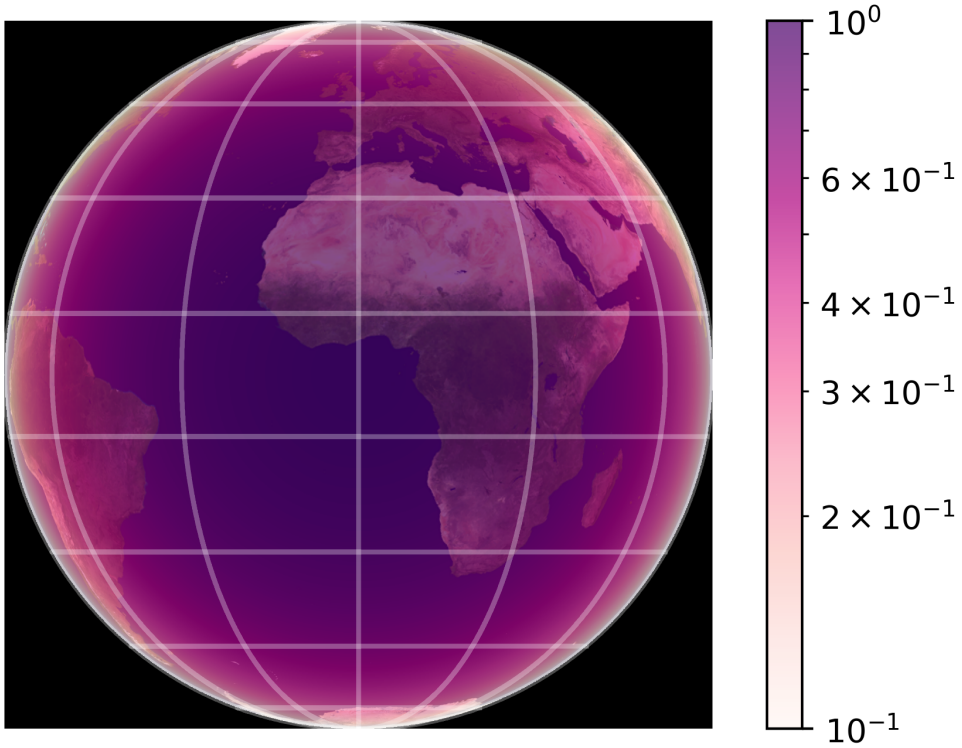

Figure 42: Orthographic projection area distortion heatmap. Here, $\phi_1 = 0$ as in Figure 40. The area distortion is highest at the edge of the map.

Here, h' and k' are not the scale factors along the parallels and meridians. Rather, h' is the scale factor in the direction of a straight line radiating from the center of the projection and k' is the scale factor in the direction perpendicular to such a radiating line.

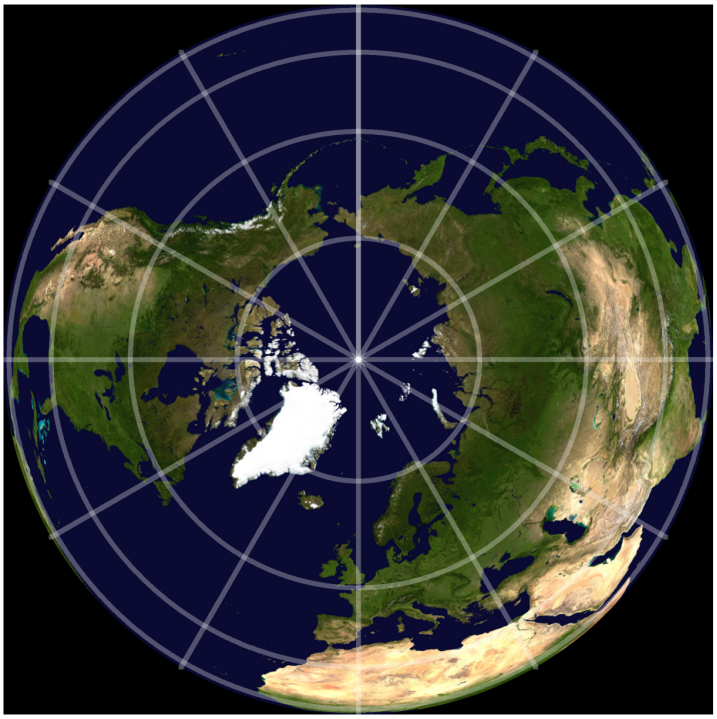

Figure 43: Orthographic projection. The equations are given by (3.3.1.1) and (3.3.1.2). Here, $\phi_1 = \pi/2$ such that the center of the map corresponds to the coordinates $(\pi/2, 0)$ on the sphere. The Orthographic projection resembles the Earth as viewed from infinity.

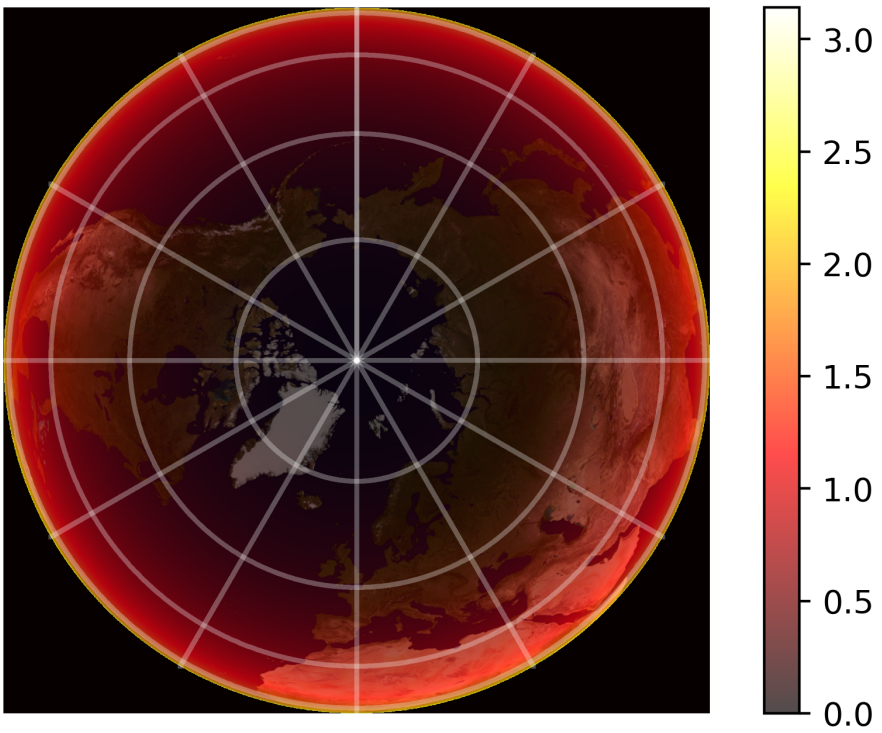

Figure 44: Orthographic projection angular distortion heatmap. Here, $\phi_1 = \pi/2$ as in Figure 43. The angular distortion is highest at the edge of the map.

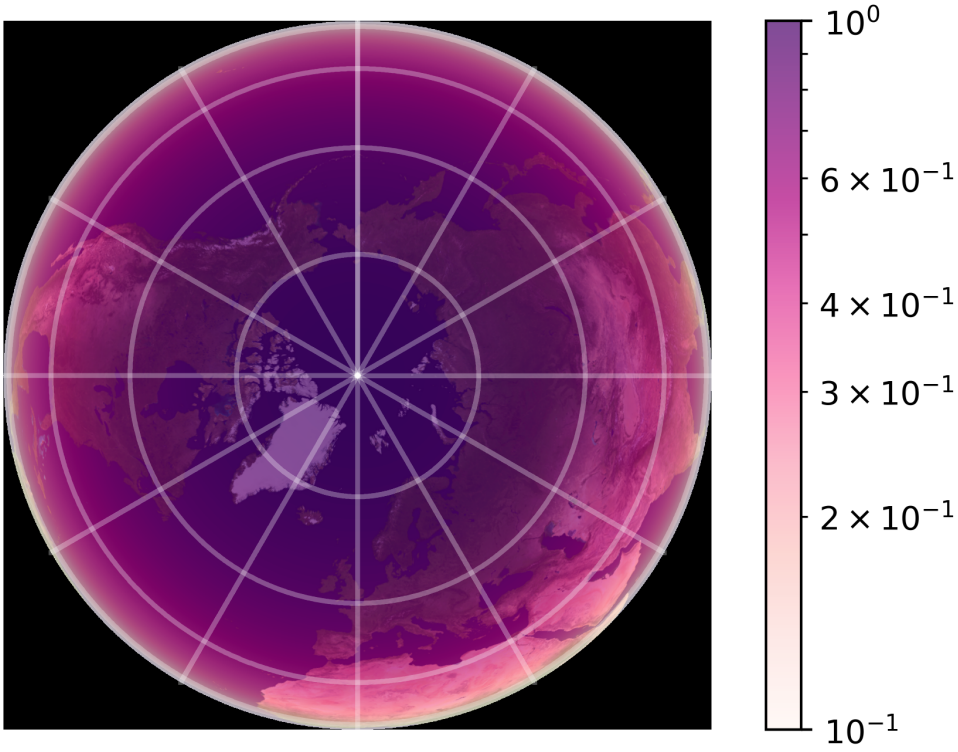

Figure 45: Orthographic projection area distortion heatmap. Here, $\phi_1 = \pi/2$ as in Figure 43. The area distortion is highest at the edge of the map.

3.3.2 Stereographic projection

The Stereographic projection is created by placing the point of perspective on the surface of the sphere opposite the point where the plane is tangent to the sphere (which is also the center of the projection). For example, if the North Pole is the center of the projection, the point of perspective is at the South Pole. Even though more than one hemisphere can be projected, it is not possible to show the entirety of the sphere; the point of perspective is projected at an infinite distance from the center. An important feature of this projection is that it is conformal. The equations are:

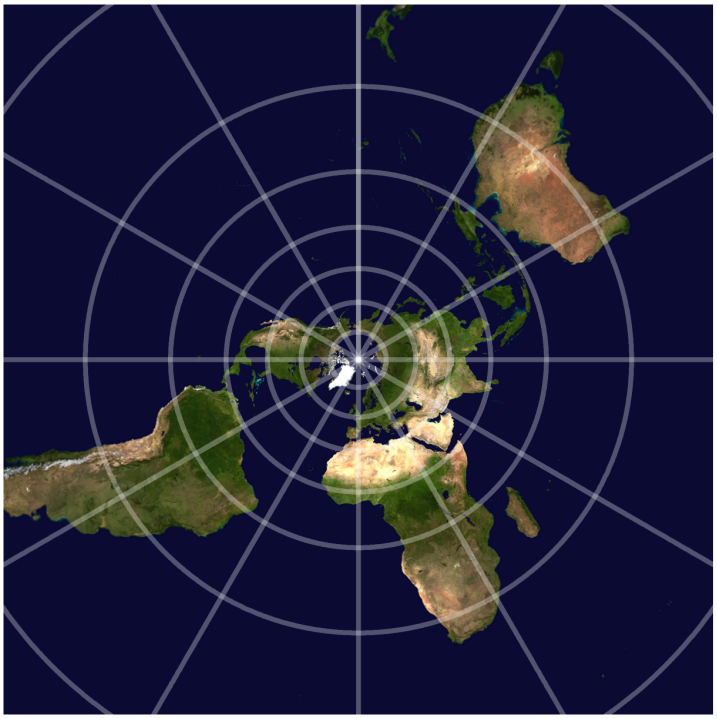

Figure 46: Stereographic projection. The equations are given by (3.3.2.1) and (3.3.2.2). Here, $\phi_1 = \pi/2$ such that the center of the map corresponds to the coordinates $(\pi/2, 0)$ on the sphere. The projection is conformal. The parallels are concentric circles and the meridians are straight lines radiating from the center.

$$x(\phi, \lambda) = Rk\cos(\phi)\sin(\lambda), \tag{3.3.2.1}$$
$$y(\phi, \lambda) = Rk(\cos(\phi_1)\sin(\phi) - \sin(\phi_1)\cos(\phi)\cos(\lambda)), \tag{3.3.2.2}$$

where

$$k = \frac{2}{1+\cos(c)} = \frac{2}{1+\sin(\phi_1)\sin(\phi)+\cos(\phi_1)\cos(\phi)\cos(\lambda)}. \tag{3.3.2.3}$$

Here, c is angular distance in radians on the sphere from the center of the projection. Furthermore, the center point of the map corresponds to the coordinates $(\phi_1, 0)$ on the sphere. If one desires (ϕ_1, λ_1) to be the center, all instances of λ are to be replaced by $\lambda - \lambda_1$. As the Stereographic projection is conformal, k is the scale factor in every direction. The domain is the whole sphere, except for the point of perspective. The range is $\mathbb{R}^2$. The inverse equations are:

$$\phi(x, y) = \arcsin(\cos(c)\sin(\phi_1) + (y\sin(c)\cos(\phi_1)/\rho)), \tag{3.3.2.4}$$
$$\lambda(x, y) = \operatorname{atan2}\left(x\sin(c),\ \rho\cos(\phi_1)\cos(c) - y\sin(\phi_1)\sin(c)\right), \tag{3.3.2.5}$$
$$\rho = \sqrt{x^2+y^2}, \tag{3.3.2.6}$$
$$c = 2\operatorname{atan2}\left(\rho,\ 2R\right). \tag{3.3.2.7}$$

Here, c is again the angular distance on the sphere from the center of the projection, but now given in terms of x and y. If $\phi_1 = \pm\pi/2$, we have

$$\lambda(x, y) = \operatorname{atan2}\left(x,\ -\operatorname{sgn}(\phi_1)y\right). \tag{3.3.2.8}$$

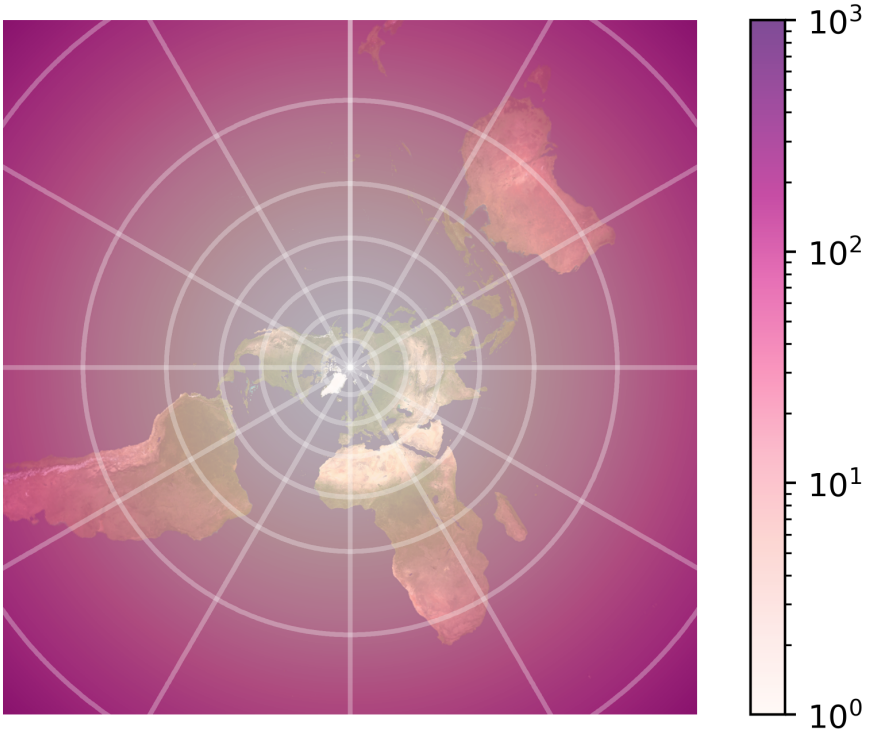

Figure 47: Stereographic projection area distortion heatmap. Here, $\phi_1 = \pi/2$ as in Figure 46. As the area distortion tends to infinity as one moves away from the center of the projection, the legend has been capped at a factor of 10^3 to obtain a coherent heatmap.

The distortions are given by

$$\omega = 0, \tag{3.3.2.9}$$

$$s = k^2. \tag{3.3.2.10}$$

As one moves away from the center of the projection, the area distortion increases rapidly.

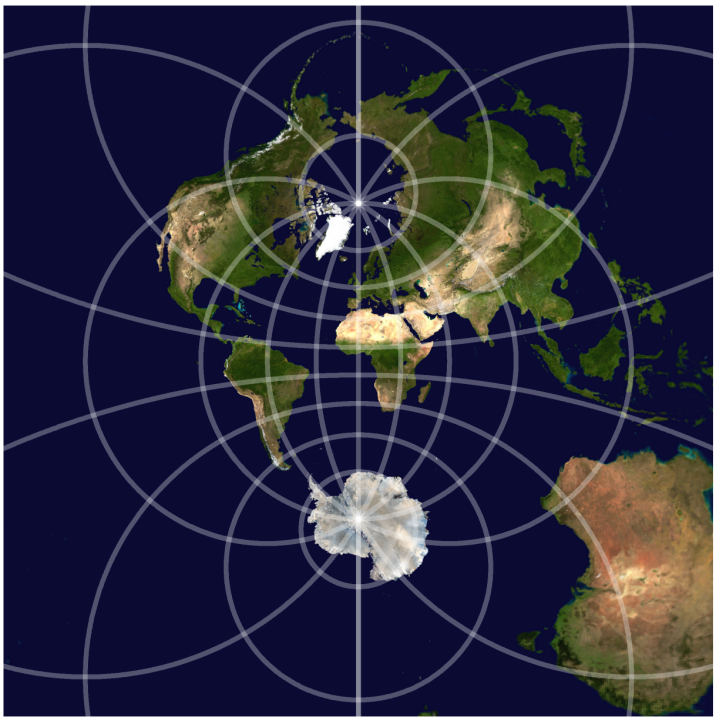

Figure 48: Stereographic projection with $\phi_1 = 0$. Hence the center of the map corresponds to the coordinates $(0, 0)$ on the sphere. The map is conformal and the parallels and meridians are complex curves.

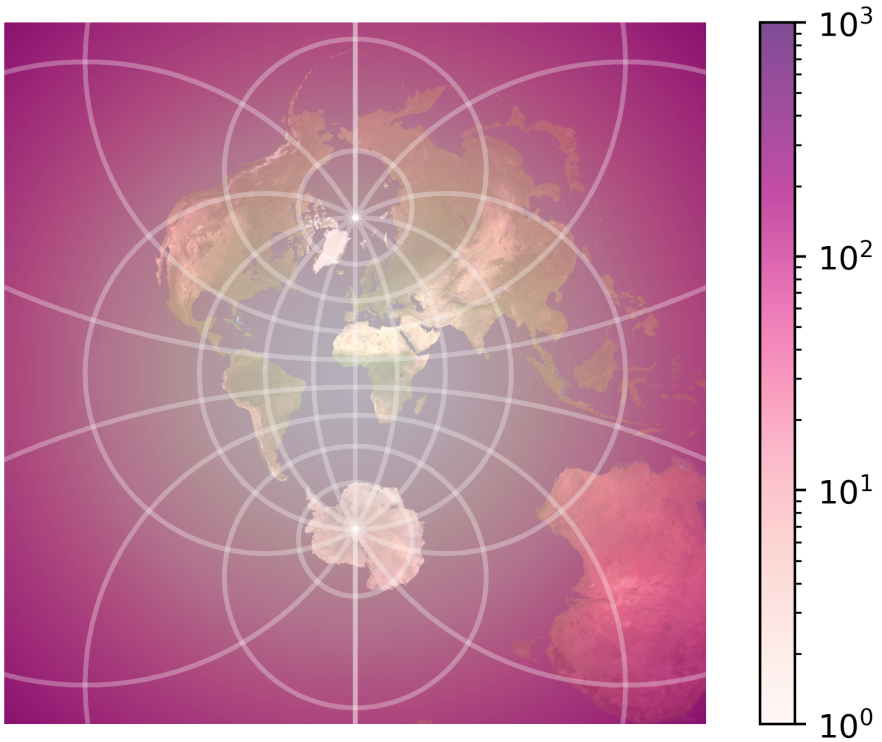

Figure 49: Stereographic projection area distortion heatmap. Here, $\phi_1 = 0$ as in Figure 48. As the area distortion tends to infinity as one moves away from the center of the projection, the legend has been capped at a factor of 10^3 to obtain a coherent heatmap.

3.3.3 Gnomonic projection

The characteristic feature of the Gnomonic projection is the fact that every great circle arc (also known as a geodesic), which determines the shortest route between two points, is projected as a straight line. This is the result of placing the point of perspective at the center of the sphere: all great circles lie in a plane that passes through the center of the sphere. As a result it is impossible to show a full hemisphere, and also implies much distortion. Furthermore, the meridians and the Equator become straight lines. The other parallels are ellipses, parabolas or hyperbolas. The equations and scale factors are given by:

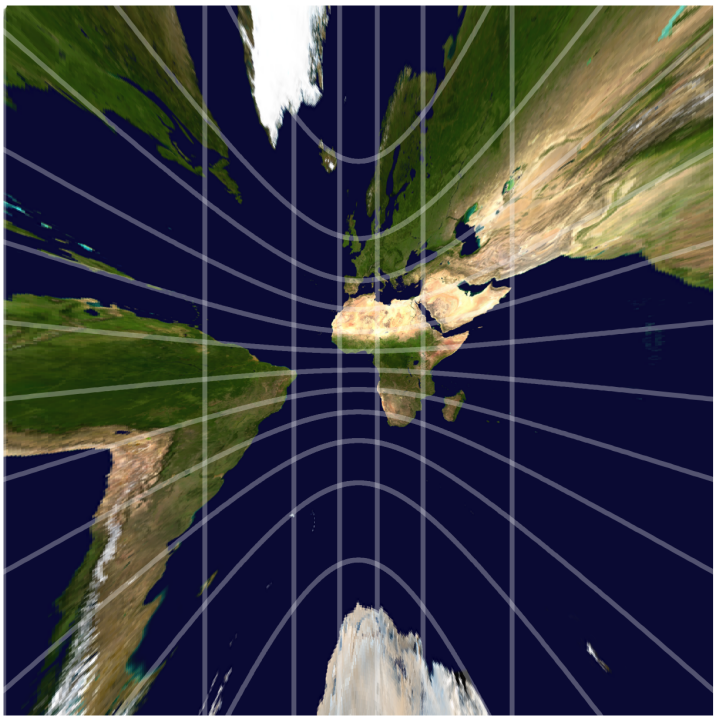

Figure 50: Gnomonic projection with $\phi_1 = 0$. Hence, the center of the map corresponds to the coordinates $(0, 0)$ on the sphere. The map is neither conformal nor equal-area, but has the property that the shortest route between any two points is projected as a straight line. Furthermore, only one hemisphere can be displayed at once. The meridians are drawn as straight lines and the parallels as complex curves, except for the Equator.

$$x(\phi, \lambda) = Rk' \cos(\phi) \sin(\lambda), \tag{3.3.3.1}$$

$$y(\phi, \lambda) = Rk'(\cos(\phi_1) \sin(\phi) - \sin(\phi_1) \cos(\phi) \cos(\lambda)), \tag{3.3.3.2}$$

$$k' = \frac{1}{\cos(c)}, \tag{3.3.3.3}$$

$$h' = \frac{1}{\cos(c)^2}. \tag{3.3.3.4}$$

Here, $\cos(c)$ is the cosine of the angular great circle distance c in radians from section (2.5),

$$\cos(c) = \sin(\phi_1) \sin(\phi) + \cos(\phi_1) \cos(\phi) \cos(\lambda).$$

The center point of the map corresponds to the coordinates $(\phi_1, 0)$ on the sphere. If one desires (ϕ_1, λ_1) to be the center, all instances of λ are to be replaced by $\lambda - \lambda_1$. Furthermore, h' and k' are not the scale factors along the parallels and meridians. Rather, h' is the scale factor in the direction of a straight line radiating from the center of the projection and k' is the scale factor in the direction perpendicular to such a radiating line. As mentioned before, not even a full (closed, to be precise) hemisphere can be projected by the Gnomonic projection. As the boundary is not in the domain, only the points with an angular distance to the center c on the sphere that is strictly smaller than $\frac{\pi}{2}$ are projected. Thus, the domain

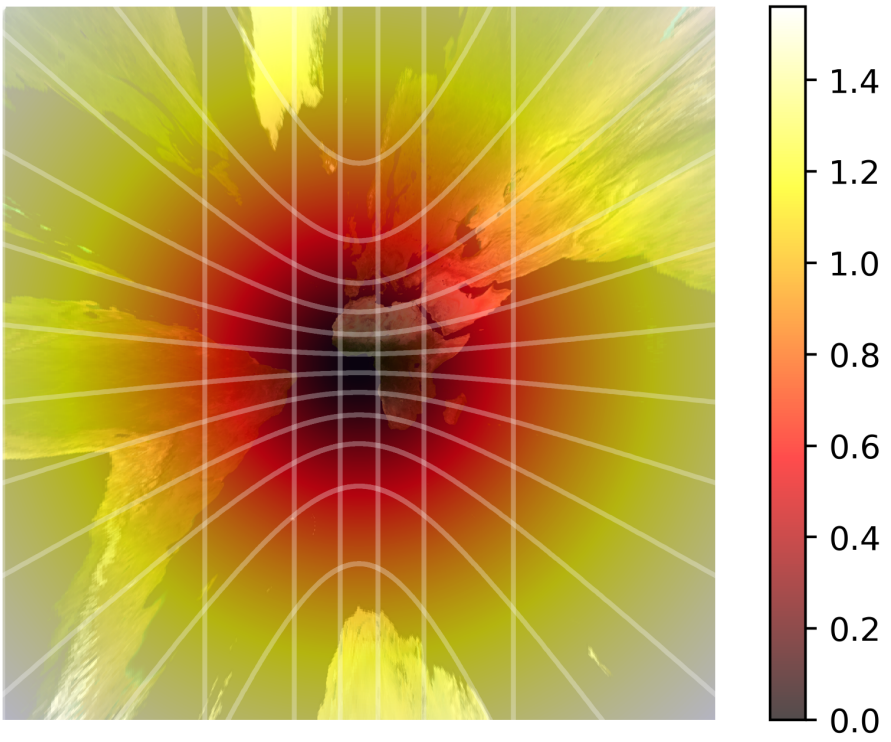

Figure 51: Gnomonic projection angular distortion heatmap with $\phi_1 = 0$. Hence, the center of the map corresponds to the coordinates $(0, 0)$ on the sphere. The angular distortion increases very quickly as one moves away from the center.

is the open hemisphere $\{(\phi, \lambda)|\ \cos(c) = \sin(\phi_1)\sin(\phi) + \cos(\phi_1)\cos(\phi)\cos(\lambda) > 0.)\}$. The range of the projection is $\mathbb{R}^2$. The inverse equations are:

$$\phi(x, y) = \arcsin\Big(\cos(c)\sin(\phi_1) + (y\sin(c)\cos(\phi_1)/\rho)\Big), \tag{3.3.3.5}$$

$$\lambda(x, y) = \operatorname{atan2}\left(x\sin(c),\ \rho\cos(\phi_1)\cos(c) - y\sin(\phi_1)\sin(c)\right) \tag{3.3.3.6}$$

$$\rho = \sqrt{x^2 + y^2} \tag{3.3.3.7}$$

$$c = \operatorname{atan2}(\rho,\ R). \tag{3.3.3.8}$$

Here, c is again the angular distance to the center on the sphere in radians, but now given in terms of x and y. If $\phi_1 = \pm\pi/2$, we have

$$\lambda(x, y) = \operatorname{atan2}\left(x,\ -\operatorname{sgn}(\phi_1)y\right). \tag{3.3.3.9}$$

The distortions are given by

$$\omega = 2\arcsin\left(\frac{|\sec(c) - \sec(c)^2|}{\sec(c) + \sec(c)^2}\right), \tag{3.3.3.10}$$

$$s = \sec(c)^3. \tag{3.3.3.11}$$

As one moves away from the center, both the angular distortion, as well as the distortion in area, diverges to infinity.

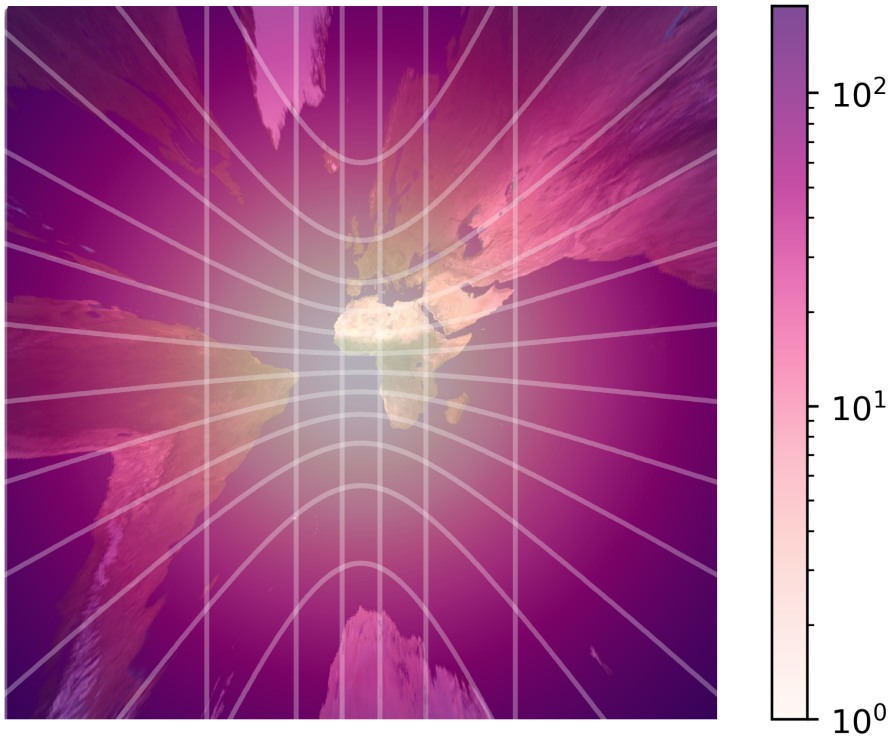

Figure 52: Gnomonic projection area distortion heatmap with $\phi_1 = 0$. Hence, the center of the map corresponds to the coordinates $(0, 0)$ on the sphere. The area distortions goes to infinity as one moves away from the center of the projection.

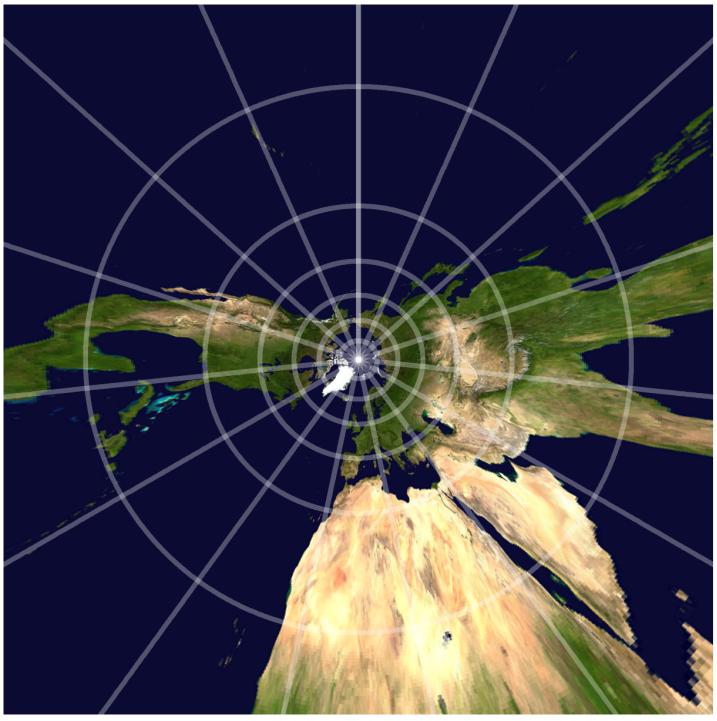

Figure 53: Gnomonic projection with $\phi_1 = \pi/2$. Hence, the center of the map corresponds to the coordinates $(\pi/2, 0)$ on the sphere. The parallels are concentric circles and the meridians straight lines radiating from the center of the projection.

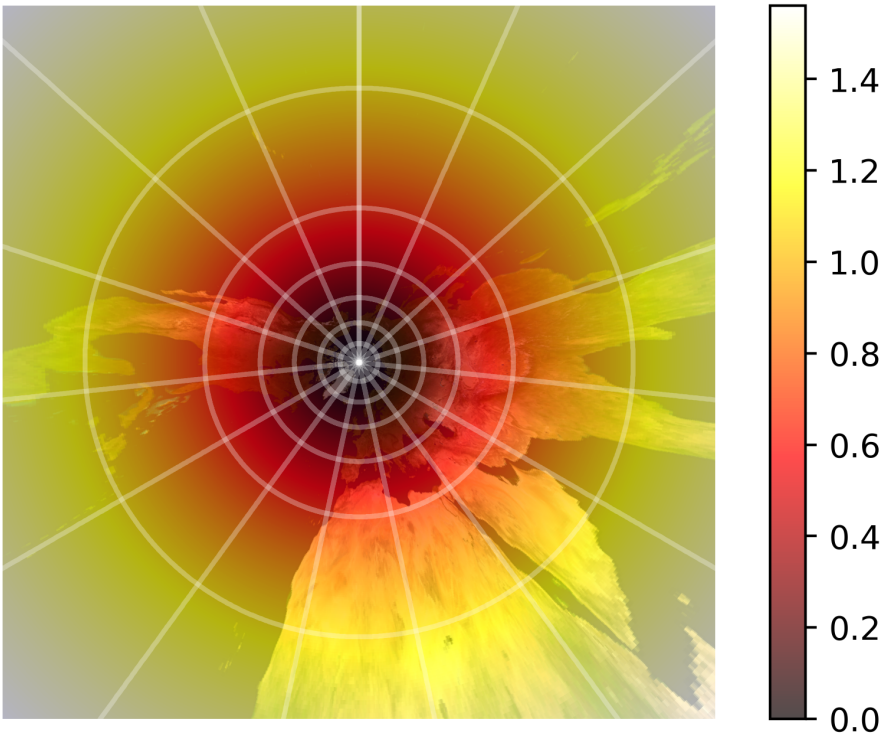

Figure 54: Gnomonic projection angular distortion heatmap with $\phi_1 = \pi/2$. Hence, the center of the map corresponds to the coordinates $(\pi/2, 0)$ on the sphere. The angular distortion increases rapidly as one moves away from the center.

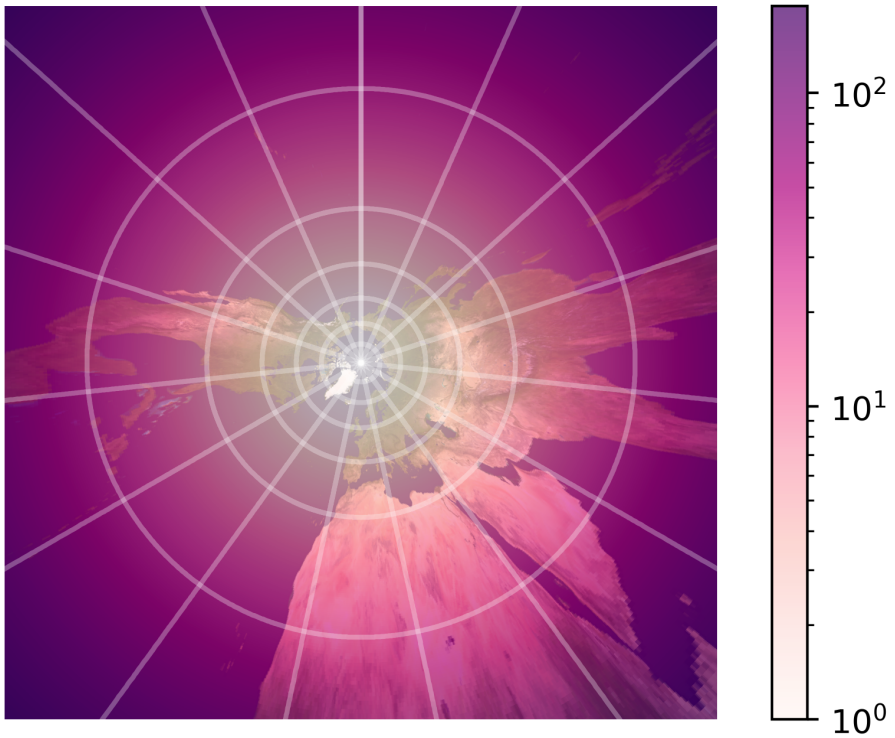

Figure 55: Gnomonic projection area distortion heatmap with $\phi_1 = \pi/2$. Hence, the center of the map corresponds to the coordinates $(\pi/2, 0)$ on the sphere. The area distortion increases rapidly as one moves away from the center.

3.3.4 Lambert azimuthal equal-area projection

In contrast to the other azimuthal projections that have been discussed, the Lambert azimuthal equal-area projection is not a perspective projection. It does, like the other azimuthal projections, have true direction with respect to the center. As the name suggests, it is equal-area. Furthermore, almost all meridians and parallels are complex curves. The equations and scale factors are given by:

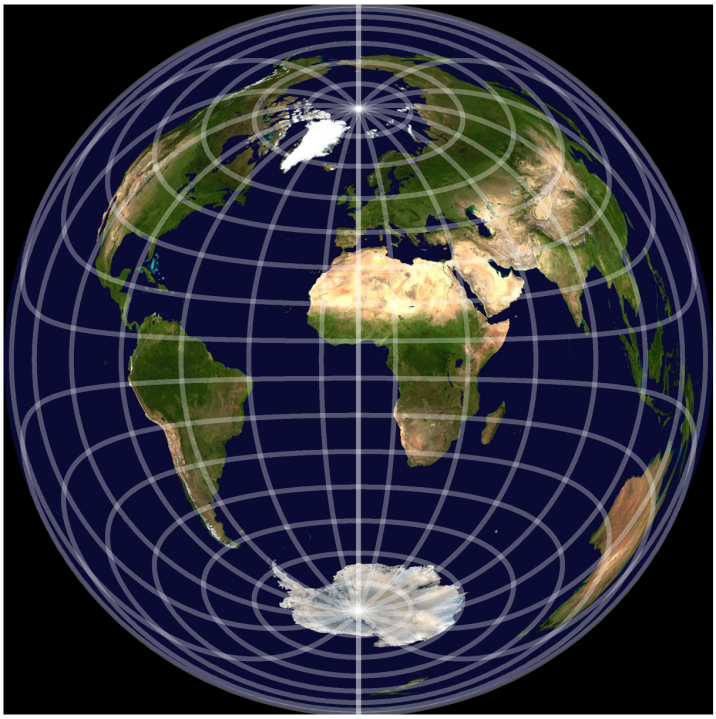

Figure 56: Lambert azimuthal equal-area projection with $\phi_1 = 0$. Hence, the center of the map corresponds to the coordinates $(0, 0)$ on the sphere. The equations are given by (3.3.4.1) and (3.3.4.2). The map is equal-area and most of the parallels and meridians are complex curves.

$$x(\phi, \lambda) = Rk' \cos(\phi) \sin(\lambda), \tag{3.3.4.1}$$

$$y(\phi, \lambda) = Rk'(\cos(\phi_1) \sin(\phi) - \sin(\phi_1) \cos(\phi) \cos(\lambda)), \tag{3.3.4.2}$$

$$k' = \sqrt{\frac{2}{1 + \sin(\phi_1) \sin(\phi) + \cos(\phi_1) \cos(\phi) \cos(\lambda)}}, \tag{3.3.4.3}$$

$$h' = 1/k'. \tag{3.3.4.4}$$

Here, the center point of the map corresponds to the coordinates $(\phi_1, 0)$ on the sphere. If one desires (ϕ_1, λ_1) to be the center, all instances of λ are to be replaced by $\lambda - \lambda_1$. Furthermore, h' and k' are not the scale factors along the parallels and meridians. Rather, h' is the scale factor in the direction of a straight line radiating from the center of the projection and k' is the scale factor in the direction perpendicular to such a radiating line. We see that h' decreases as the distance to the center increases, whereas k' increases as this distance grows. The range is simply a circle of radius $2R$: $\{(x, y) |\ x^2 + y^2 \leq 4R^2\}$. The inverse equations are given by:

$$\phi(x, y) = \arcsin\Big(\cos(c) \sin(\phi_1) + (y \sin(c) \cos(\phi_1)/\rho)\Big), \tag{3.3.4.5}$$

$$\lambda(x, y) = \operatorname{atan2}\left(x \sin(c),\ \rho \cos(\phi_1) \cos(c) - y \sin(\phi_1) \sin(c)\right), \tag{3.3.4.6}$$

$$\rho = \sqrt{x^2 + y^2}, \tag{3.3.4.7}$$

$$c = 2 \arcsin\left(\frac{\rho}{2R}\right). \tag{3.3.4.8}$$

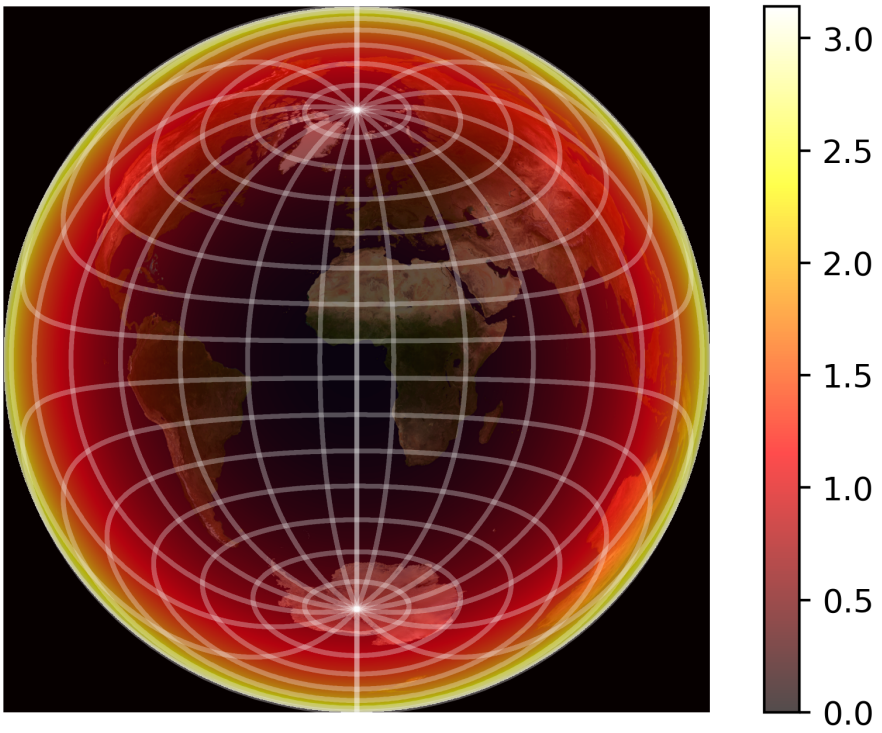

Figure 57: Lambert Azimuthal Equal-Area projection angular distortion heatmap. Here, $\phi_1 = 0$ as in Figure 56. The angular distortion is greatest at the edge of the map.

Here, c is again the angular distance on the sphere to the center of the map, but now given in terms of x and y. If $\phi_1 = \pm\pi/2$, we have

$$\lambda(x, y) = \operatorname{atan2}\left(x,\ -\operatorname{sgn}(\phi_1)y\right). \tag{3.3.4.9}$$

The distortions are given by

$$\omega = 2\arcsin\left(\frac{|k' - 1/k'|}{k' + 1/k'}\right), \tag{3.3.4.10}$$

$$s = 1. \tag{3.3.4.11}$$

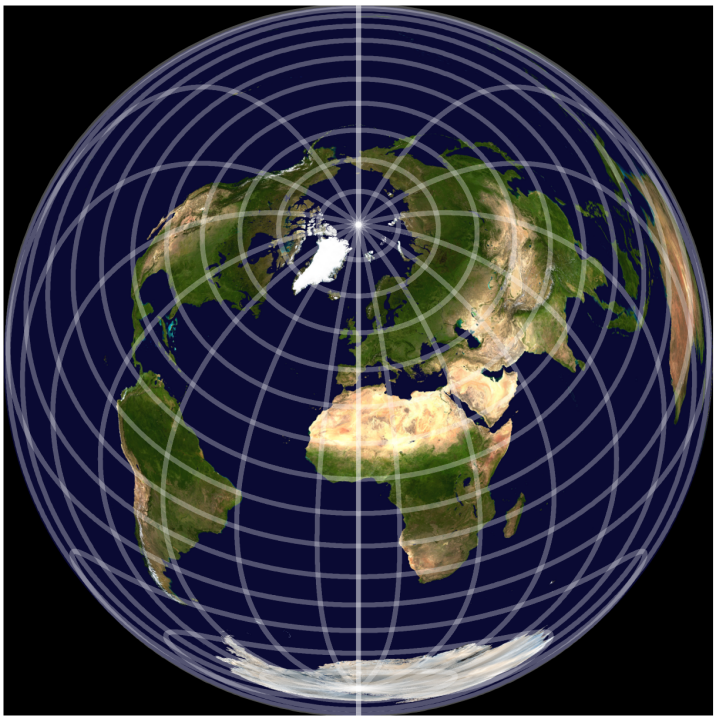

Figure 58: Lambert azimuthal equal-area projection with $\phi_1 = \pi/4$. Hence, the center of the map projection corresponds to the coordinates $(\pi/4, 0)$ on the sphere.

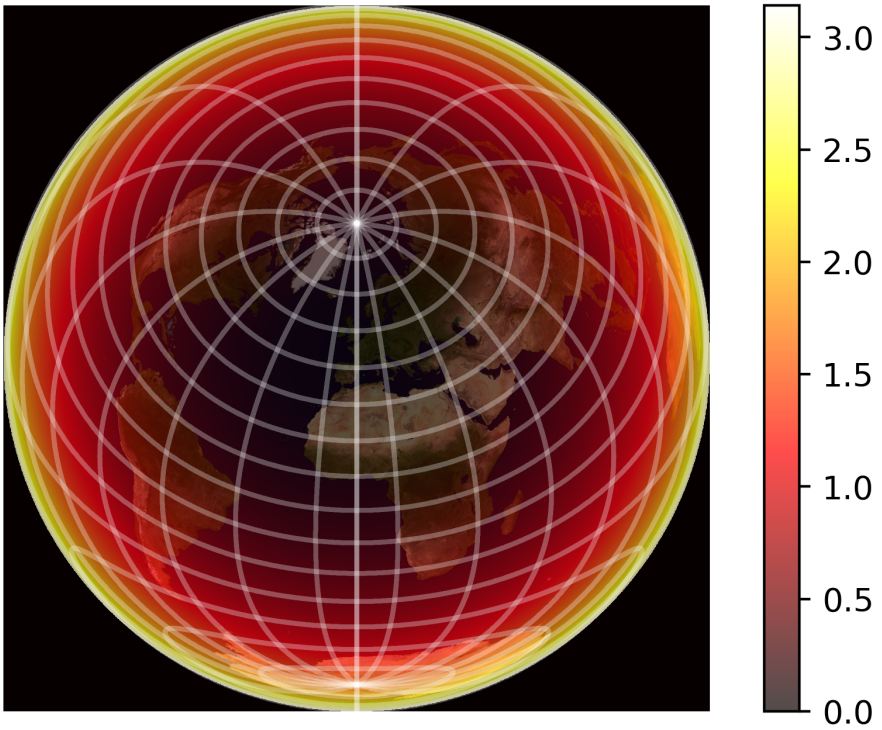

Figure 59: Lambert azimuthal equal-area projection angular distortion heatmap with $\phi_1 = \pi/4$ as in Figure 58. The angular distortion is greatest at the edge of the map.

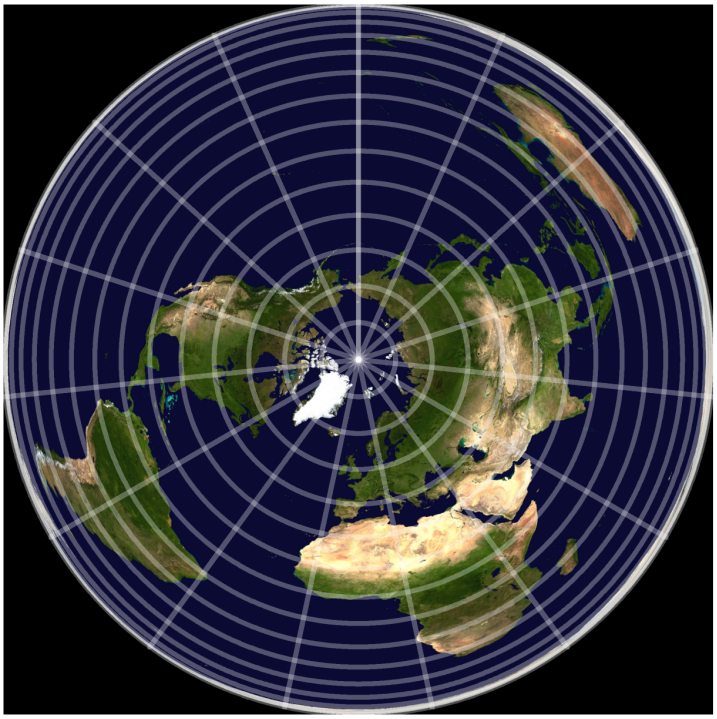

Figure 60: Lambert azimuthal equal-area projection with $\phi_1 = \pi/2$. Hence, the center of the map corresponds to the coordinates $(\pi/2, 0)$ on the sphere. The parallels are concentric circles intersecting the radiating straight meridians at right angles.

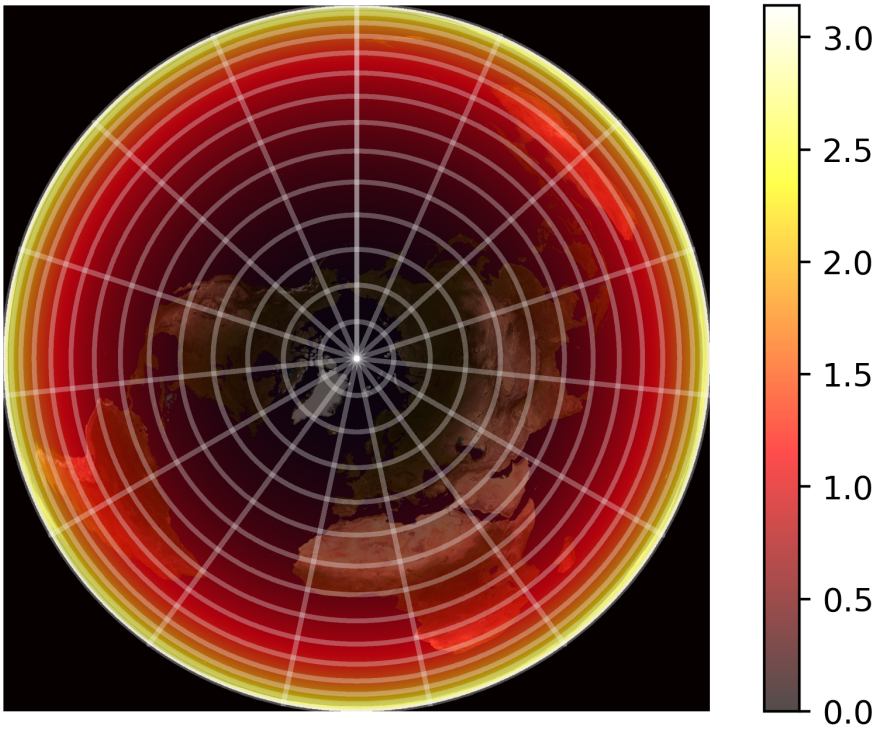

Figure 61: Lambert azimuthal equal-area projection angular distortion heatmap with $\phi_1 = \pi/2$ as in Figure 60. The angular distortion is greatest the edge of the map.

3.4 Miscellaneous projections

A lot of projections do not neatly fall in any of the former categories, but are still very much worth discussing, be it for having little distortion or being mathematically interesting. The following projections will be reviewed:

- Sinusoidal projection
- Mollweide projection
- Eckert IV projection
- Eckert VI projection
- Van der Grinten projection

3.4.1 Sinusoidal projection

The Sinusoidal projection is an equal-area pseudocylindrical projection. As is the case with regular cylindrical projections, the parallels are equally spaced straight lines, but contrary to cylindrical projections, the meridians in the Sinusoidal projection are equally-spaced sinusoidal curves (except for the central meridian, which is a straight line). Furthermore, along the central meridian and all parallels, the scale is preserved and the poles are represented as points. The equations for the Sinusoidal projection are:

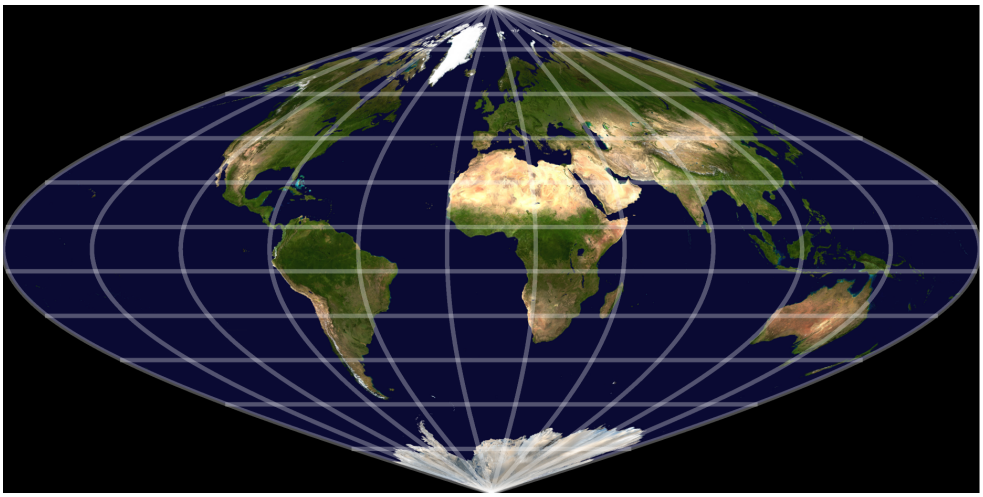

Figure 62: Sinusoidal projection. The equations are given by (3.4.1.1) and (3.4.1.2). The map is equal-area, but not conformal. The parallels are drawn as equally spaced straight horizontal lines and the meridians as sinusoidal curves. The poles are represented as points.

$$x(\phi, \lambda) = R\lambda\cos(\phi), \tag{3.4.1.1}$$
$$y(\phi, \lambda) = R\phi. \tag{3.4.1.2}$$

The range of the transformation is

$$\{(x, y)| - R\pi\cos(y/R) \leq x \leq R\pi\cos(y/R),\ -R\pi/2 \leq y \leq R\pi/2\}.$$

The inverse equations are:

$$\lambda(x, y) = \frac{x}{R\cos(\phi)}, \tag{3.4.1.3}$$
$$\phi(x, y) = \frac{y}{R}. \tag{3.4.1.4}$$

The scale factors and distortions are given by

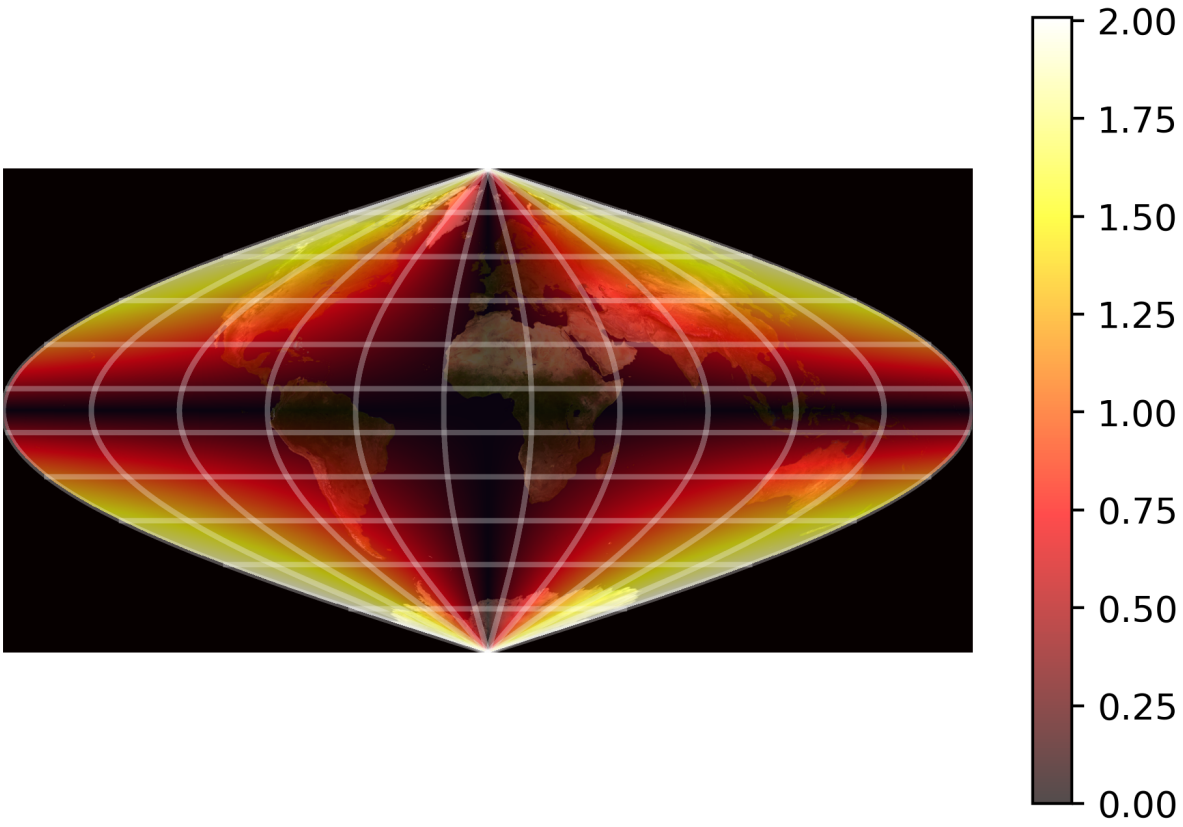

Figure 63: Sinusoidal projection angular distortion heat map as in Figure 62. As one moves away from the Equator and the Central Meridian, the angular distortion increases, becoming relatively large.

$$k = 1, \tag{3.4.1.5}$$

$$h = \sqrt{1 + \lambda^2 \sin(\phi)^2}, \tag{3.4.1.6}$$

$$\omega = 2 \arctan \left| \frac{1}{2} \lambda \sin(\phi) \right|, \tag{3.4.1.7}$$

$$s = 1. \tag{3.4.1.8}$$

As one moves away from the Equator and the Central meridian, the angular distortion increases.

3.4.2 Mollweide projection

Analogous to the Sinusoidal projection, the Mollweide projection is also an equal-area pseudocylindrical projection. The Central Meridian is a straight line; all other meridians are elliptical arcs, where the meridians $\frac{\pi}{2}$ radians East and West of the central meridian form a circle. The parallels are straight lines that are spaced unequally and the poles are points. The equations are given by:

$$x(\phi, \lambda) = \frac{\sqrt{8}}{\pi} R\lambda \cos(\theta), \tag{3.4.2.1}$$

$$y(\phi, \lambda) = \sqrt{2} R \sin(\theta), \tag{3.4.2.2}$$

where θ is found from

$$2\theta + \sin(2\theta) = \pi \sin(\phi). \tag{3.4.2.3}$$

Geometrically, θ can be seen as the parametric angle made between between the center point of the Equator and the point of latitude on the circle formed by the meridians $\frac{\pi}{2}$ radians

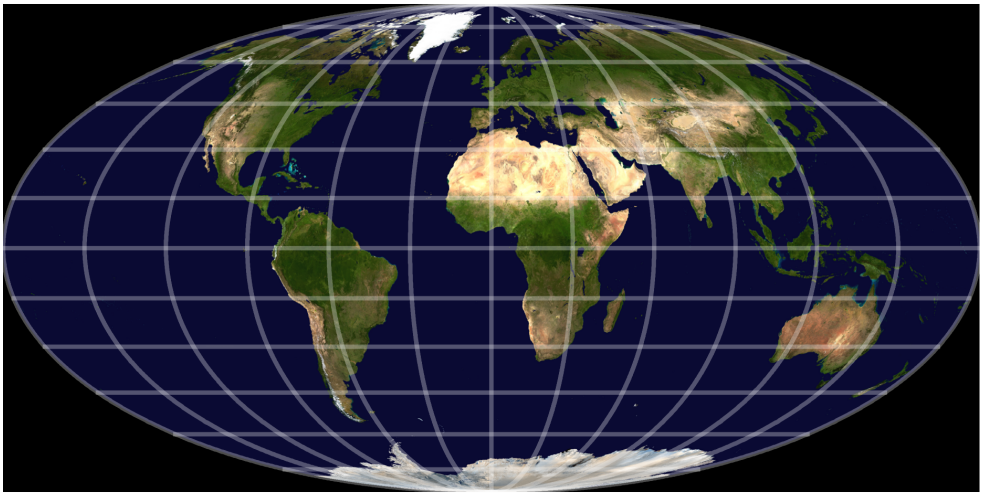

Figure 64: Mollweide projection. The equations are given by (3.4.2.1) and (3.4.2.2). The projection is equal-area, but not conformal. The parallels are unequally spaced lines and the meridians are drawn as elliptical arcs.

East and West of the central meridian and takes values in $[-\pi/2, \pi/2]$. Equation (3.4.2.3) can be solved using a Newton-Raphson iteration [12] with ϕ as initial guess:

$$\Delta\theta' = -\frac{\theta' + \sin(\theta') - \pi\sin(\phi)}{1 + \cos(\theta')}. \tag{3.4.2.4}$$

$\Delta\theta'$ is then added to the previous iteration θ' to obtain the next θ' to use in the next calculation of $\Delta\theta'$. When $\Delta\theta'$ is smaller than a predetermined $\epsilon \in \mathbb{R}_{>0}$, θ is calculated to be

$$\theta = \frac{\theta'}{2}. \tag{3.4.2.5}$$

The range of the transformation is the ellipse $\{(x, y) | \ \frac{x^2}{8R^2} + \frac{y^2}{2R^2} \leq 1\}$. The inverse equations do not require any iterations:

$$\theta = \arcsin\left(\frac{y}{\sqrt{2}R}\right), \tag{3.4.2.6}$$

$$\lambda(x, y) = \frac{\pi x}{\sqrt{8}R\cos(\theta)}, \tag{3.4.2.7}$$

$$\phi(x, y) = \arcsin\left(\frac{2\theta + \sin(2\theta)}{\pi}\right). \tag{3.4.2.8}$$

If $\phi = \pm\frac{\pi}{2}$, equation (3.4.2.8) is indeterminate as $\theta = \pm\frac{\pi}{2}$, in which case we define

$$\lambda(x, y) = 0, \tag{3.4.2.9}$$

$$\phi(x, y) = \pm\frac{\pi}{2}. \tag{3.4.2.10}$$

The scale factors and distortions can be found by implicit differentiation of equation (3.4.2.3). They are given by

$$k = \frac{\sqrt{8}}{\pi}\frac{1}{\cos(\phi)}\cos(\theta), \tag{3.4.2.11}$$

$$h = \frac{\sqrt{\sec^2(\theta)\cos^2(\phi)(4\lambda^2\tan^2(\theta) + \pi^2)}}{2\sqrt{2}}, \tag{3.4.2.12}$$

$$a' = \sqrt{k^2 + h^2 + 2}, \tag{3.4.2.13}$$

$$b' = \sqrt{k^2 + h^2 - 2}, \tag{3.4.2.14}$$

$$\omega = 2\arcsin\left(\frac{b'}{a'}\right), \tag{3.4.2.15}$$

$$s = 1. \tag{3.4.2.16}$$

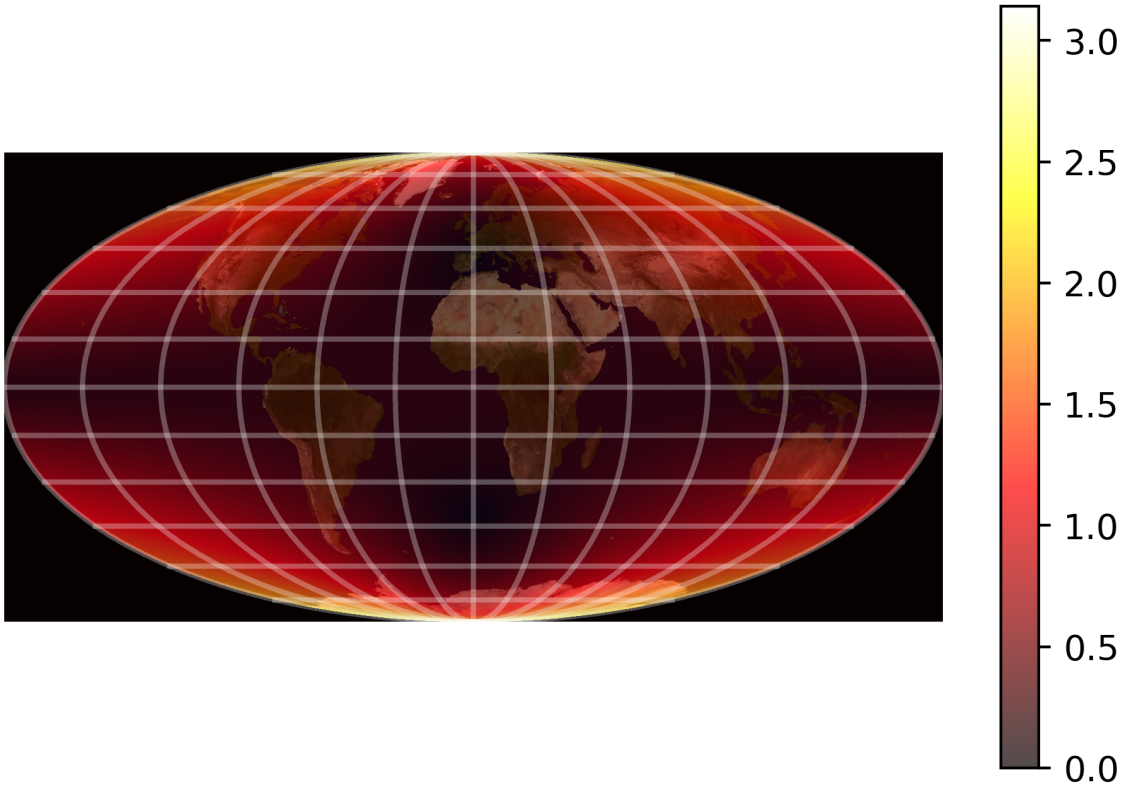

Figure 65: Mollweide projection angular distortion heat map. The angular distortion increases as one moves away from the Equator and the Central Meridian.

Similar to the Sinusoidal projection, the angular distortion increases as one moves away from the Equator and the Central meridian.

3.4.3 Eckert IV projection

Continuing with equal-area pseudocylindrical projections, the Eckert IV projection has equally spaced elliptical arcs and unequally-spaced straight lines for meridians and parallels respectively. The poles are straight lines, half as long as the Equator. The equations are given by:

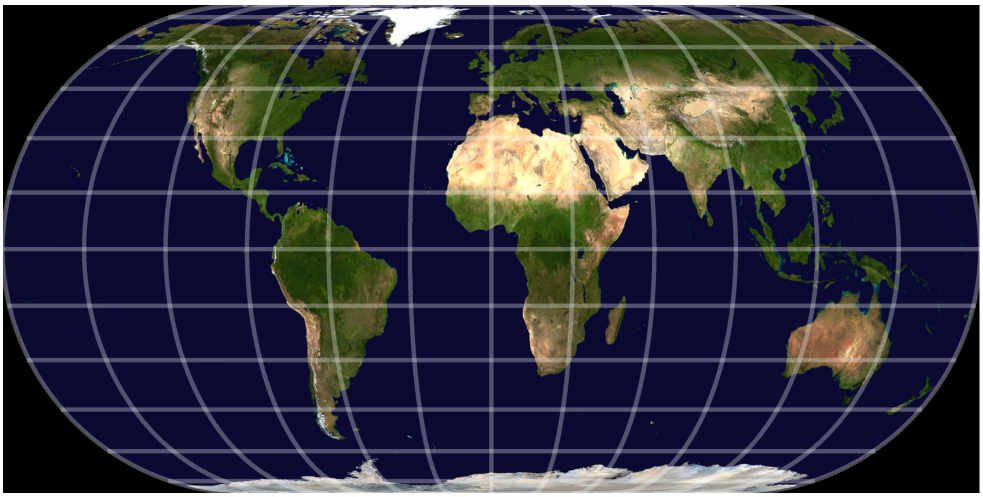

Figure 66: Eckert IV projection. The equations are given by (3.4.3.1) and (3.4.3.2). The map is equal-area, but not conformal. It has equally spaced elliptical arcs for meridians and unequally-spaced straight lines for parallels. The poles are represented as straight lines which are half as long as the Equator.

$$x(\phi,\lambda) = \frac{2}{\sqrt{\pi(4+\pi)}} R\lambda\left(1+\cos(\theta)\right), \tag{3.4.3.1}$$

$$y(\phi,\lambda) = 2\sqrt{\frac{\pi}{4+\pi}} R\sin(\theta), \tag{3.4.3.2}$$

where θ is found from

$$\theta + \sin(\theta)\cos(\theta) + 2\sin(\theta) = (2+\pi/2)\sin(\phi). \tag{3.4.3.3}$$

We have that θ takes values approximately in the range $[-5.49247, 5.49247]$. Equation (3.4.3.3) can be solved using a Newton-Raphson iteration [12] with $\phi/2$ as initial guess:

$$\Delta\theta = -\frac{\theta + \sin(\theta)\cos(\theta) + 2\sin(\theta) - (2+\pi/2)\sin(\phi)}{2\cos(\theta)\Big(1+\cos(\theta)\Big)}. \tag{3.4.3.4}$$

$\Delta\theta$ is to be added to the preceding θ to obtain the next θ. This calculation is repeated until $\Delta\theta$ is smaller than a predetermined value $\epsilon \in \mathbb{R}_{>0}$, in which case the requested accuracy for θ has been obtained. The range is the union of two ellipes and a rectangle:

$$\left\{(x,y)|\ \left(x - \frac{2R\pi}{\sqrt{\pi(4+\pi)}}\right)^2 \frac{\pi(4+\pi)}{4R^2\pi^2} + y^2\frac{4+\pi}{4R^2\pi} \le 1\right\}$$
$$\cup \left\{(x,y)|\ \left(x + \frac{2R\pi}{\sqrt{\pi(4+\pi)}}\right)^2 \frac{\pi(4+\pi)}{4R^2\pi^2} + y^2\frac{4+\pi}{4R^2\pi} \le 1\right\}$$
$$\cup \left\{(x,y)|\ x \in \left[\frac{-2R\pi}{\sqrt{\pi(4+\pi)}}, \frac{2R\pi}{\sqrt{\pi(4+\pi)}}\right], y \in \left[-2R\sqrt{\frac{\pi}{4+\pi}}, 2R\sqrt{\frac{\pi}{4+\pi}}\right]\right\}.$$

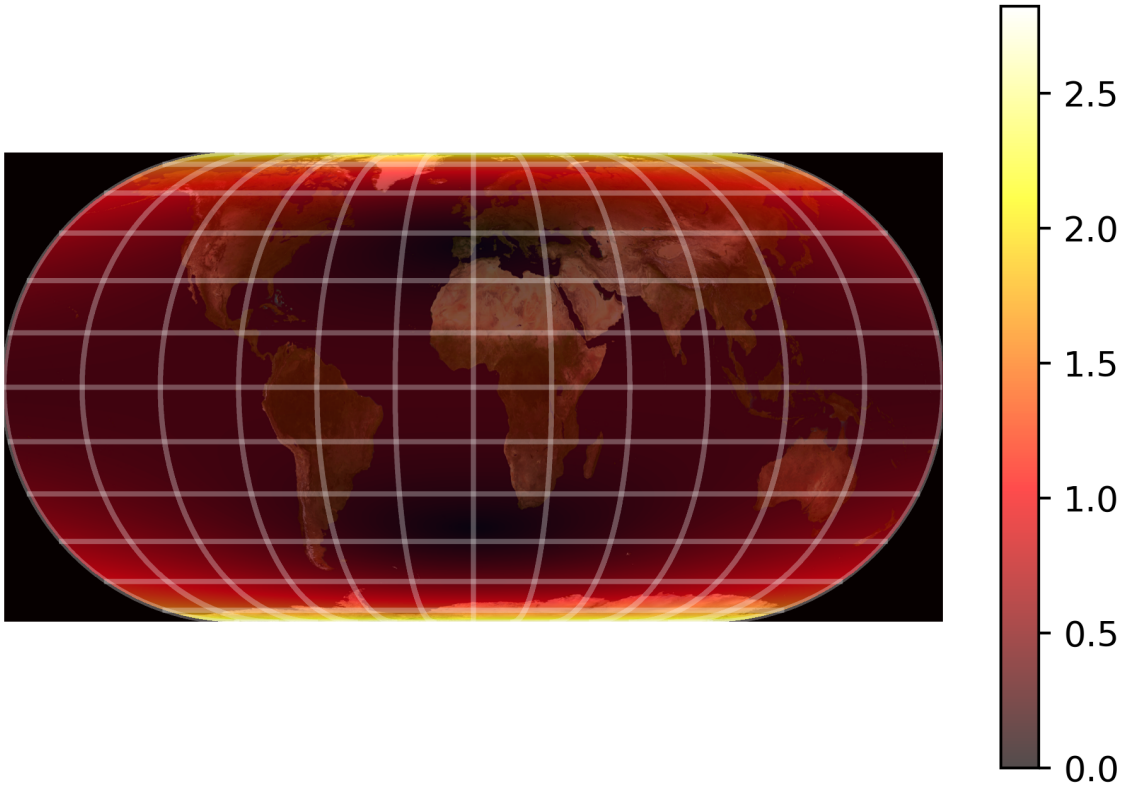

Figure 67: Eckert IV projection angular distortion heat map corresponding to Figure 66. The only two parallels with correct scale are at $\phi = \pm\frac{9\pi}{40}$. The only points without angular distortion are at the intersection of these parallels and the Central Meridian. As one moves away from these points, and especially towards the poles, the angular distortion increases, but overall is rather low.

The inverse equations do not require any iteration:

$$\theta = \arcsin\left(\frac{y\sqrt{4+\pi}}{2\sqrt{\pi}R}\right), \tag{3.4.3.5}$$

$$\lambda(x,y) = \frac{\sqrt{\pi(4+\pi)}x}{2R(1+\cos(\theta))}, \tag{3.4.3.6}$$

$$\phi(x,y) = \arcsin\left(\frac{\theta + \sin(\theta)\cos(\theta) + 2\sin(\theta)}{2+\pi/2}\right). \tag{3.4.3.7}$$

The scale factors and distortions can be found by implicit differentiation and are given by

$$k = \frac{2}{\sqrt{\pi(4+\pi)}}\frac{1}{\cos(\phi)}(1+\cos(\theta)), \tag{3.4.3.8}$$

$$h = \frac{4+\pi}{8}\sqrt{\sec^4(\theta/2)\cos^2(\theta)\left(\frac{4\pi}{4+\pi}\lambda^2\tan^2(\theta) + \frac{4}{\pi(4+\pi)}\right)}, \tag{3.4.3.9}$$

$$a' = \sqrt{k^2+h^2+2}, \tag{3.4.3.10}$$

$$b' = \sqrt{k^2+h^2-2}, \tag{3.4.3.11}$$

$$\omega = 2\arcsin\left(\frac{b'}{a'}\right), \tag{3.4.3.12}$$

$$s = 1. \tag{3.4.3.13}$$

The only two parallels with correct scale are at $\phi = \pm\frac{9\pi}{40}$. Where these parallels intersect the Central Meridian are the only two points without angular distortion. Moving away from these points, and especially towards the poles, the distortion increases. Overall, however, the angular distortion is rather low.

3.4.4 Eckert VI projection

Related to the Eckert IV projection, the Eckert VI is an equal-area psuedocylindrical projection which has unequally-spaced straight lines for parallels. Furthermore, the poles are depicted as straight, horizontal lines half as long as the Equator. In contrast to the Eckert IV, however, the meridians are equally spaced sinusoidal curves, except for the Central meridian, which is a straight line. Again, the equations require iteration and are given by:

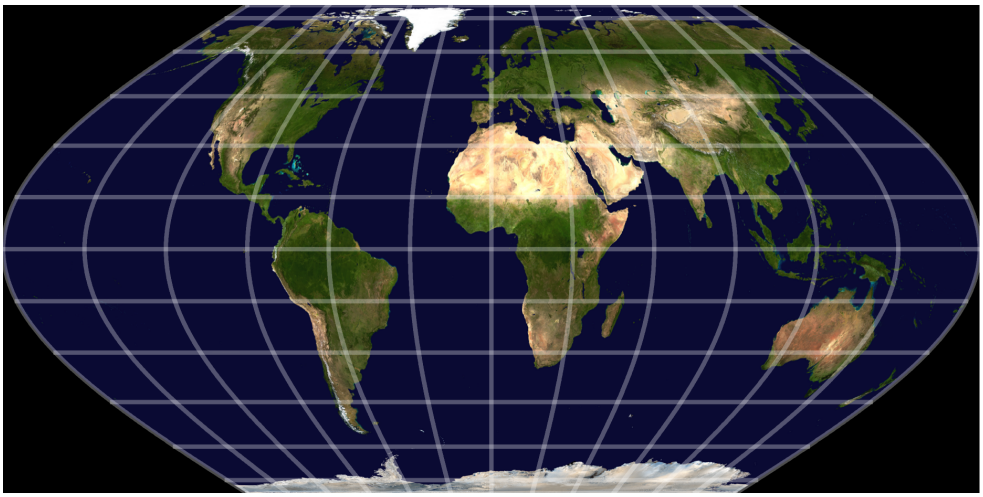

Figure 68: Eckert VI projection. The equations are given by (3.4.4.1) and (3.4.4.2). It is equal-area, but not conformal. Similar to the Sinusoidal projection, the parallels are drawn as unequally spaced straight lines and the meridians as equally spaced sinusoidal curves. In contrast to the Sinusoidal projection, the poles are not represented as points, but as straight lines half as long as the Equator.

$$x(\phi,\lambda) = \frac{R\lambda\,(1+\cos(\theta))}{\sqrt{2+\pi}}, \tag{3.4.4.1}$$

$$y(\phi,\lambda) = \frac{2R\theta}{\sqrt{2+\pi}}. \tag{3.4.4.2}$$

where θ is found from

$$\theta + \sin(\theta) = (1+\pi/2)\sin(\phi). \tag{3.4.4.3}$$

We have that θ takes values in $[-\pi/2, \pi/2]$. Equation (3.4.4.3) can be solved using a Newton-Raphson iteration [12] with ϕ as initial guess:

$$\Delta\theta = -\frac{\theta + \sin(\theta) - (1+\pi/2)\sin(\phi)}{1+\cos(\theta)}. \tag{3.4.4.4}$$

Every iteration, $\Delta\theta$ is added to θ to obtain the next value for θ. This is repeated until $\Delta\theta$ is smaller than a predetermined $\epsilon \in \mathbb{R}_{>0}$. The value of θ is then used to obtain the x and y-coordinates. The range is given by

$$\left\{(x,y)|\ -\frac{R\pi}{\sqrt{2+\pi}}\left(1+\cos\left(\frac{y\sqrt{2+\pi\}}}{2R}\right)\right) \le x \le \frac{R\pi}{\sqrt{2+\pi}}\left(1+\cos\left(\frac{y\sqrt{2+\pi\}}}{2R}\right)\right),\right.$$
$$\left. -\frac{R\pi}{\sqrt{2+\pi}} \le y \le \frac{R\pi}{\sqrt{2+\pi}}\right\}. \tag{3.4.4.5}$$

The inverse equations do not require iteration and are given by:

$$\theta = \frac{y\sqrt{2+\pi}}{2R}, \tag{3.4.4.6}$$

$$\lambda(x,y) = \frac{\sqrt{2+\pi}x}{R(1+\cos(\theta))}, \tag{3.4.4.7}$$

$$\phi(x,y) = \arcsin\left(\frac{\theta+\sin(\theta)}{1+\pi/2}\right). \tag{3.4.4.8}$$

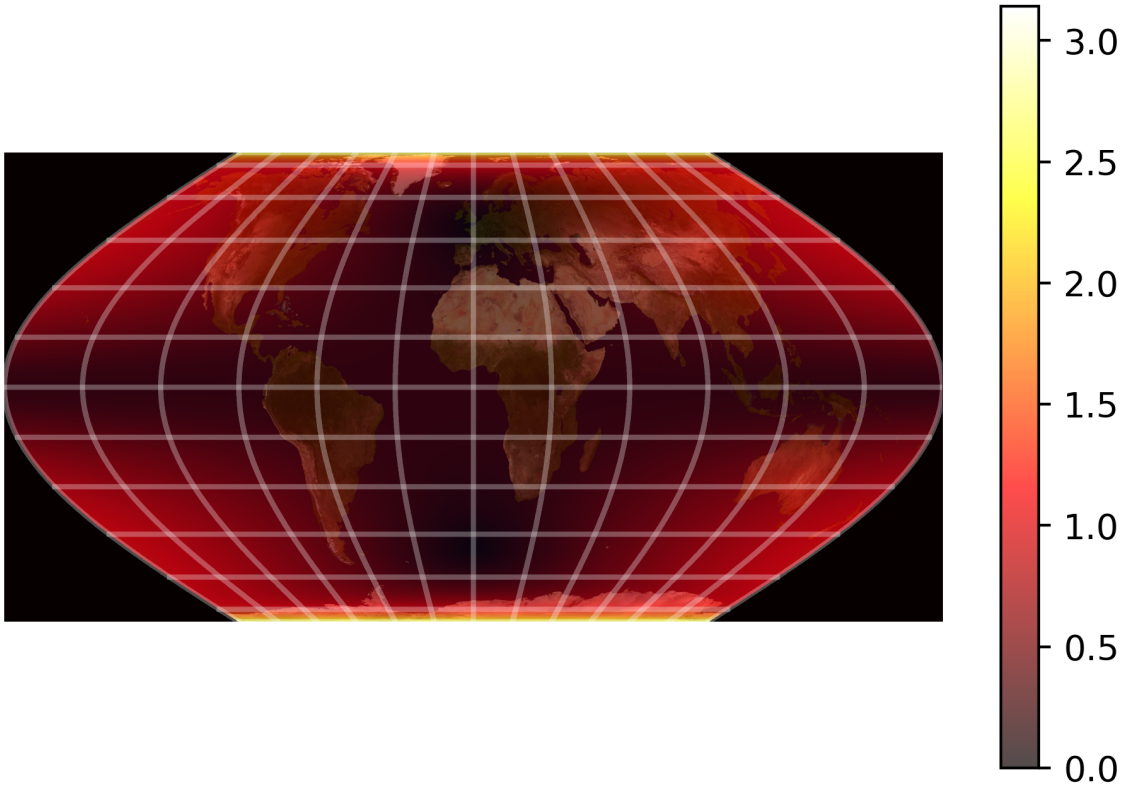

Figure 69: Eckert VI projection angular distortion heat map. The only two parallels with correct scale are at $\phi = \pm\frac{739\pi}{2700}$. Where these parallels intersect the Central Meridian are the only two points without angular distortion. Moving away from these points, and especially towards the poles, the distortion increases.

The scale factors and distortions can be found by using implicit differentiation and are given by

$$k = \frac{(1+\cos(\theta))}{\cos(\phi)\sqrt{2+\pi}}, \tag{3.4.4.9}$$

$$h = \frac{\sqrt{2+\pi}}{2}\frac{\cos(\phi)}{1+\cos(\phi)}\sqrt{\lambda^2\sin^2(\theta)+4}, \tag{3.4.4.10}$$

$$a' = \sqrt{k^2+h^2+2}, \tag{3.4.4.11}$$

$$b' = \sqrt{k^2+h^2-2}, \tag{3.4.4.12}$$

$$\omega = 2\arcsin\left(\frac{b'}{a'}\right), \tag{3.4.4.13}$$

$$s = 1. \tag{3.4.4.14}$$

The only two parallels with correct scale are at $\phi = \pm\frac{739\pi}{2700}$. Where these parallels intersect the Central meridian are the only two points without angular distortion. Moving away from these points, and especially towards the poles, the distortion increases.

3.4.5 Van der Grinten projection

The Van der Grinten projection was created by combining the Mercator projection with the curves of the Mollweide projection [12]. This resulted in a projection which is neither conformal nor equal-area, but does have limited distortion, except at the poles. It encloses the entire surface of the sphere in a circle and apart from the Central meridian and the Equator, all parallels and meridians are arcs of circles. Furthermore, the Equator is true to scale. The equations are given by:

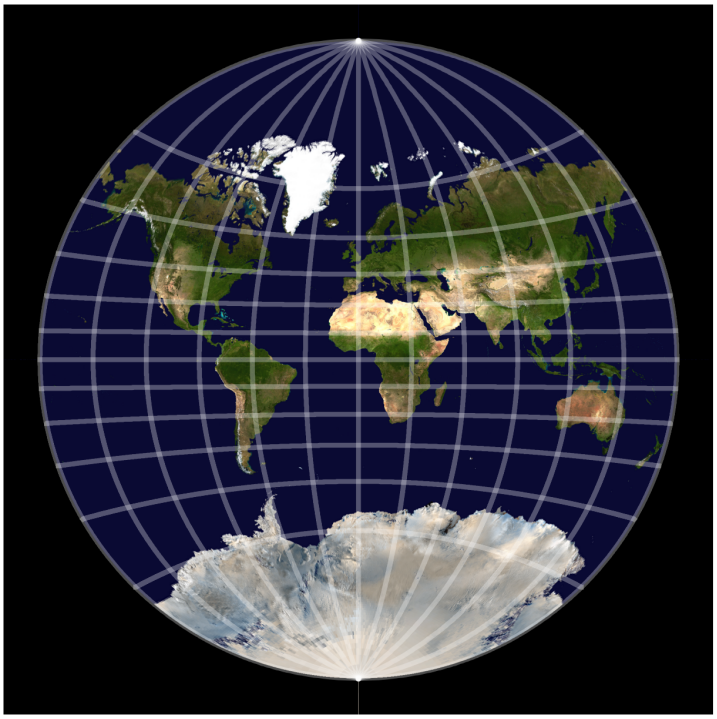

Figure 70: Van der Grinten projection. The equations are given by (3.4.5.1 - 3.4.5.7). The whole map is contained in a circle and except for the Central Meridian and Equator, all meridians and parallels are circular arcs. It is neither conformal nor equal-area.

$$x(\phi,\lambda) = \operatorname{sgn}(\lambda)\pi R\frac{A(G-P^2)+\sqrt{A^2(G-P^2)^2-(P^2+A^2)(G^2-P^2)}}{P^2+A^2}, \tag{3.4.5.1}$$

$$y(\phi,\lambda) = \operatorname{sgn}(\phi)\pi R\frac{PQ-A\sqrt{(A^2+1)(P^2+A^2)-Q^2}}{P^2+A^2}, \tag{3.4.5.2}$$

where

$$A = \frac{1}{2}\left|\frac{\pi}{\lambda}-\frac{\lambda}{\pi}\right|, \tag{3.4.5.3}$$

$$G = \frac{\cos(\theta)}{\sin(\theta)+\cos(\theta)-1}, \tag{3.4.5.4}$$

$$P = \frac{2G}{\sin(\theta)}-G, \tag{3.4.5.5}$$

$$\theta = \arcsin\left|\frac{2\phi}{\pi}\right|, \tag{3.4.5.6}$$

$$Q = A^2+G. \tag{3.4.5.7}$$

If $\phi = 0$, however, G and P given by equations (3.4.5.4) and (3.4.5.5) are indeterminate and instead we have that along the Equator, the x-coordinate is simply the longitude:

$$x(\phi,\lambda) = R\lambda, \tag{3.4.5.8}$$

$$y(\phi,\lambda) = 0. \tag{3.4.5.9}$$

Furthermore, if $\lambda = 0$ or $\phi = \pm\pi/2$, A or G given by equations (3.4.5.3) and (3.4.5.4) are indeterminate, in which case

$$x(\phi,\lambda) = 0, \tag{3.4.5.10}$$

$$y(\phi,\lambda) = \operatorname{sgn}(\phi)\pi R\tan(\theta/2). \tag{3.4.5.11}$$

The range of the projection is the circle $\{(x,y)|\ x^2+y^2 \le \pi^2R^2\}$. The inverse equations are

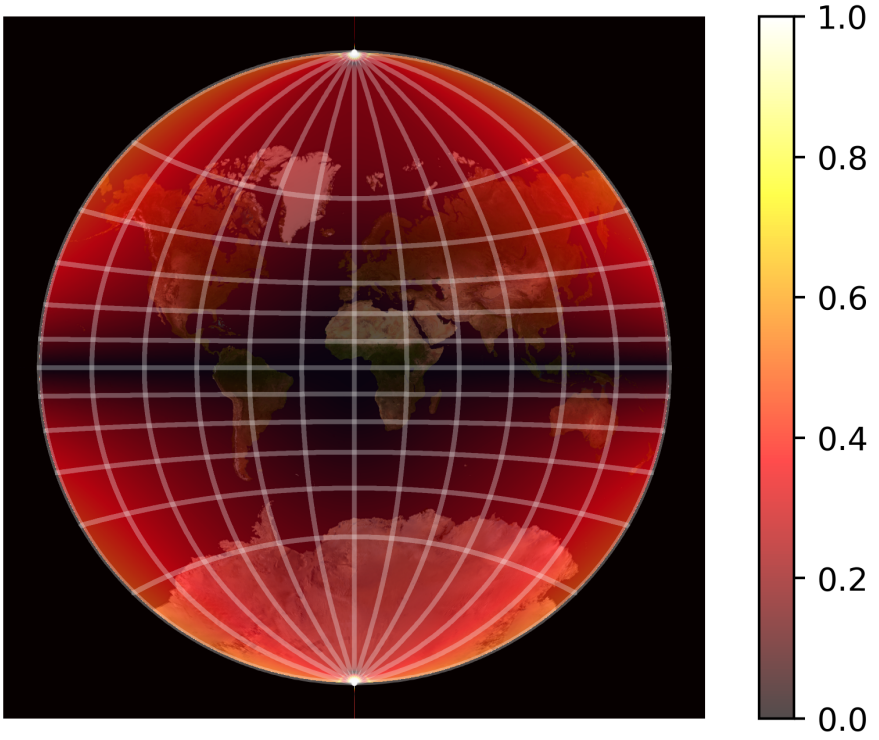

Figure 71: Van der Grinten projection angular distortion heat map. The angular distortion is lowest along the Equator as well as a part of the Central Meridian.

given in order of use:

$$X = x/(\pi R), \tag{3.4.5.12}$$

$$Y = y/(\pi R), \tag{3.4.5.13}$$

$$c_1 = -|Y|(1 + X^2 + Y^2), \tag{3.4.5.14}$$

$$c_2 = c_1 - 2Y^2 + X^2, \tag{3.4.5.15}$$

$$c_3 = -2c_1 + 1 + 2Y^2 + (X^2 + Y^2)^2, \tag{3.4.5.16}$$

$$d = \frac{Y^2}{c_3} + \frac{2c_2^3}{27c_3^3} - \frac{9c_1c_2}{27c_3^2}, \tag{3.4.5.17}$$

$$a_1 = \frac{3c_1c_3 - c_2^2}{3c_3^2}, \tag{3.4.5.18}$$

$$m_1 = 2\sqrt{-a_1/3}, \tag{3.4.5.19}$$

$$\theta_1 = \frac{1}{3}\arccos\left(\frac{3d}{a_1m_1}\right), \tag{3.4.5.20}$$

$$\phi(x, y) = \pi\,\mathrm{sgn}(y)\left(-m_1\cos(\theta_1 + \pi/3) - \frac{c_2}{3c_3}\right), \tag{3.4.5.21}$$

$$\lambda(x, y) = \frac{\pi\left(X^2 + Y^2 - 1 + \sqrt{1 + 2(X^2 - Y^2) + (X^2 + Y^2)^2}\right)}{2X},\ X \neq 0, \tag{3.4.5.22}$$

If $X = 0$, equation (3.4.5.22) is indeterminate, in which case we set $\lambda = 0$.

The formulas for the scale factors and distortions are rather complicated and lengthy and are hence not included. Instead, singular value decomposition and central differences are used to obtain the plots for the distortions. From reviewing the Figures (71) and (72), the distortion in area increases rapidly as one approaches the poles. The angular distortion seems to be limited, and increases as one moves away from the Equator and Central meridian.

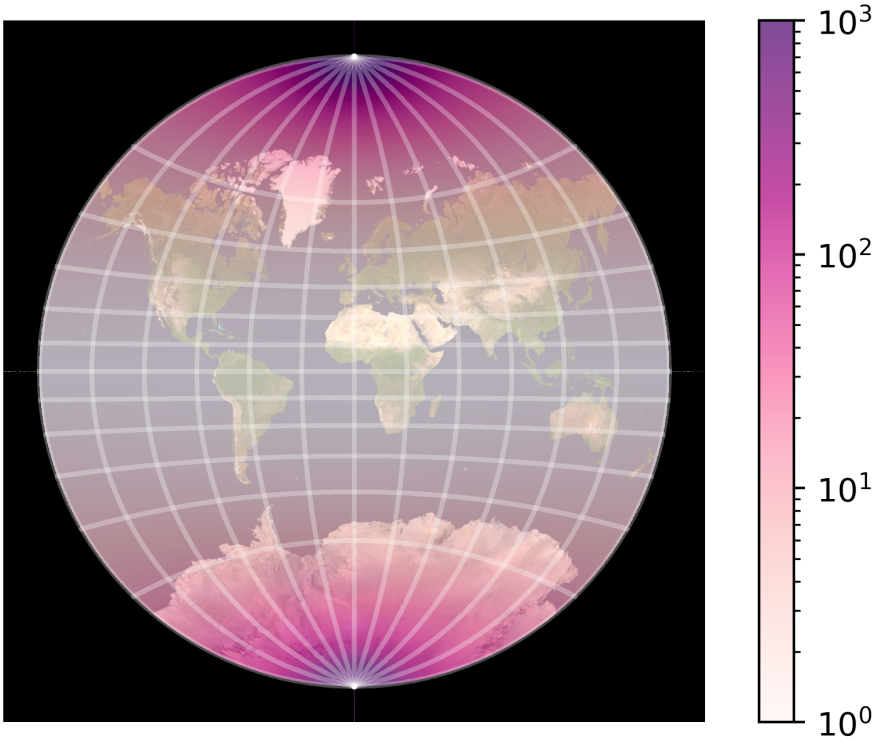

Figure 72: Van der Grinten projection area distortion heatmap. In order to produce a coherent heatmap, the legend has been capped at a factor of 10^3. The distortion in area is especially noticeable in the polar regions, where it approaches infinity.

4 Methodology and results

This chapter will tackle the main question: "What is the best map projection?" To do so, we will first address the methodology, after which the results will be given and discussed.

4.1 Methodology

To answer the question of what the best map projection is, we will rank the projections according to their distortions on three different values: angular distortion, distortion in area size and a combination of both. In order to do so, we must define a measure that quantifies these distortions, which henceforth will be called a distortion number.

For the area distortion number μ_s, we use the average of the absolute value of the natural logarithm of the area distortion factor s over the whole sphere:

$$\mu_s = \frac{1}{4\pi} \int_{-\pi/2}^{\pi/2} \int_{-\pi}^{\pi} |\ln(s(\phi,\lambda))| \cos(\phi)\, d\lambda d\phi. \tag{4.1.0.1}$$

Here, we use that

$$\frac{1}{4\pi} \int_{-\pi/2}^{\pi/2} \int_{-\pi}^{\pi} f(\phi,\lambda)\cos(\phi) d\lambda d\phi,$$

is the average of a function $f(\phi,\lambda)$ over the sphere; the cosine factor represents the Jacobian. As the local area distortion s is a multiplicative factor, we want an area inflation by a factor of 100 to contribute to the average equally as much as a factor of $\frac{1}{100}$. Hence, the absolute value of the natural logarithm of s is taken, which ensures that a number and its reciprocal give the same value when taking the average. Furthermore, as $\ln(1) = 0$, we have that a factor of 1, indicating no area distortion, correctly contributes with 0 when taking the average. The closer μ_s is to zero, the lower the area distortion is and hence the better the projection scores.

For the angular distortion number μ_ω, we rank according to the average angular distortion over the whole sphere:

$$\mu_\omega = \frac{1}{4\pi} \int_{-\pi/2}^{\pi/2} \int_{-\pi}^{\pi} \omega(\phi,\lambda)\cos(\phi)\, d\lambda d\phi, \tag{4.1.0.2}$$

Here, $\omega(\phi,\lambda)$ is the angular distortion at a given point (ϕ,λ). Again, the closer μ_ω is to 0, the better the map projections scores. As desired, conformal maps will have $\mu_\omega = 0$, which follows from the fact that conformal maps have the property that $\omega(\phi,\lambda) = 0$ for all ϕ and for all λ.

We now define the (combined) distortion number μ with the Tissot's Indicatrix in mind. As the semi-minor and semi-major axes a and b (which are the maximum and minimum scale factors in a point) of the ellipse respectively are related to both the area distortion and angular distortion by equations (2.9.1.17) and (2.9.2.10):

$$\sin\left(\frac{\omega}{2}\right) = \frac{|a-b|}{a+b},$$
$$s = ab,$$

we have that the closer a and b are to 1, the lower the angular and area distortion will be. Geometrically, this makes sense, as this implies that the Tissot's Indicatrix will remain a circle of the same area. Hence, we will rank according to the average of the sum of the natural logarithm of a and b:

$$\mu = \frac{1}{4\pi} \int_{-\pi/2}^{\pi/2} \int_{-\pi}^{\pi} (|\ln(a(\phi,\lambda))| + |\ln(b(\phi,\lambda))|)\cos(\phi)\, d\lambda d\phi. \tag{4.1.0.3}$$

With the same reasoning as before, as a and b are scale factors, the absolute value of the natural logarithm equally weighs a factor and its reciprocal when taking the average. Furthermore, when a and b are close to 1, $|\ln(a)|$ and $|\ln(b)|$ will be close to zero and hence taking the average of their sum serves as a good measure for ranking the projections.

For the azimuthal projections, which sometimes display only part of the sphere, all of the distortion numbers will only be determined by the points which are actually in the range. For the Orthographic projection, these are the points (ϕ, λ) for which the distance to the center is smaller than or equal to $\frac{\pi}{2}$. In section (2.5), we found that this is equivalent to

$$\cos(c) = \sin(\phi_1)\sin(\phi) + \cos(\phi_1)\cos(\phi)\cos(\lambda) \geq 0, \tag{4.1.0.4}$$

where $(\phi_1, 0)$ is the center of the projection. For a set A, an indicator function is defined as

$$\mathbb{1}_A(x) = \begin{cases} 1 & \text{if } x \in A, \\ 0 & \text{if } x \notin A. \end{cases} \tag{4.1.0.5}$$

Hence, the average for a function $f(\phi, \lambda)$ used in the distortion numbers for the Orthographic projection is given by

$$\frac{1}{2\pi}\int_{-\pi/2}^{\pi/2}\int_{-\pi}^{\pi} f(\phi,\lambda)\cos(\phi)\mathbb{1}_{\{(\phi,\lambda)|\cos(c)\geq 0\}}(\phi,\lambda)d\lambda d\phi, \tag{4.1.0.6}$$

where $\mathbb{1}_{\{(\phi,\lambda)|\cos(c)\geq 0\}}(\phi,\lambda)$ is an indicator function. Consequently, the averages for the Gnomonic projection are calculated as

$$\frac{1}{2\pi}\int_{-\pi/2}^{\pi/2}\int_{-\pi}^{\pi} f(\phi,\lambda)\cos(\phi)\mathbb{1}_{\{(\phi,\lambda)|\cos(c)> 0\}}(\phi,\lambda)d\lambda d\phi. \tag{4.1.0.7}$$

As not all of these distortion numbers can be calculated analytically, they will be computed numerically using Python [13]. An example of numerically calculating these averages is the following piece of pseudocode:

```
total = 0
total_normal = 0
steps = 1000
lambdas = np.linspace(-math.pi, math.pi, num=steps*2)
phis = np.linspace(-math.pi/2, math.pi/2, num=steps)
for phi in phis:
    for lambda in lambdas:
        distortion_value = *FUNCTION OF PHI AND LAMBDA*
        total  = total + distortion_value*math.cos(phi)
        total_normal = total_normal + math.cos(phi)
return total/total_normal.
```

For the Orthographic and Gnomonic projection, it is checked whether the point is actually projected before using it in the average:

```
total = 0
total_normal = 0
steps = 1000
lambdas = np.linspace(-math.pi, math.pi, num=steps*2)
phis = np.linspace(-math.pi/2, math.pi/2, num=steps)
for phi in phis:
    for lambda in lambdas:
        if (cos(c) < 0) continue  # if using Orthographic, or
        if (cos(c) <= 0) continue # if using Gnomonic
        distortion_value = *FUNCTION OF PHI AND LAMBDA*
        total  = total + distortion_value*math.cos(phi)
        total_normal = total_normal + math.cos(phi)
return total/total_normal
```

In the next section, the results are computed according to the discussed methodology and collected into a table, after which they are analysed.

Projection	μ_ω	μ_s	μ
Central cylindrical projection	0.2938	0.9205	0.9205
Mercator projection	0	0.6137	0.6137
Cylindrical equal-area projection	0.5390	0	0.6137
Transverse Mercator	0	0.6131	0.6131
Albers equal-area conic projection ($\phi_1 = 0$ and $\phi_2 = -\pi/3$)	0.5364	0	0.6084
Albers equal-area conic projection ($\phi_1 = \pi/4$ and $\phi_2 = \pi/3$)	0.7142	0	0.8290
Lambert conformal conic projection ($\phi_1 = \pi/5$ and $\phi_2 = -\pi/3$)	0	0.7062	0.7062
Bonne projection	0.6993	0	0.7513
Lambert azimuthal equal-area projection ($\phi_1 = 0$)	0.8596	0	1.001
Orthographic projection ($\phi_1 = 0$)	0.8606	1.003	1.003
(polar) Orthographic projection ($\phi_1 = \pi/2$)	0.8584	0.9989	0.9989
Stereographic projection ($\phi_1 = 0$)	0	1.998	1.998
(polar) Stereographic projection ($\phi_1 = \pi/2$)	0	1.999	1.999
Gnomonic projection ($\phi_1 = 0$)	0.8605	3.010	3.010
(polar) Gnomonic projection ($\phi_1 = \pi/2$)	0.8583	2.997	2.997
Sinusoidal projection	0.6807	0	0.7282
Mollweide projection	0.5636	0	0.5928
Eckert IV projection	0.5016	0	0.5287
Eckert VI projection	0.5664	0	0.5929
Van der Grinten projection	0.1409	0.5458	0.5471

Table 2: Distortion results. For every projection, the values for the distortion numbers μ_ω, μ_s and μ defined in the previous section are given. Projections that include a parameter may occur multiple times, as this parameter could influence the values of the distortion numbers.

4.2 Distortion results

This section will discuss the results of ranking the projections according to the distortion numbers defined in the previous section. Table 2 shows the values of the distortion numbers of the map projections. The rows represent the different map projections, whereas the columns are the three different distortion numbers defined in the previous section.

A number of observations can be made from Table 2. For one, as expected, the μ_ω and the μ_s are 0 for all conformal and equal-area projections, respectively. Not counting the conformal projections, the Van der Grinten projection appears to have the lowest angular distortion according to our angular distortion number. Similarly, apart from the equal-area projections, it is again the Van der Grinten projection that scores best in the area distortion category. However, if we examine the distortion number μ, we find the Eckert IV to have the lowest overall distortion, winning by a small margin from the Van der Grinten projection.

More interestingly however, one may notice that μ_s and μ are equal for many projections. Examining these projections, as well as our definitions for μ_s and μ given by (4.1.0.1) and (4.1.0.3),

$$\mu_s = \frac{1}{4\pi} \int_{-\pi/2}^{\pi/2} \int_{-\pi}^{\pi} |\ln(s(\phi,\lambda))| \cos(\phi)\, d\lambda d\phi,$$

$$\mu = \frac{1}{4\pi} \int_{-\pi/2}^{\pi/2} \int_{-\pi}^{\pi} (|\ln(a(\phi,\lambda))| + |\ln(b(\phi,\lambda))|) \cos(\phi)\, d\lambda d\phi,$$

we have found the scale factors of these projections to be greater or equal to one, meaning these maps only feature scale expansion and no scale compression. From this follows that both the area distortion factor $s(\phi,\lambda)$ as well as the maximum and minimum scale factors

of a point a and b are greater or equal to one. Thus, if $a \geq 1$ and $b \geq 1$, we have that

$$|\ln(s(\phi,\lambda))| = |\ln(ab)| = |\ln(a) + \ln(b)| = \ln(a) + \ln(b) = |\ln(a)| + |\ln(b)|. \tag{4.2.0.1}$$

Hence, if the scale factors are greater or equal to one, μ_s and μ will be equal. This also implies that as μ and μ_s are equal, μ does not take into account the angular distortion for said projections.

Another interesting observation is the values of μ and μ_s for the azimuthal projections. These values are approximately 1, 2 and 3 for the Orthographic, Stereographic and Gnomonic projection respectively. Numerically, the error is less than 1%. We can confirm this analytically for the North Polar perspectives, which is sufficient as the value for μ is invariant under rotation for these three projections. We start with the Orthographic projection:

$$\begin{aligned}
a &= k' = 1, \\
b &= h' = \sin(\phi), \\
\mu &= \frac{1}{2\pi}\int_0^{\pi/2}\int_{-\pi}^{\pi}(|\ln(a(\phi,\lambda))| + |\ln(b(\phi,\lambda))|)\cos(\phi)d\lambda d\phi \\
&= \frac{1}{2\pi}\int_0^{\pi/2}\int_{-\pi}^{\pi}(|\ln(1)| + |\ln(\sin(\phi))|)\cos(\phi)d\lambda d\phi \\
&= \int_0^{\pi/2}|\ln(\sin(\phi))|\cos(\phi)d\phi \\
&= -\int_0^{\pi/2}\ln(\sin(\phi))d(\sin(\phi)) \\
&= [-\sin(\phi)\ln(\sin(\phi)) + \sin(\phi)]_0^{\pi/2} \\
&= 1.
\end{aligned} \tag{4.2.0.2}$$

The calculation for the North Polar Stereographic projection is as follows:

$$\begin{aligned}
a = b = k &= \frac{2}{1+\sin(\phi)}, \\
\mu &= \frac{1}{4\pi}\int_{-\pi/2}^{\pi/2}\int_{-\pi}^{\pi}(|\ln(a(\phi,\lambda))| + |\ln(b(\phi,\lambda))|)\cos(\phi)d\lambda d\phi \\
&= \frac{1}{4\pi}\int_{-\pi/2}^{\pi/2}\int_{-\pi}^{\pi}\left(\left|\ln\left(\frac{2}{1+\sin(\phi)}\right)\right| + \left|\ln\left(\frac{2}{1+\sin(\phi)}\right)\right|\right)\cos(\phi)d\lambda d\phi \\
&= \frac{1}{2}\int_{-\pi/2}^{\pi/2}\left(\left|\ln\left(\frac{2}{1+\sin(\phi)}\right)\right| + \left|\ln\left(\frac{2}{1+\sin(\phi)}\right)\right|\right)\cos(\phi)d\phi \\
&= \int_{-\pi/2}^{\pi/2}(\ln(2) - \ln(1+\sin(\phi))\cos(\phi)d\phi \\
&= \int_{\phi=-\pi/2}^{\phi=\pi/2}(\ln(2) - \ln(1+\sin(\phi))d(\sin(\phi)) \\
&= 2.
\end{aligned} \tag{4.2.0.3}$$

The calculation for the North Polar Gnomonic projection is as follows:

$$\begin{aligned}
a &= k' = \frac{1}{\sin(\phi)}, \\
b &= h' = \frac{1}{\sin(\phi)^2}, \\
\mu &= \frac{1}{2\pi}\int_0^{\pi/2}\int_{-\pi}^{\pi}(|\ln(a(\phi,\lambda))| + |\ln(b(\phi,\lambda))|)\cos(\phi)d\lambda d\phi \\
&= \frac{1}{2\pi}\int_0^{\pi/2}\int_{-\pi}^{\pi}\left(\left|\ln\left(\frac{1}{\sin(\phi)}\right)\right| + \left|\ln\left(\frac{1}{\sin(\phi)^2}\right)\right|\right)\cos(\phi)d\lambda d\phi \\
&= \int_0^{\pi/2}\left(\left|\ln\left(\frac{1}{\sin(\phi)}\right)\right| + \left|\ln\left(\frac{1}{\sin(\phi)^2}\right)\right|\right)\cos(\phi)d\phi \\
&= -3\int_{\phi=0}^{\phi=\pi/2}\ln(\sin(\phi))d(\sin(\phi)) \\
&= 3. \qquad (4.2.0.4)
\end{aligned}$$

In the next section, the flaw exposed by μ and μ_s being equal is examined and an attempt at an improvement in the area and combined distortion numbers is made.

4.3 Normalising the map projections

If we enlarge or shrink a map by scaling the x and y coordinates by a factor $c \in \mathbb{R}_{>0}$, the scaling factors will also be multiplied by c, which will lead to arbitrary $\ln(c)$ terms to appear in the calculations of our distortion numbers μ and μ_s. Thus, by linearly scaling the map, one can arbitrarily change the distortion numbers, which obviously is not desired. To remedy this, the finite map projections will be normalised to produce maps with an area of 4π (the area of a unit sphere, hence we choose the radius of the sphere $R = 1$ in this section). For the Orthographic projection, this will be 2π, as it can only display one hemisphere. In theory, this will allow for a fairer comparison of the projections. The following projections have a finite domain and can hence be normalised:

- Albers equal-area conic projection
- Lambert conformal conic projection
- Lambert azimuthal equal-area projection
- Orthographic projection
- Sinusoidal projection
- Mollweide projection
- Eckert IV projection
- Eckert VI projection
- Van der Grinten projection

The Orthographic projection, the Lambert azimuthal equal-area projection and the Van der Grinten projection are all circles of radius 1, 2 and π respectively. Hence, the maps are scaled by the factors 2, 1 and $\frac{4}{\pi^2}$ to obtain maps of area 2π, 4π and 4π respectively. The area of the Albers Equal-Area Conic projection can be calculated using polar coordinates $(r\cos(\theta), r\sin(\theta))$:

$$\iint_A dxdy = \int_{-n\pi}^{n\pi}\int_{\frac{C-2n}{n^2}}^{\frac{C+2n}{n^2}} rdrd\theta, \qquad (4.3.0.1)$$

if $n > 0$. Else, the upper and lower bounds of the integrals swap. Computing this for the standard parallels $\phi_1 = 0$ and $\phi_2 = -\pi/3$ gives 2π and hence requires a factor 2. For $\phi_1 = \pi/3$ and $\phi_2 = \pi/4$ we obtain an area of 4π and hence no scaling needs to be done. The areas of the Sinusoidal projection, Mollweide, Eckert IV projection and Eckert VI projection

Projection	Former μ_s	New μ_s	Former μ	New μ
Albers equal-area conic projection ($\phi_1 = 0$ and $\phi_2 = -\pi/3$)	0	0	0.6084	1.512
Albers equal-area conic projection ($\phi_1 = \pi/4$ and $\phi_2 = \pi/3$)	0	0	0.8290	0.8290
Lambert azimuthal equal-area projection ($\phi_1 = 0$)	0	0	1.001	1.001
Orthographic projection ($\phi_1 = 0$)	1.003	0.6962	1.003	1.111
(polar) Orthographic projection ($\phi_1 = \pi/2$)	0.9989	0.6921	0.9989	1.1063
Sinusoidal	0	0	0.7282	0.7282
Mollweide	0	0	0.5928	0.5928
Eckert IV	0	0	0.5287	0.5287
Eckert VI	0	0	0.5929	0.5929
Van der Grinten	0.5458	1.3453	0.5471	1.3527

Table 3: Normalised area and overall distortion results compared to the distortion results from the previous section. The rows correspond to the projections, for which both the former and new values obtained by normalising the maps for μ and μ_s are listed.

are simple double integrals over the ranges given in Chapter 3 and produce maps of area 4π, hence requiring no scaling either.

The results of the normalised maps are stated in Table 3. Firstly, for the Sinusoidal, Mollweide, Eckert IV and VI, one of the Albers equal-area conic projection and the Lambert azimuthal equal-area projection, no scaling was required and hence there is no change in their values. The value of μ for the Albers equal-area projection with $\phi_1 = 0$ and $\phi_2 = \pi/3$ increased significantly, now scoring much worse than the version with the standard parallels $\phi_1 = \pi/4$ and $\phi_2 = \pi/3$. From reviewing the figures of the maps, this is plausible, but it is difficult to say with certainty. Furthermore, the Orthographic projection is the only projection with a better score on its area distortion, but a slightly worse score on its combined distortion number μ. Lastly, the Van der Grinten has a stark increase in both its area and overall distortion score, now ranking among the worst discussed in this paper. Given that the Van der Grinten projection does not appear to have this much distortion when reviewing the map by eye, this leads us to believe that the distortion numbers in this section again do not provide a fair comparison. In the next section, a different approach for obtaining a fair ranking is discussed.

4.4 Minimising μ_s and μ

Rather than scaling the x and y-coordinates by a factor $c \in \mathbb{R}_{>0}$ such that the area of the maps are fixed at 4π, one can also find the values of c for which the distortion numbers μ_s and μ have the lowest values. These factors will be denoted by c_{μ_s} and c_μ respectively. Since this can be done for all projections, it is an improvement over the former method, which only considered projections with a finite area. To obtain the factors for which the distortion numbers are minimal, the Golden-section search algorithm [6] is used. However, this algorithm requires that there be only one minimum in the given interval in which we search for the minimum. Considering our problem intuitively, this is feasible; given that the factor c is simply a shift of all scaling factors, the logarithmic distance to 1 changes by the same value for all scale factors (as long as these are continuous). Taking the limit of c to 0 or to infinity both results in μ_s and μ going to infinity. Hence we can assume that, per projection, there exists one $c \in \mathbb{R}_{>0}$ for which the distortion numbers are minimal. To further justify this, one can consider Figure 73. It portrays the value of μ for the Van der Grinten projection for different values of c in the interval $[0.1, 5]$. As there appears to be only one minimum for this relatively complex projection, it is likely to assume this holds for all other (continuous) projections discussed in this paper.

A single step of the algorithm goes as follows: the algorithm takes three points u, v and w, for which the one in the in between the two other points, say w, has the lowest function value f_w. From this setup it is clear that the minimum must be in between the two points u and v adjacent to the point w with the lowest function value. Now a new point x is chosen

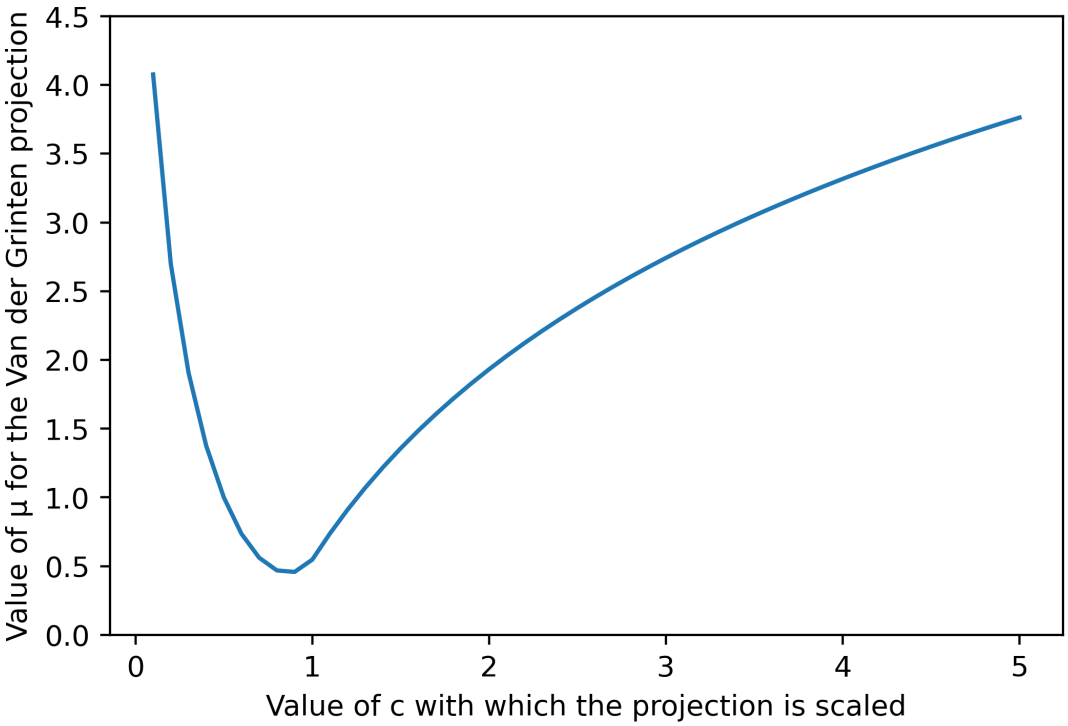

Figure 73: Plot of the value of μ for the Van der Grinten projection for 50 evenly spaced values of c in the interval $[0.1, 5]$. There appears to be only one minimum.

in between u and v. Independent of if f_x is larger or smaller than f_w, a new set of three points for which the point with the lowest function value is in between the other two can always be chosen, hence reducing the interval in which the minimum lies. The algorithm now continues with the newly chosen three points. This progressively reduces the size of the interval until it is smaller than a predetermined $\epsilon \in \mathbb{R}_{>0}$. For maximum efficiency, the four points are chosen such that their three intervals are in the ratio $\varphi : 1 : \varphi$, where φ is the golden ratio. The algorithm is demonstrated in the following piece of Python code. This particular implementation assumes the minimum is not at the edges u or v of the interval, but at the points w or x.

```
varphi = (math.sqrt(5) + 1) / 2
def gss(f, u, v, eps=1e-3):
    w = v - (v - u) / varphi
    x = u + (v - u) / varphi
    while abs(v - u) > eps:
        fw = f(w)
        fx = f(x)
        if fw < fx:
            v = x
        else:
            u = w
        w = v - (v - u) / varphi
        x = u + (v - u) / varphi

    return (((v + u) / 2), f((v + u) /2))
```

The minimised values for the distortion numbers μ_s and μ are given in Table 4. The rows represent the projections and the columns the values for c_{μ_s} and c_μ that produce the lowest scores for μ_s and μ, as well as the non-minimised ('former', as stated in the table) values from Section (4.2), for convenience. From the new values, a number of interesting observations can be made. For one, many of the values for c_{μ_s} and c_μ appear to either be

Projection	c_{μ_s}	Former μ_s	μ_s	c_μ	Former μ	μ
Central cylindrical projection	0.806	0.9205	0.7849	0.819	0.9205	0.7954
Mercator projection	0.866	0.6137	0.5232	0.866	0.6137	0.5232
Cylindrical equal-area projection	N/A	0	0	0.866	0.6137	0.5685
Transverse Mercator	0.866	0.6131	0.5230	0.866	0.6131	0.5230
Albers equal-area conic projection ($\phi_1 = 0$, $\phi_2 = -\frac{\pi}{3}$)	N/A	0	0	1.00	0.6084	0.6083
Albers equal-area conic projection ($\phi_1 = \frac{\pi}{4}$, $\phi_2 = \frac{\pi}{3}$)	N/A	0	0	0.999	0.8290	0.8290
Lambert conformal conic projection ($\phi_1 = \frac{\pi}{5}$, $\phi_2 = -\frac{\pi}{3}$)	1.28	0.7062	0.5763	1.28	0.7062	0.5763
Bonne projection ($\phi_1 = -\frac{\pi}{8}$)	N/A	0	0	1.00	0.7513	0.7513
Lambert azimuthal equal-area projection ($\phi_1 = 0$)	N/A	0	0	1.00	1.001	1.001
Orthographic projection ($\phi_1 = 0$)	1.414	1.003	0.6962	1.00	1.003	1.003
(polar) Orthographic projection ($\phi_1 = \frac{\pi}{2}$)	1.414	0.9989	0.6921	1.00	0.9989	0.9989
Stereographic projection ($\phi_1 = 0$)	0.500	1.998	1.388	0.500	1.998	1.338
(polar) Stereographic projection ($\phi_1 = \frac{\pi}{2}$)	0.500	1.999	1.386	0.500	1.999	1.386
Gnomonic projection ($\phi_1 = 0$)	0.353	3.010	2.089	0.382	3.010	2.170
(polar) Gnomonic projection ($\phi_1 = \frac{\pi}{2}$)	0.354	2.997	2.076	0.381	2.997	2.158
Sinusoidal	N/A	0	0	0.999	0.7282	0.7282
Mollweide	N/A	0	0	1.00	0.5928	0.5928
Eckert IV	N/A	0	0	1.00	0.5287	0.5287
Eckert VI	N/A	0	0	1.00	0.5929	0.5929
Van der Grinten	0.858	0.5458	0.4356	0.863	0.5471	0.4522

Table 4: Minimised distortion results. For every projection, the minimum values of μ_s and μ, as well as the values c_{μ_s} and c_μ that produce these minimal values, are listed. Furthermore, the values of μ_s and μ from Section (4.2) are also listed for comparison. Some projection as listed multiple times, as these include parameters that could influence the distortion numbers. If a map projections is equal-area, μ_s naturally cannot be improved and hence c_{μ_s} is given the value N/A.

well-known fractions or square roots such as:

$$\begin{aligned} 0.866 &\approx \frac{1}{2}\sqrt{3}, \\ 1.414 &\approx \sqrt{2}, \\ 0.500 &\approx \frac{1}{2}, \\ 0.353 &\approx \frac{1}{4}\sqrt{2}, \\ 1.00 &\approx 1. \end{aligned}$$

The surfacing of these numbers in the minimisation of a distortion number consisting of the double integral of the absolute value of natural logarithms multiplied by a cosine term is a curious phenomena. Furthermore, as to why this is not the case for the Central cylindrical projection, the Lambert conformal conic projection and the Van der Grinten projection is perhaps worth exploring more in-depth.

Continuing with the area distortion number μ_s, apart from those with the equal-area property, all projections improved significantly on their scores. Among the highest gainers are the three perspective azimuthal projections and the Central Cylindrical projection. Unfortunately, however, these projections still rank rather poorly compared to the other projections. The Van der Grinten again rates best of the non equal-area projections, scoring almost 0.1 lower than the second best: the (Transverse) Mercator projection. The worst projection in this category is the Gnomonic projection, having by far the most distortion in area size.

Whereas the Eckert IV projection scored better than the Van der Grinten projection in Section (4.2) on the overall rating μ, the Van der Gritten projection now overtakes the Eckert IV projection by a significant margin. Interestingly enough, the (Transverse) Mercator projection is now also slightly better than the Eckert IV in overall distortion, even though one is conformal and the other equal-area, and also rates significantly higher than the Mollweide and Eckert VI projections, as does the Lambert conformal conic projection. Furthermore, the Cylindrical equal-area projection also rates higher than the Mollweide and Eckert VI, despite being mathematically simpler and having the equal-area property as well. Among the worst projections are again the azimuthal projections, with the Gnomonic being the worst by far. The Bonne, Central cylindrical, Albers equal-area conic and Sinusoidal projection have a somewhat average score compared to the rest.

5 Conclusion

Over the years, numerous maps have replaced each other as the 'standard' world map used in atlases. Often, however, these were justified by imprecise reasons, leaving the user without any option other than to trust the atlas publishers that these maps were in fact 'better'. Even though maps should be chosen with the requirements in mind, an ordered list of map projections based on an accurate and exact criterion is desired. To accomplish this, in Chapter 2 we define map projections and gradually works our way towards a way of quantifying the angular and area distortion that occur in the attempt of projecting the surface of a sphere onto a flat surface. Using the theory of Chapter 2, Chapter 3 then presents an analysis of a number of map projections. It displays figures of the maps, presents a short summary of the map's features and gives the angular and area distortion, both of which are also accompanied by a visualisation of the distortion. In Chapter 4, a choice of a distortion number that takes both the angular and area distortion into account allows us to compare and rate projections. Multiple perspectives for defining a suitable distortion number have been discussed and substantiated in Chapter 4. It is important to keep in mind, however, that selecting an appropriate distortion number is naturally somewhat subjective. The first distortion numbers discussed in Sections (4.1) and (4.2) are defined by logically considering the properties of the distortion values and how they should contribute to the ranking. For the angular distortion number μ_ω we simply take the average of the angular distortion over the whole sphere. For the area distortion number μ_s, given that that the area distortion is a multiplicative factor, we take the average of the absolute value of the natural logarithm of the area distortion factor over the whole sphere. This allows for a factor and its reciprocal to contribute equally to the distortion number, which is desired. For the (combined) distortion number μ, it is created considering the maximum and minimum scale factors of a point; if these are both close to one, both the angular and area distortion are small. Hence, the average of the absolute value of the maximum scale factor plus the absolute value of the minimum scale factor over the whole sphere is taken. The appearance of $\mu \approx \mu_s \approx 1.0$ for the Orthographic projection, $\mu \approx \mu_s \approx 2.0$ for the Stereographic projection and $\mu \approx \mu_s \approx 3.0$ for the Gnomonic projection for these choices of distortion numbers is interesting and may point to their efficacy. Unfortunately, μ_s and μ often being equal, and hence μ not including the angular distortion, points to a flaw in their definitions. Section (4.3) and (4.4) improve these distortion numbers by eliminating the dependence on the scaling inherent to μ and μ_s. In section (4.3), the projections are scaled to produce maps with a fixed area of 4π, where possible. An issue with this approach is that only the finite maps can be considered. Furthermore, for some projections the new values of the distortion number did not really appear to be in unison with a visual assessment of the distortion, hence calling for a different solution to the scaling issue. Consequently, in section (4.4), this is solved by finding the minimum values of the distortion numbers with respect to the size of the map. For this, the Golden-section search algorithm is used. Although the somewhat bold assumption is made that there exist only one minimum, we still believe Section (4.4) provides the best results. Hence, the best map projections according to our criterion are, in order:

1. Van der Gritten projection
2. (Transverse) Mercator projection
3. Eckert IV projection
4. Lambert conformal conic projection ($\phi_1 = \frac{\pi}{5}$, $\phi_2 = -\frac{\pi}{3}$)
5. Cylindrical equal-area projection
6. Mollweide projection
7. Eckert VI projection
8. Albers equal-area conic projection ($\phi_1 = 0$, $\phi_2 = -\frac{\pi}{3}$)
9. Sinusoidal projection
10. Bonne projection
11. Central cylindrical projection

12. Albers equal-area conic projection ($\phi_1 = \frac{\pi}{4}$, $\phi_2 = \frac{\pi}{3}$)
13. Lambert azimuthal equal-area projection ($\phi_1 = 0$)
14. Orthographic projection
15. Stereographic projection
16. Gnomonic projection

The list of projection discussed here is rather limited as compared to the large number of known projections. With the distortion numbers discussed in this paper, however, expanding upon this list can be done easily to create a more complete list. Furthermore, based on the distortion values discussed in this paper, one can improve upon this paper by creating other distortion numbers, thereby obtaining a different list. One example of an improvement to the distortion numbers discussed is to consider the circumference of the map; the lower, the better. Maps not taking a rectangular or elliptical shape, but rather one with a very high circumference can be designed to produce very low distortion everywhere, but may not necessarily be useful as these have odd shapes or awkward cutoff lines. With the current distortion numbers used, the orange peel map in Figure (2) would rate rather high, despite not being useful in all cases.

References

[1] Cmglee. Comparison of cartography surface development, 2019. http://commons.wikimedia.org/wiki/File:Globe_Atlantic.svg, (accessed: 29/6/2023).

[2] Schøyen Collection. Cyclon (yurda), possibly with map of darling river. https://www.schoyencollection.com/24-smaller-collections/maps/cylcon-darling-river-ms-5087-36, (accessed: 4/18/2023).

[3] Figure from Journey North. Understanding latitude and longitude. https://journeynorth.org/tm/LongitudeIntro.html, (accessed: 4/24/2023).

[4] C. F. Gaus and Peter Pesic. *General Investigations of Curved Surfaces*. Dover publications, 2005.

[5] Ebrahim Ghaderpour. Map projections. *Journal of Applied Geodesy*, 2014.

[6] J. Kiefer. Sequential minimax search for a maximum. *Proceedings of the American Mathematical Society*, 4(3):502–506, 1953.

[7] Stefan Kühn. Mercator projection map with tissot's indicatrices. https://commons.wikimedia.org/wiki/File:Tissot_mercator.png, (accessed: 30/6/2023).

[8] A. C. Hamilton L. Hradilek. *Systematic analysis of distortions in map projections*. Dept. of Surveying Engineering, University of New Brunswick, 1973.

[9] D.H. Maling. *Coordinate Systems and Map Projections*. Elsevier Science, 2013.

[10] BBC News. Ice age star map discovered, 2000. http://news.bbc.co.uk/2/hi/science/nature/871930.stm, (accessed: 4/18/2023).

[11] L.A. Sadun. *Applied Linear Algebra: The Decoupling Principle*. Monograph Bks. American Mathematical Society, 2007.

[12] John P. Snyder. *Map projections: A working manual*. U.S. Government Printing Office, 1987.

[13] Guido Van Rossum and Fred L. Drake. *Python 3 Reference Manual*. CreateSpace, Scotts Valley, CA, 2009.

[14] C. Vuik, P. van Beek, F. Vermolen, and J. van Kan. *Numerical Methods for Ordinary Differential Equations*. VSSD, 2007.

[15] A. Wolodtschenko and T. Forner. Prehistoric and early historic maps in europe: Conception of cd-atlas. 2:114–116, 01 2007.

[16] ZevRoss. Coordinate reference systems. https://s3.amazonaws.com/files.zevross.com/workshops/spatial/slides/html/4-crs.html#23, (accessed: 4/26/2023).